Title
A Fuel-Based Approach to Estimating Motor Vehicle Exhaust Emissions

Author
Craig, Brett

Publication Date
1998-09-01

A Fuel-Based Approach to Estimating Motor Vehicle Exhaust Emissions

by

Brett Craig Singer

B.S. (Temple University) 1991
M.S. (University of California, Berkeley) 1994

A dissertation submitted in partial satisfaction of the

requirements for the degree of

Doctor of Philosophy

in

Engineering:

Civil and Environmental Engineering

in the

GRADUATE DIVISION

of the

UNIVERSITY OF CALIFORNIA, BERKELEY

Committee in charge:

Professor Robert A. Harley, Chair
Professor William W. Nazaroff
Professor Robert F. Sawyer

Fall 1998

A Fuel-Based Approach to Estimating Motor Vehicle Exhaust Emissions

by

Brett Craig Singer

The dissertation of Brett Craig Singer is approved:

Robert Harley 11/20/98

Chair Date

Robert F Sawyer 11/20/98

Date

Wm W Nazaroff 12/1/98

Date

University of California, Berkeley

Fall 1998

Abstract

A Fuel-Based Approach to Estimating Motor Vehicle Exhaust Emissions

by

Brett Craig Singer

Doctor of Philosophy in Engineering: Civil and Environmental Engineering

University of California, Berkeley

Professor Robert A. Harley, Chair

Motor vehicles contribute significantly to air pollution problems; accurate motor vehicle emission inventories are therefore essential to air quality planning. Current travel-based inventory models use emission factors measured from potentially biased vehicle samples and predict fleet-average emissions which are often inconsistent with on-road measurements. This thesis presents a fuel-based inventory approach which uses emission factors derived from remote sensing or tunnel-based measurements of on-road vehicles. Vehicle activity is quantified by statewide monthly fuel sales data resolved to the air basin level.

Development of the fuel-based approach includes (1) a method for estimating cold start emission factors, (2) an analysis showing that fuel-normalized emission factors are consistent over a range of positive vehicle loads and that most fuel use occurs during loaded-mode driving, (3) scaling factors relating infrared hydrocarbon measurements to total exhaust volatile organic compound (VOC) concentrations, and (4) an analysis

showing that economic factors should be considered when selecting on-road sampling sites.

The fuel-based approach was applied to estimate carbon monoxide (CO) emissions from warmed-up vehicles in the Los Angeles area in 1991, and CO and VOC exhaust emissions for Los Angeles in 1997. The fuel-based CO estimate for 1991 was higher by a factor of 2.3±0.5 than emissions predicted by California's MVEI 7F model. Fuel-based inventory estimates for 1997 were higher than those of California's updated MVEI 7G model by factors of 2.4±0.2 for CO and 3.5±0.6 for VOC. Fuel-based estimates indicate a 20% decrease in the mass of CO emitted, despite an 8% increase in fuel use between 1991 and 1997; official inventory models predict a 50% decrease in CO mass emissions during the same period. Cold start CO and VOC emission factors derived from parking garage measurements were lower than those predicted by the MVEI 7G model. Current inventories in California appear to understate total exhaust CO and VOC emissions, while overstating the importance of cold start emissions. The fuel-based approach yields robust, independent, and accurate estimates of on-road vehicle emissions. Fuel-based estimates should be used to validate or adjust official vehicle emission inventories before society embarks on new, more costly air pollution control programs.

Robert Harley 12/3/98

To My Father

Louis Singer,

Of Blessed Memory

and

To My Mother

Annette Singer,

May She Reach 120 In Good Health!

ACKNOWLEDGEMENTS

I have been blessed with tremendous technical, financial, and emotional support throughout my research career at the University of California. I extend my most sincere gratitude to all those who have helped to make this dissertation a reality. My only regret is that I can name but a few of the individuals to whom I am indebted.

My esteemed advisor, Robert Harley, is of course most responsible for sending me back into the world with extra letters following my name. His patience, encouragement, and belief in me nurtured my growth as a researcher; his wisdom, guidance, and dedication to quality taught me to be a professional. Thanks, Rob, for allowing me to work on my own schedule and to pursue some dead ends along the way.

The recently annointed Dr. Thomas W. Kirchstetter also deserves more credit than I can express here. Tom contributed directly to the parking garage measurements and was a sounding board for many of the ideas which are presented in this thesis. Tom has also been a great friend, office-mate, workout partner, and listener. Rock On, Tom!

Waymond Chan, now retired from the Bay Area Air Quality Management District (BAAQMD), taught Tom and me to stand on our own feet as field researchers, consulted on the parking garage project, and offered much warm encouragement along the way.

Addtional field sampling assistance was provided by Mike Traverse, Grahams Scovell, and Chris Gee of the BAAQMD. Parking garage air samples were analyzed for

speciated VOC by Jim Hesson at the BAAQMD lab in San Francisco. Thanks also to Gary Kendall who offered BAAQMD resources to the parking garage study.

David Littlejohn, of Lawrence Berkeley National Laboratory, provided the instrumentation and much of the technical expertise for the infrared and flame ionization detector measurements of VOC concentrations presented in Chapter 4. Thanks, Dave, for all of your help and support!

The individual vehicle speciated VOC exhaust measurements presented in Chapter 4 would not have been possible without the efforts of many individuals at the California Air Resources Board; most significant among them were Thu Vo and Jerry Ho. I am likewise indebted to Jeff Long and all those at CARB who were responsible for making the remote sensor measurements referenced in Chapter 6.

Many researchers in the field of motor vehicle emissions have been incredibly generous with their support; the technical advice and encouragement offered by Don Stedman, Gary Bishop, Bob Slott, Marc Ross, Bob Stephens, Michael St. Denis, Tom Wenzel, John Sagebiel, and Alan Gertler, to name but a few, have meant a great deal to me. Thanks to Bob Sawyer for encouraging me to utilize existing emissions data!

On the issue of finances, I must again thank my advisor, Rob Harley, for insisting that I worry about research while he worried about funding. My first year of graduate work was financed by scholarships administered by the Department of Civil and Environmental Engineering at U.C. Berkeley. Later work was supported by Environmental Protection Agency and National Science Foundation grants awarded to Professor Harley, by U.S. Department of Transportation and Caltrans grants

administered through the U.C. Transportation Center, and by a dissertation scholarship from the U.C. Transportation Center.

Lastly, and most importantly, I owe a tremendous debt of gratitude to my family and the many friends who have supported me unconditionally during the past five years. My wife, Maia, has tolerated my crazy work schedule, raised my spirits with her twinkling eyes and energetic hugs, and done her very best to ensure that I eat more green vegetables than chocolate chip cookies. Thanks Jay for your support and for being a great brother; I love you, Man! Thank you Sally and David for making me feel at home from the moment I arrived to the Bay Area. Thank you Lynne-Rachel for giving me a chance. Thanks to David, Alan, Matt, Evan, Abra and all those who hung around the dungeon doing late-night problem sets. Yo, Angus! Credit is due to Linsey Marr and Greg Noblet, who postponed office re-organization until I was able to (almost) finish. Extra special thanks to Rula Deeb, Shelly Miller, and Doug Black, truly great people whose warmth and wit have made Davis Hall almost bearable. Mark, what can I say? You've been a brother, a best friend, a running partner, a role model, a chuppah bearer, and a basket case...Thanks for all of it.

Cheers!

TABLE OF CONTENTS

LIST OF FIGURES

LIST OF TABLES

CHAPTER ONE

Introduction

1.1 MOTIVATION

The emission inventory is an important tool in our efforts to understand and control air pollution problems. An inventory is developed by quantifying mass emissions from each pollutant source in an area. Sources can include stationary facilities such as power plants and factories, mobile units such as on-road vehicles and aircraft, and diffuse activities such as house painting. Individual source emissions are typically estimated as the product of an emission factor (mass of pollutant emitted per unit of activity) and estimates or measurements of total source activity. For pollutants which are formed in the atmosphere, such as tropospheric ozone, inventories must be calculated for precursor compounds. Photochemical models which are used to relate ozone formation to precursor emissions require accurate volatile organic compound (VOC) and nitrogen oxides (NO_x) emissions inventories (Harley et al., 1993).

Emission inventories are used to target sources for control and to develop air quality improvement strategies; it is therefore essential that they be as accurate as possible. For example, the official 1995 emission inventory for the South Coast Air Basin (SoCAB)

attributes 45% of reactive organic gases (ROG, essentially non-methane VOC), 64% of NO_x, and 70% of carbon monoxide (CO) emissions to the on-road motor vehicle fleet (CARB, 1997). Reflecting these estimates, California's official plan to meet federal clean air standards in the SoCAB depends largely on reducing vehicle emissions (SCAQMD, 1996).

Official vehicle emission inventories are calculated by models which combine emission factors and activity estimates for a matrix of vehicle groups. In California, vehicles are grouped by body type (e.g. passenger cars, light-duty trucks, etc.), engine and emission control technology, and model year (CARB, 1995). Emission factors are measured primarily in the laboratory from vehicles which have been recruited through mailings to registered vehicle owners (Devesh, 1994). With the laboratory-based approach, individual vehicles are pre-conditioned and tested under controlled environmental conditions. Exhaust emissions are normalized to travel and measured while each vehicle is driven through a standard dynamometer cycle intended to simulate on-road driving. Travel demand models and fuel use data are used to estimate total travel, as well as the breakdown of travel by vehicle type and speed. Since travel-normalized emission factors vary with driving mode, a subset of vehicles are tested on additional driving cycles to quantify the dependence of emissions on engine load.

The laboratory-based approach yields precise emission measurements for individual vehicles driven under prescribed conditions, but may result in biased and/or highly uncertain estimates of fleet-average emissions. On-road studies have shown that the distribution of vehicle exhaust emissions is highly skewed, with about 10% of the fleet

accounting for more than half the emissions of each pollutant (CO, VOC, and NO_x) (Lawson et al., 1990; Zhang et al., 1993; Stedman et al., 1994; Zhang et al., 1994). Emission rates of the highest-emitting vehicles can also vary substantially from test to test (Bishop et al., 1996). Accurate characterization of fleet emissions thus requires large numbers of emissions measurements from unbiased samples of vehicles. Contrary to this objective, the high cost and time requirements associated with dynamometer testing limits the number of vehicles tested and the number of repeat tests performed. The vehicle sample recruited for testing may be inherently biased because it is drawn exclusively from the officially-registered fleet; the on-road fleet also includes unregistered vehicles and vehicles registered in other states. Recruitment of an unbiased vehicle sample is further complicated by the unwillingness of some vehicle owners to submit their vehicles for testing. Vehicles driven by people who decline to participate in roadside test programs have higher emissions, on average, than vehicles which are volunteered willingly (Stedman et al., 1994; Hughes Environmental Systems, 1995).

On-road vehicle emissions can be measured directly by sampling the ventilation air in roadway tunnels (Kirchstetter et al., 1996; Pierson et al., 1996; Kirchstetter, 1998) and through the use of remote emissions sensors (Bishop et al., 1989; Lawson et al., 1990; Stephens and Cadle, 1991; Zhang et al., 1993; Stedman et al., 1994; Guenther et al., 1995; Zhang et al., 1996; Jimenez et al., 1997). The term "real-world" is often used to describe such studies because vehicles are sampled as they are maintained and operated under everyday conditions. On-road techniques allow for large numbers of vehicles to be sampled, including the entire population of vehicles at each sampling site. The primary

criticism of real-world studies is that many uncontrolled factors may influence emissions at the time and place of sampling. An alternate perspective is that real world studies directly account for the influence of all factors which affect on-road emissions. For example, the effect of increased air conditioner usage is measured directly when sampling occurs on a hot summer day. Wintertime sampling can likewise capture any emissions changes which result from lower ambient temperatures. When sited at economically and geographically diverse locations throughout an air basin, remote sensors can measure a representative sample of the on-road vehicle population (Klausmeier et al., 1995; Walsh and Gertler, 1997).

Tunnel studies characterize emissions from the population of vehicles traveling through the tunnel, often under a narrow range of driving modes. Emission factors measured at a single tunnel may not represent the overall vehicle population in an area or the full distribution of on-road driving, but they may be used as calibration points for official emission factor models (Gertler et al., 1997). Such comparisons have revealed inconsistencies between model predictions and on-road measurements of fleet-average emissions. For example, California's EMFAC 7C emission factor model underpredicted CO and HC emission factors by factors of 2.7±0.7 and 3.8±1.5 respectively, but correctly predicted the NO_x emission factors measured at a tunnel in Van Nuys, CA in 1987 (Ingalls, 1989; Ingalls et al., 1989; Pierson et al., 1990). Emission factor ratios predicted by the EMFAC 7F model matched the VOC/NO_x ratio but still underpredicted by a factor of 1.5-2.2 the CO/NO_x ratio measured at the Caldecott tunnel in Oakland, CA in 1994 (Kirchstetter et al., 1996). CO emission factors predicted by EMFAC 7F were

about 55% of those measured at the Van Nuys and Sepulveda tunnels in 1995, while model-predicted ROG and NO_x emission factors were comparable to those measured in the tunnels (Gertler et al., 1997).

Unquantified uncertainties and potential biases associated with current motor vehicle emission inventory models may result in unnecessarily costly or, at the other extreme, insufficiently stringent motor vehicle emission control programs. For this reason, the development of independent and potentially more accurate methods to calculate vehicle emission inventories has been identified as a high priority for air quality research (National Research Council, 1991). In California, state law requires the independent validation of official emission inventories (Polanco, 1996).

1.2 RESEARCH OBJECTIVES

The goal of this research was to develop and demonstrate a robust, independent, and accurate approach to estimating on-road motor vehicle exhaust emissions. The defining features of the approach are that emissions are normalized to fuel consumption rather than distance traveled, and that fleet-average emission factors are derived directly from on-road measurements. Specific objectives included (1) evaluation of motor vehicle exhaust emission inventories for southern California, (2) development and application of a fuel-based approach to estimating cold start emissions, (3) analysis of driving mode effects on fuel-normalized emission factors, and (4) assessment of progress in reducing vehicle emissions in southern California during the 1990s.

1.3 OVERVIEW

This dissertation presents, develops, and applies a fuel-based methodology for calculating motor vehicle emission inventories. The fuel-based approach uses emission factors normalized to fuel consumption, i.e. mass of pollutant emitted per quantity of fuel burned, and measures activity by fuel consumption. Emission factors are calculated from direct measurements of on-road vehicle emissions, primarily from infrared remote sensors but also from measurements in roadway tunnels and parking garages. Total fuel use is estimated from fuel sales which are tracked monthly by each state.

A detailed description of the fuel-based approach is presented in Chapter 2. The approach was used to estimate hot stabilized[1] CO emissions in California's South Coast Air Basin during summer 1991. Fuel-based estimates are compared to predictions of California's MVEI 7F motor vehicle emission inventory model.

The importance of cold start emissions is evaluated in Chapter 3, which describes a fuel-based approach to estimating cold start emissions. Fuel-normalized emission factors were measured as vehicles entered in hot stabilized mode, and exited in cold start mode, from an underground parking garage in Oakland, CA. The amount of fuel used during cold start was evaluated from dynamometer test data. Cold start emission factors measured in the garage are compared with those predicted by the EMFAC 7G model.

Chapter 4 describes the development of an adjustment factor which relates infrared to

---

[1] The term "hot stabilized" is used to describe vehicle operation after the engine and emission controls have reached normal operating temperatures. For vehicles with functioning oxygen sensors and catalytic converters, emission factors during hot stabilized driving are much lower than emission levels during the first few minutes after the vehicle is started cold. This issue is discussed further in Chapter 3.

flame ionization detector measurements of total VOC concentrations in vehicle exhaust. Adjustment is needed because infrared remote sensors do not respond equally to all individual organic compounds in vehicle exhaust.

The fuel-based inventory approach was motivated in part by evidence that emission factors normalized to fuel consumption vary much less than travel-normalized emission factors across different driving modes. The impact of driving mode on fuel-based emission factors is examined in Chapter 5. The analysis makes use of speed and acceleration measurements paired to on-road remote emissions measurements in Phoenix, AZ.

In Chapter 6, the fuel-based approach is applied to calculate an inventory of stabilized CO and VOC emissions for the South Coast Air Basin in 1997. Results presented in Chapter 4 are used to adjust infrared remote sensor measurements to represent the total VOC mass emission rate. Fuel-based inventory estimates for 1997 are compared to predictions of the current version of California's motor vehicle emission inventory model, MVEI 7G. Progress in reducing vehicle emissions is assessed by comparing the fuel-based inventory estimates for 1991 and 1997.

The important results of this work are summarized, and recommendations for future research are presented in Chapter 7.

1.4 REFERENCES

Bishop, G. A., J. R. Starkey, A. Ihlenfeldt, W. J. Williams and D. H. Stedman (1989). IR long-path photometry: a remote sensing tool for automobile emissions. *Anal. Chem.* **61**:671A-677A.

Bishop, G. A., D. H. Stedman and L. Ashbaugh (1996). Motor vehicle emissions variability. *J. Air Waste Manage. Assoc.* **46**:667-675.

CARB (1995). *Methodology for estimating emissions from on-road motor vehicles, MVEI 7G*. Mobile Source Emission Inventory Branch, California Air Resources Board, Sacramento, CA. Volumes I-V.

CARB (1997). *Emission Inventory 1995*. Emission Inventory Branch, Technical Support Division, California Air Resources Board, El Monte, CA. Data accessed via the internet at www.arb.ca.gov.

Devesh, S. (1994). *Test report of the light-duty vehicle surveillance program, series 12 (LDVSP 12)*. Mobile Source Division, California Air Resources Board, El Monte, CA. MS-94-04.

Gertler, A. W., J. C. Sagebiel, D. N. Wittorff, W. R. Pierson, W. A. Dippel, D. Freeman and L. Sheetz (1997). *Vehicle emissions in five urban tunnels*. Desert Research Institute, Reno, NV. Report to the Coordinating Research Council, Atlanta, GA. Project No. E-5.

Guenther, P. L., D. H. Stedman, G. A. Bishop, S. P. Beaton, J. H. Bean and R. W. Quine (1995). A hydrocarbon detector for the remote sensing of vehicle exhaust emissions. *Rev. Sci. Instrum.* **66**:3024-3029.

Harley, R. A., A. G. Russell, G. J. McRae, G. R. Cass and J. H. Seinfeld (1993). Photochemical modeling of the Southern California Air Quality Study. *Environ. Sci. Technol.* **27**:378-388.

Hughes Environmental Systems (1995). *City of Los Angeles remote sensing pilot project.* Prepared for the Mobile Sources Air Pollution Reduction Committee under the AB2766 Program and the City of Los Angeles Environmental Affairs Department. City Contract #C87060-1.

Ingalls, M. N. (1989). On-road vehicle emission factors from measurements in a Los Angeles area tunnel. *82nd Annual Meeting of the Air & Waste Management Association*, Anaheim, CA, June 25-30.

Ingalls, M. N., L. R. Smith and R. E. Kirksey (1989). *Measurement of on-road vehicle emission factors in the California South Coast Air Basin. Volume I: regulated emissions*. Southwest Research Institute, San Antonio, TX.

Jimenez, J. L., D. D. Nelson, M. S. Zahniser and C. E. Kolb (1997). Remote sensing measurements of on-road vehicle emissions of an important greenhouse gas: nitrous oxide. *Seventh CRC On-Road Vehicle Emissions Workshop*, San Diego, CA, April 9-11, 1997. Coordinating Research Council, Atlanta, GA.

Kirchstetter, T. (1998). *Impact of reformulated fuels on motor vehicle emissions.* Ph.D. Dissertation, Department of Civil and Environmental Engineering, University of California, Berkeley, CA.

Kirchstetter, T. W., B. C. Singer, R. A. Harley, G. R. Kendall and W. Chan (1996). Impact of oxygenated gasoline use on California light-duty vehicle emissions. *Environ. Sci. Technol.* **30**:661-670.

Klausmeier, R., S. Kishan, A. Burnette and J. McFarland (1995). *Evaluation of the California pilot inspection/maintenance (I/M) program.* Radian Corporation, Austin, TX. Draft Final Report to the California Bureau of Automotive Repair, Sacramento, CA.

Lawson, D. R., P. J. Groblicki, D. H. Stedman, G. A. Bishop and P. L. Guenther (1990). Emissions from in-use motor vehicles in Los Angeles: a pilot study of remote sensing and the inspection and maintenance program. *J. Air Waste Manage. Assoc.* **40**:1096-1105.

National Research Council (1991). *Rethinking the ozone problem in urban and regional pollution.* National Academy Press: Washington, DC.

Pierson, W. R., A. W. Gertler and R. L. Bradow (1990). Comparison of the SCAQS tunnel study with other on-road vehicle emission data. *J. Air Waste Manage. Assoc.* **40**:1495-1504.

Pierson, W. R., A. W. Gertler, N. F. Robinson, J. C. Sagebiel, B. Zielinska, G. A. Bishop, D. H. Stedman, et al. (1996). Real-world automotive emissions – summary of recent tunnel studies in the Fort McHenry and Tuscarora Mountain tunnels. *Atmos. Environ.* **30**:2233-2256.

Polanco (1996). SB 2174 and Section 39607.3 of Health and Safety Code, California Code of Regulations.

SCAQMD (1996). *Final 1997 air quality management plan.* South Coast Air Quality Management District, Diamond Bar, CA.

Stedman, D. H., G. A. Bishop, S. P. Beaton, J. E. Peterson, P. L. Guenther, I. F. McVey and Y. Zhang (1994). *On-road remote sensing of CO and HC emissions in California.* Final Report to the California Air Resources Board, Contract No. A032-093.

Stephens, R. D. and S. H. Cadle (1991). Remote sensing measurements of carbon monoxide emissions from on-road vehicles. *J. Air Waste Manage. Assoc.* **41**:39-46.

Walsh, P. A. and A. W. Gertler (1997). *Texas 1996 remote sensing feasibility study.* Desert Research Institute, Energy and Environmental Engineering Center, Reno, NV.

Final Report to the Texas Natural Resources Conservation Commission, Austin, TX.

Zhang, Y., G. A. Bishop and D. H. Stedman (1994). Automobile emissions are statistically gamma-distributed. *Environ. Sci. Technol.* **28**:1370-1374.

Zhang, Y., D. H. Stedman, G. A. Bishop, S. P. Beaton, P. L. Guenther and I. F. McVey (1996). Enhancement of remote sensing for mobile source nitric oxide. *J. Air Waste Manage. Assoc.* **46**:25-29.

Zhang, Y., D. H. Stedman, G. A. Bishop, P. L. Guenther, S. P. Beaton and J. E. Peterson (1993). On-road hydrocarbon remote sensing in the Denver area. *Environ. Sci. Technol.* **27**:1885-1891.

CHAPTER TWO

The Fuel-Based Approach

2.1 INTRODUCTION

Official emission inventories attribute a large fraction of total anthropogenic carbon monoxide (CO), nitrogen oxides (NO_x), and volatile organic compound (VOC) emissions to motor vehicles (EPA, 1994; CARB, 1997). Consequently, it is anticipated that reductions in vehicle emissions will result in significant air quality benefits (SCAQMD, 1996). However, as discussed in Chapter 1, conventional motor vehicle emission inventory models may not accurately reflect emissions from the current on-road fleet. Future vehicle emission inventories are even more uncertain, since they are based on projected decreases from current emission levels. Accurate, independent estimates of on-road vehicle emissions are needed to validate current inventory model predictions and to establish a baseline from which future emission reduction scenarios may be evaluated.

This chapter describes a fuel-based approach to calculating vehicle exhaust emission inventories. Pollutant emissions are related to the amount of fuel consumed and activity is tracked by fuel consumption. A fuel-based method was chosen over the more

---

Derived with permission from Singer, B.C. and R.A. Harley (1996). A fuel-based motor vehicle emission inventory. *J. Air Waste Manage. Assoc.* **46:** 581-593. ©1996 Air & Waste Management Association.

conventional travel-based approaches to estimating vehicle emissions based on the following considerations.

First, fuel consumption can be quantified more readily and in most cases more accurately than travel. Activity data for travel-based emissions models, such as the California Air Resources Board MVEI model (CARB, 1995), are developed using travel demand models and fuel use data. While travel-demand models provide valuable information about the spatial and temporal distribution of vehicle activity, total travel estimates are calculated from fuel use data and estimates of fleet-average on-road fuel economy (Caltrans, 1995). Direct use of fuel consumption data as the measure of vehicle activity eliminates one source of uncertainty in the final emission inventory. For locations outside the U.S., detailed travel estimates may not be available, whereas fuel sales data generally are available (Sawyer et al., 1998). In the U.S., monthly fuel sales are reported by each state to the national Department of Transportation (USDOT, 1998).

The second factor motivating the fuel-based approach is that fuel-normalized emission factors can be calculated directly from on-road emissions measurements. Remote sensors measure exhaust concentration ratios (e.g. CO/CO_2, HC/CO_2, and NO/CO_2) rather than absolute mass emission rates (Bishop et al., 1989; Stephens and Cadle, 1991; Guenther et al., 1995; Zhang et al., 1996). Since essentially all of the carbon in gasoline is emitted as CO_2, CO, or volatile organic compounds (VOC, includes HC and carbonyls), emissions of these compounds and any other pollutant which is measured concurrenty can be related directly to fuel consumption. Calculation of travel-normalized emission factors requires an uncertain estimate of individual vehicle fuel economy. In roadway tunnel studies, fuel-normalized emission rates can be calculated directly from the

concentrations of CO_2, CO, VOC, and other pollutants which are measured in tunnel exhaust air (Kirchstetter et al., 1996). Travel-normalized emission factors can be calculated only if tunnel ventilation rates are also measured; uncertainty in ventilation measurements adds uncertainty to the calculated travel-normalized emission factors (Rogak et al., 1998).

Finally, fuel-normalized emissions vary much less than travel-normalized emissions across different driving modes. Travel-based models predict emission factors for a range of average speed driving cycles. Since the relationship between emissions and average cycle speed is measured from a small sample of vehicles (on the order of dozens) (CARB, 1995), it is uncertain whether the models accurately reflect the effect of driving mode on real-world travel-normalized emission factors. The effect of driving mode on fuel-normalized emission factors is analyzed in Chapter 5.

2.2 APPROACH

A fuel-based emission inventory uses emission factors normalized to fuel consumption (e.g., grams of pollutant emitted per liter or kg of fuel burned). Average emission factors for subgroups of vehicles are weighted by the fraction of total fuel used by each vehicle subgroup (e.g. light-duty trucks vs. passenger cars) to obtain an overall fleet-average emission factor. The fleet-average emission factor is multiplied by regional fuel sales to compute pollutant emissions.

2.2.1 Emission Factors

By carbon balance, it is possible to relate the amount of pollutant emitted to the amount of fuel burned if the molar exhaust concentrations of CO_2, CO, and VOC are measured. An emission factor E_P for pollutant P can be computed as follows:

$$E_P = \left(\frac{[P]}{[CO_2]+[CO]+[VOC]} \right) \cdot w_c \rho_f \left(\frac{M_P}{12} \right) \qquad (2.1)$$

where E_P is in units of grams of pollutant P emitted per unit volume of fuel consumed, $[P]$ is the exhaust concentration of pollutant P, w_c is the carbon weight fraction of the fuel, ρ_f is the fuel density, and M_P is the molecular weight of P. The denominator of eq 2.1 represents a sum of carbon atoms in the exhaust; the factor of 12 is the atomic mass of carbon. The inclusion of the VOC term in the denominator of eq 2.1 is generally unimportant since CO_2 and CO account for more than 99% of fuel carbon for all but the highest VOC-emitting vehicles. Very small amounts (<0.1%) of fuel carbon may also be emitted in the form of particulate matter.

Infrared remote sensor measurements of Q_1 = [CO]/[CO_2] and Q_2 = [HC]/[CO_2] (with HC expressed on a propane equivalent basis) can be used to calculate CO emission factors as follows:

$$E_{CO} = \left(\frac{Q_1}{1+Q_1+3Q_2} \right) \cdot w_c \rho_f \left(\frac{28}{12} \right) \qquad (2.2)$$

where the factor of 3 in the denominator converts from propane molecules to carbon atoms. As discussed in Chapter 4, infrared remote sensor HC data reflect a partial reporting of total VOC concentrations in vehicle exhaust. The value of Q_2 in the denominator could be adjusted to reflect the discrepancy between infrared-reported HC

and total exhaust VOC, but the adjustment will have no significant effect on calculated emission factors (recall that VOC represents <1% of carbon emissions). Although remote sensors measure Q_1 and Q_2 directly, remote sensing data are generally reported as exhaust gas concentrations such as %CO and ppm HC. Q_1 and Q_2 may be back-calculated as the ratios of these values to the $\%CO_2$ value which is also available, but not always presented or discussed in the literature.

Each remote sensor measurement is coupled to a video image of the vehicle license plate. License plate numbers are matched to registration records from the state Department of Motor Vehicles (DMV) to obtain the information needed to classify each vehicle. In California, vehicle registration records include the vehicle make, model, model year, fuel type, body code (which identifies the functional capabilities of the vehicle; e.g., pick-up truck, school bus, passenger vehicle, etc.), body type (e.g., 4-door, hatchback, station wagon, etc.), vehicle identification number, and whether the vehicle is registered for commercial or private use. With this information it is possible to disaggregate the vehicle fleet and compute average emission factors for subgroups of vehicles. For the application presented in this chapter, vehicles are grouped by model year i and vehicle class j. Thus, EP_{ij} represents the average emission factor for all sampled vehicles of model year i and vehicle class j.

Vehicle emissions also can be measured in roadway tunnels, where elevated levels of motor vehicle exhaust are present. Tunnel measurements provide composite emission factors, weighted by fuel use, for the entire fleet of vehicles traveling through the tunnel. Measured emissions are weighted by fuel use because the total mass of pollutant emitted by each vehicle is related to the amount of fuel used by the vehicle as it travels through

the fixed length of the tunnel. If the fleet composition within the tunnel is variable over time, separate emission factors can be derived for different vehicle types (Gorse, 1984). For example, Pierson et al. (1996) used this technique to compute emission factors for heavy-duty trucks at the Tuscarora tunnel, where trucks varied from 6 to 80% of the vehicles travelling through the tunnel at various times of day. Tunnel studies are also valuable because a wide range of pollutants, including individual VOC, can be measured from a single exhaust air sample.

2.2.2 Vehicle Activity

In a fuel-based inventory, vehicle activity is measured by fuel use. Precise fuel sales data are available at the statewide level from records of taxes collected at initial points of sale. Monthly fuel sales are reported by the states to the U.S. Department of Transportation (USDOT, 1998). Calculation of the emission inventory for individual air basins requires that fuel use be resolved to the same spatial scale. Fuel use can be apportioned by tracking fuel shipments from major suppliers, through surveys of filling stations, or according to the distribution of population and/or the number of registered vehicles among all air basins in the state.

The fuel used in each air basin may be further apportioned among vehicle subgroups. Fuel-based emission factors cannot be weighted by travel fractions because different vehicles use different amounts of fuel to travel the same distance. For example, light-duty trucks use more fuel on average than light-duty passenger cars per km traveled (Murrell et al., 1993). In addition, vehicle fuel economy has improved dramatically over the last two decades, as shown in Table 2.1. The U.S. EPA has calculated average fuel economy values, weighted by new vehicle sales, for all vehicles of each class (cars and

Table 2.1. Fuel economy data for cars and trucks.[a]

Model Year	Fuel economy (km L^{-1})[b]		Fuel economy (mpg)	
	Cars	Trucks	Cars	Trucks
Pre-75[c]	6.0	5.8	14.2	13.7
1975	6.7	5.8	15.8	13.7
1976	7.4	6.1	17.5	14.4
1977	7.7	6.6	18.3	15.6
1978	8.4	6.4	19.9	15.2
1979	8.6	6.2	20.3	14.7
1980	9.9	7.9	23.5	18.6
1981	10.6	8.5	25.1	20.1
1982	11.0	8.7	26.0	20.5
1983	11.0	8.8	25.9	20.9
1984	11.1	8.7	26.3	20.5
1985	11.4	8.7	27.0	20.6
1986	11.8	9.1	27.9	21.4
1987	11.9	9.1	28.1	21.6
1988	12.1	9.0	28.6	21.2
1989	11.9	8.8	28.1	20.9
1990	11.7	8.8	27.7	20.7
1991	11.9	9.0	28.0	21.3

(a) Combined city/highway fuel economy estimates from Murrell et al. (1993). Values are fleet-average estimates weighted by new vehicle sales. Values listed here have not been adjusted to account for lower fuel economy observed in real-world driving.

(b) The units of km L^{-1} are used in place of the more conventional SI units of L per 100 km so that fuel economy can be expressed as distance traveled per volume of fuel consumed.

(c) All vehicles of model year 1974 and earlier. The fuel economy for cars shown here is for the 1974 model year from AAMA Facts and Figures (1993). The fuel economy for pre-1975 model year trucks is estimated using the same value reported for the 1975 model year.

trucks), for all vehicles sold by each manufacturer, and for foreign and domestic vehicles (Murrell et al., 1993). The actual fuel economy realized by vehicles on the road varies with vehicle model, but is lower on average than unadjusted EPA estimates by about 20% (Mintz et al., 1993). In 1985, the average shortfall associated with light-duty trucks was

20.1%, compared to a shortfall of 18.7% for cars. No significant trends in fuel economy shortfall have been correlated to automobile size or to vehicle age (Mintz et al., 1993). Since the calculation of fuel use by each vehicle subgroup requires only that the relative fuel economies be known (note that the fuel economy FE_{ij} appears in the summations in both the numerator and the denominator of eq 2.3 below), EPA fuel economy values were used without adjustment for the present analysis.

The travel fractions v_{ij} of each vehicle subgroup are estimated as the frequencies at which vehicles of each subgroup pass a remote sensor. For example, if a total sample of N vehicles drive by a remote sensor, then $v_{ij} = n_{ij}/N$ where n_{ij} is the count of vehicles in subgroup (i,j). Using the average fuel economy FE_{ij} and vehicle travel fraction v_{ij}, the fraction f_{ij} of total fuel used by each vehicle subgroup (i,j) is:

$$f_{ij} = \frac{\left(v_{ij} / FE_{ij} \right)}{\sum_{j=1}^{C} \sum_{i=Y_1}^{Y_n} \left(v_{ij} / FE_{ij} \right)} \tag{2.3}$$

where Y_1 is the model year of the oldest vehicles, Y_n is the most recent model year, and C is the number of vehicle classes being considered.

2.2.3 Combining Activity and Emission Factors

The overall fleet-average emission factor for pollutant P,

$$\overline{E}_P = \sum_{j=1}^{C} \sum_{i=Y_1}^{Y_n} f_{ij} \, E_{P_{ij}} \tag{2.4}$$

is multiplied by total fuel use to compute vehicular emissions of pollutant P. Emissions can be calculated by vehicle class by applying eqs 2.3 and 2.4 separately for each class j.

2.3 APPLICATION

The fuel-based methodology described above was applied to California's South Coast Air Basin (SoCAB). Stabilized exhaust emissions of carbon monoxide were calculated for gasoline-powered light-duty cars and light/medium-duty trucks for the summer of 1991.

Emission factors were calculated from remote sensing measurements made by Stedman, Bishop, and co-workers from the University of Denver as part of a study of on-road CO and HC emissions in California (Stedman et al., 1994). The complete data set received from the Unversity of Denver contained 91,679 valid CO and HC measurements matched to vehicle registration records (Stedman and Bishop, 1994). HC emission factors were not calculated for this analysis because the infrared HC sensor used by Stedman et al. in 1991 was subject to water vapor interference (Guenther et al., 1995). Use of HC remote sensor measurements is addressed in detail in Chapter 4. Vehicles were sampled at 13 sites in the Los Angeles and San Francisco Bay areas during May-July of 1991. Sites were selected to include a range of socioeconomic levels and driving modes. The current analysis for the SoCAB was based on data from Los Angeles area sites. Data from a parking lot were not used because vehicles were measured while operating in cold start mode. Summary descriptions of the sites (Stedman et al., 1994) are given below.

ROSEMEAD: Rosemead Blvd. north of the cloverleaf intersection with the Pomona Freeway (I-60) in south El Monte. Rosemead Blvd. is a flat, six-lane divided highway with traffic signals and a posted speed limit of 50 mph (80 km hr^{-1}); however, vehicles were measured while traveling at speeds ranging from nearly 0 to 80 km hr^{-1}. During the monitoring, all southbound traffic was funneled into a single lane to increase the measurement rate. Because this site was used for a random pullover study which lasted

about two weeks, more data are available for the Rosemead site than for all of the other sites combined. General Motors Research used their own remote sensor to obtain side-by-side measurements at this site; these results have been reported elsewhere (Stephens, 1994).

PECK: Interchange of Peck Road to I-10. Driving modes consisted of moderate accelerations on the on-ramp and decelerations on the curved off-ramp.

BEACH: Beach Boulevard to Southbound I-405. Two remote sensors were placed beyond the metering lights on the curved, 2% uphill grade. Vehicles were monitored as they accelerated past both units to merge with the freeway. Heavy congestion on the freeway restricted traffic flow during the morning hours.

LYNWOOD: Long Beach Blvd. one block north of Norton. Long Beach Blvd. is a level, four-lane surface street with light traffic and average speeds of 15-40 km hr^{-1}. In the afternoon, one of the lanes was closed so that more vehicles could be sampled.

EL SEGUNDO: El Segundo Blvd. to Southbound I-405. Two instruments were located past the metering lights on an uphill on-ramp, approximately 6 and 30 m from the ramp exit. Vehicles were observed to be gently accelerating as they passed the first sensor, and in cruise mode as they passed the second sensor.

BROADWAY: Northbound Broadway to Northbound I-101. Two units were used to monitor vehicles along a downhill on-ramp. Driving modes included light accelerations and cruises at ~30-65 km hr^{-1}.

VERMONT: Southbound Vermont Ave. to Westbound I-10. Vehicles were monitored as they accelerated past the first unit, located on a steep (~5% slope) uphill

on-ramp, and as they cruised or decelerated slightly past a second sensor, located 43 m away on a more gentle slope.

Using fuel-code data from the vehicle registration records, all vehicles burning fuels other than gasoline were excluded. Of 80,775 measurements at the seven sampling sites, 1424 measurements of non-gasoline vehicles were excluded. No fuel code was designated in the registration records matched to 1189 of the emissions measurements; these vehicles were assumed to be predominantly gasoline-powered and thus included in the calculation. Measurements of 110 vehicles registered with a model year of 1992 were grouped together with the 4690 measurements of 1991 vehicles.

Vehicles were classifed as either cars or trucks according to body code and/or body type information in the registration records. The truck category includes both light-duty and medium-duty trucks. It was not possible to track these truck classes separately because the division is based on gross vehicle weight, a parameter that was not included with the registration data. However, since remote sensors are designed to sample emissions from vehicle tailpipes that are about 30 cm from the ground, light-duty trucks were sampled more efficiently than medium-duty trucks. Emissions were not measured from heavy-duty vehicles with elevated exhaust pipes.

On many of the sampling days, a single remote sensor was used. For one day of sampling at the Rosemead site, and for all sampling at the Beach, Broadway, El Segundo, and Vermont sites, two instruments were positioned in series to measure the same stream of vehicles. This arrangement allowed for a greater fraction of the passing vehicles to be sampled at least once, and for a large fraction of the vehicles to be sampled twice.

Duplicate measurements for a single vehicle pass were averaged together and subsequently considered as a single measurement.

An emission factor (g L^{-1}) was calculated for each remote sensor measurement using eq 2.2 along with fuel properties of industry average gasoline circa 1991, i.e., a carbon weight fraction w_c = 0.87 and a fuel density ρ_f = 750 g L^{-1} (Pahl and McNally, 1990). Average emission factors were computed for vehicles of each subgroup (i,j) at each site. All vehicles of 1974 vintage and older were grouped together, and as mentioned previously, 1992 vehicles were grouped with 1991 vehicles. Table 2.2 shows the total sample size and the mean model year for cars and trucks at each site.

Table 2.2. Vehicle counts and mean model year for Los Angeles sites.[a]

Site	Cars measured	Mean car model year[b]	Trucks measured	Mean truck model year[b]
Beach	6103	1986.0	1538	1985.8
Broad	3372	1985.8	586	1985.8
El Segundo	2925	1985.7	732	1986.5
Lynwood	1374	1981.9	419	1982.1
Peck	4167	1984.4	946	1984.3
Rosemead	32297	1985.0	10425	1985.0
Vermont	5053	1984.4	804	1985.2
Totals	55291	1985.0	15450	1985.0

(a) Data from 1991 remote sensing study of Stedman et al. (1994).

(b) Pre-1975 vehicles were considered as having a model year of 1974.

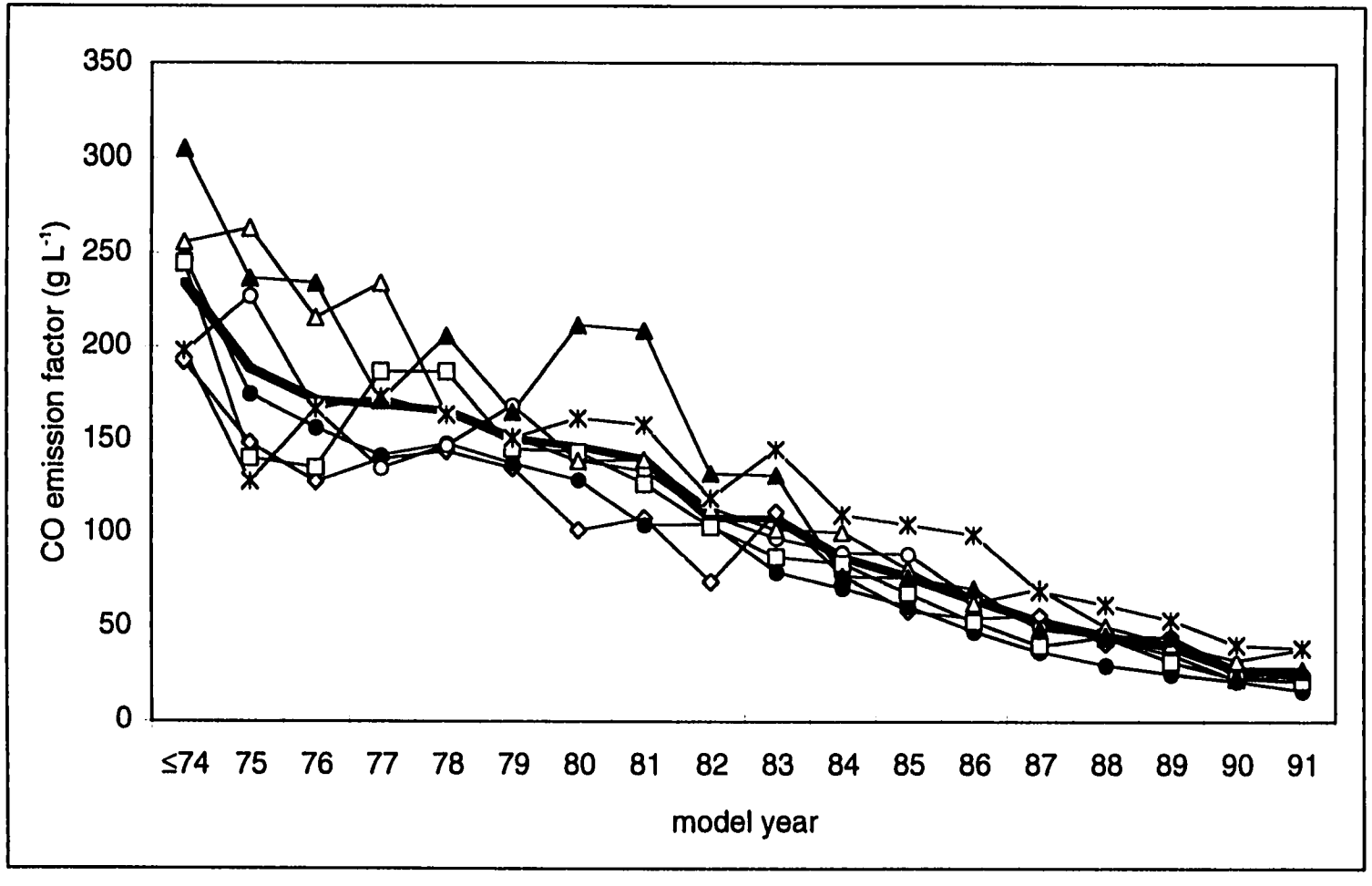

Figure 2.1. Average CO emission factors for cars of each model year at each site. The sites are: Beach (open diamond), Broadway (open circle), El Segundo (open triangle), Lynwood (filled triangle), Peck (open square), Rosemead (filled circle), Vermont (asterisk). 7-site mean emission factors are plotted as a heavy solid line.

Differences in average emissions between sites can be explained in large part by differences in average vehicle age (Stedman et al., 1994). To account for age differences in the vehicle fleets measured at individual sites, emission factors were calculated for each model year at each site. Average emission factors for each model year of cars at each site are plotted in Figure 2.1. Figure 2.1 shows that vehicles of the same age have comparable emissions even when measured at different sites. The coefficient of variation of emission factors measured at the seven sites is similar for all model years of cars. The analogous plot for trucks exhibits the same trend of increasing emissions with vehicle age, but shows greater year-to-year fluctuations at each site because the truck sample was much smaller than the car sample, as indicated in Table 2.2.

Figure 2.1 also shows that emission factors measured at the Rosemead site are lower overall than those measured at the other sites. Rosemead emission factors are lowest or second lowest for every model year of cars back through 1979, with the exception of 1982, when Rosemead cars had the third lowest average emission factor.

Recent model year vehicles at the Vermont Ave. site have emissions which are consistently higher than vehicles of the same age at the other sites. Emission factors for Vermont vehicles are 32-69% higher than the mean of the emission factors measured at the other six sites for vehicle model years 1983-1991. The positive offset in emission factors for recent model year vehicles at the Vermont site may have resulted from a portion of the fleet experiencing enrichment effects. Enrichment occurs when the computers of modern technology vehicles command a rich fuel-air ratio for increased power during high-load driving. Emissions of CO and HC from properly-functioning

vehicles can increase by 2-3 orders of magnitude when the vehicles operate in commanded enrichment mode (Kelly and Groblicki, 1993; St. Denis et al., 1994).

California statewide gasoline sales totaled 25.2×10^9 L during the period of May 1 through October 31, 1991 (USDOT, 1992); these months correspond to the official ozone planning season. It has been estimated that 2.7% of this total was purchased for use in off-road engines such as farm equipment, construction equipment, and boat engines (Macias, 1994); this amount was deducted from total gasoline sales. The fraction of fuel used in the SoCAB was calculated by considering the county-by-county breakdowns of population and registered vehicles. On a population basis, the SoCAB includes all of Orange county, 98% of Los Angeles county, 81% of San Bernardino county, and 72% of Riverside county (Asregado, 1995). In 1991, 44% of the people residing in California lived in the SoCAB (Dept. of Finance, 1992; Fay, 1993). Similarly in 1991, 40% of California vehicles were registered in the SoCAB (Dept. of Finance, 1992). Using the average of population and vehicle registration data, 42% of statewide fuel use was apportioned to the SoCAB. Heavy-duty trucks and motorcycles, which are not included in this inventory calculation, were estimated to consume 11% of the gasoline in the SoCAB (CARB, 1993). This amount was subtracted from total on-road vehicle gasoline use. Gasoline used by cars, light-duty trucks, and medium-duty trucks in the SoCAB was therefore calculated to be 49.4×10^6 L day^{-1}. Using data from Tables 2.3 and 2.4 below, 37.8×10^6 L day^{-1} were attributed to car activity and 11.6×10^6 L day^{-1} were attributed to truck use.

2.4 RESULTS

The CO exhaust emission inventory was estimated using two approaches: (1) lower bound values were calculated using emission factors measured at the Rosemead site; and (2) a "best-estimate" of the emission inventory was calculated using an equal weighting of the emission factors measured at each of the seven remote sensing sites. Measured emission factors are presented in Table 2.3 for each model year of cars. Similar emission factor data for trucks are presented in Table 2.4. Estimates of the uncertainty associated with the emission factors are included in Tables 2.3 and 2.4. For the Rosemead emission factors, the error estimates represent the standard error of the mean, a measure of the degree to which the sample mean represents the mean for the entire population (fleet) of vehicles. The uncertainty associated with the 7-site average emission factors is stated as ± one standard deviation, a measure of the site-to-site variability in average emission factors for each model year. Note that measurements from the Rosemead site make up about two-thirds of all the data and that the remaining data are not equally distributed among the other six sites, as indicated in Table 2.2.

Travel fractions for each model year of cars and trucks are presented in Tables 2.3 and 2.4, respectively. These values were calculated as the average of observed travel fractions from all seven sites for vehicles of each model year. Site-by-site age distribution data for cars are plotted in Figure 2.2. According to the observed vehicle distributions, cars account for 81% and trucks 19% of the travel for these two vehicle classes. Travel fractions shown in Tables 2.3 and 2.4 were converted to fuel use fractions using eq 2.3 and the fuel economy data presented in Table 2.1. As expected because of their lower

fuel economy, trucks account for a greater fraction of fuel used (24%) than of distance traveled (19%).

Table 2.3. Measured travel and emission factor data for cars in the SoCAB, 1991.

Model Year	Travel fraction[a] (%)	Fuel fraction[b] (%)	Rosemead Vehicles measured	Rosemead Emissions[c] (g L^{-1} CO)	7-Site Average Vehicles measured	7-Site Average Emissions[d] (g L^{-1} CO)
Pre-75	3.80 ± 1.73	6.31	1533	248 ± 5	2509	234 ± 41
1975	0.67 ± 0.39	1.00	243	175 ± 12	416	188 ± 53
1976	1.20 ± 0.98	1.61	441	157 ± 8	736	172 ± 40
1977	1.87 ± 1.34	2.41	660	142 ± 6	1117	169 ± 35
1978	2.80 ± 2.15	3.32	1010	148 ± 5	1696	165 ± 23
1979	3.09 ± 2.17	3.58	1133	138 ± 5	1911	151 ± 13
1980	3.40 ± 2.12	3.41	1107	128 ± 5	1992	146 ± 34
1981	3.33 ± 1.22	3.12	1283	104 ± 4	2176	140 ± 36
1982	3.47 ± 0.82	3.14	1301	105 ± 4	2267	108 ± 18
1983	3.60 ± 0.51	3.27	1414	79 ± 4	2430	107 ± 24
1984	5.09 ± 0.75	4.55	2177	71 ± 3	3648	87 ± 14
1985	5.79 ± 0.90	5.05	2475	61 ± 2	4155	77 ± 16
1986	6.37 ± 1.05	5.38	2482	47 ± 2	4355	64 ± 17
1987	7.49 ± 1.89	6.27	2942	37 ± 2	5197	53 ± 13
1988	7.53 ± 1.91	6.20	3289	29 ± 1	5485	45 ± 10
1989	8.70 ± 2.80	7.29	3688	25 ± 1	6311	39 ± 9
1990	7.64 ± 2.49	6.50	3271	21 ± 1	5554	27 ± 7
1991[e]	4.88 ± 1.81	4.10	1848	16 ± 1	3336	27 ± 9
All yrs.	80.7	76.5	32297	83[f]	55291	96[f]

(a) Observed $v_{ij} = n_{ij}/N$ averaged over all 7 sites ± 1 standard deviation.
(b) Percent of total gasoline use, computed using eq 2.3.
(c) Average emission factor measured at Rosemead site ± 1 standard error.
(d) Average of emission factors measured at 7 Los Angeles sites ± 1 standard deviation.
(e) Includes some 1992 vehicles; see text for discussion.
(f) Average emission factor for all model years calculated using eq 2.4.

Table 2.4. Measured travel and emission factor data for trucks in the SoCAB, 1991.

Model Year	Travel fraction[a] (%)	Fuel fraction[b] (%)	Rosemead Vehicles measured	Rosemead Emissions[c] (g L^{-1} CO)	7-Site Average Vehicles measured	7-Site Average Emissions[d] (g L^{-1} CO)
Pre-75	1.30 ± 3.95	2.23	693	231 ± 8	973	238 ± 66
1975	0.21 ± 0.43	0.36	113	192 ± 19	166	254 ± 97
1976	0.33 ± 0.88	0.53	153	227 ± 19	229	194 ± 45
1977	0.41 ± 1.13	0.61	215	224 ± 16	309	216 ± 38
1978	0.56 ± 2.04	0.87	304	144 ± 10	425	154 ± 67
1979	0.70 ± 1.53	1.12	362	165 ± 10	521	168 ± 48
1980	0.48 ± 1.16	0.61	233	199 ± 14	345	211 ± 49
1981	0.51 ± 0.91	0.59	249	128 ± 11	369	175 ± 31
1982	0.50 ± 0.66	0.57	260	123 ± 10	391	172 ± 79
1983	0.69 ± 1.47	0.78	296	152 ± 11	461	142 ± 42
1984	1.03 ± 0.95	1.19	633	110 ± 6	901	111 ± 27
1985	1.60 ± 1.38	1.83	869	92 ± 5	1304	94 ± 27
1986	1.94 ± 0.92	2.13	1101	66 ± 4	1602	89 ± 12
1987	1.91 ± 1.50	2.08	1030	45 ± 3	1550	76 ± 29
1988	2.01 ± 3.05	2.23	1085	29 ± 2	1651	49 ± 18
1989	2.29 ± 2.59	2.58	1263	25 ± 2	1895	40 ± 14
1990	1.90 ± 2.91	2.16	1014	17 ± 2	1544	33 ± 18
1991[e]	0.94 ± 0.48	1.04	552	14 ± 1	814	24 ± 17
All yrs.	19.3	23.5	10425	96[f]	15450	110[f]

(a) Observed $v_{ij}=n_{ij}/N$ averaged over all 7 sites ± 1 standard deviation.

(b) Percent of total gasoline use, computed using eq 2.3.

(c) Average emission factor measured at Rosemead site ± 1 standard error.

(d) Average of emission factors measured at 7 Los Angeles sites ± 1 standard deviation.

(e) Includes some 1992 vehicles; see text for discussion.

(f) Average emission factor for all model years calculated using eq 2.4.

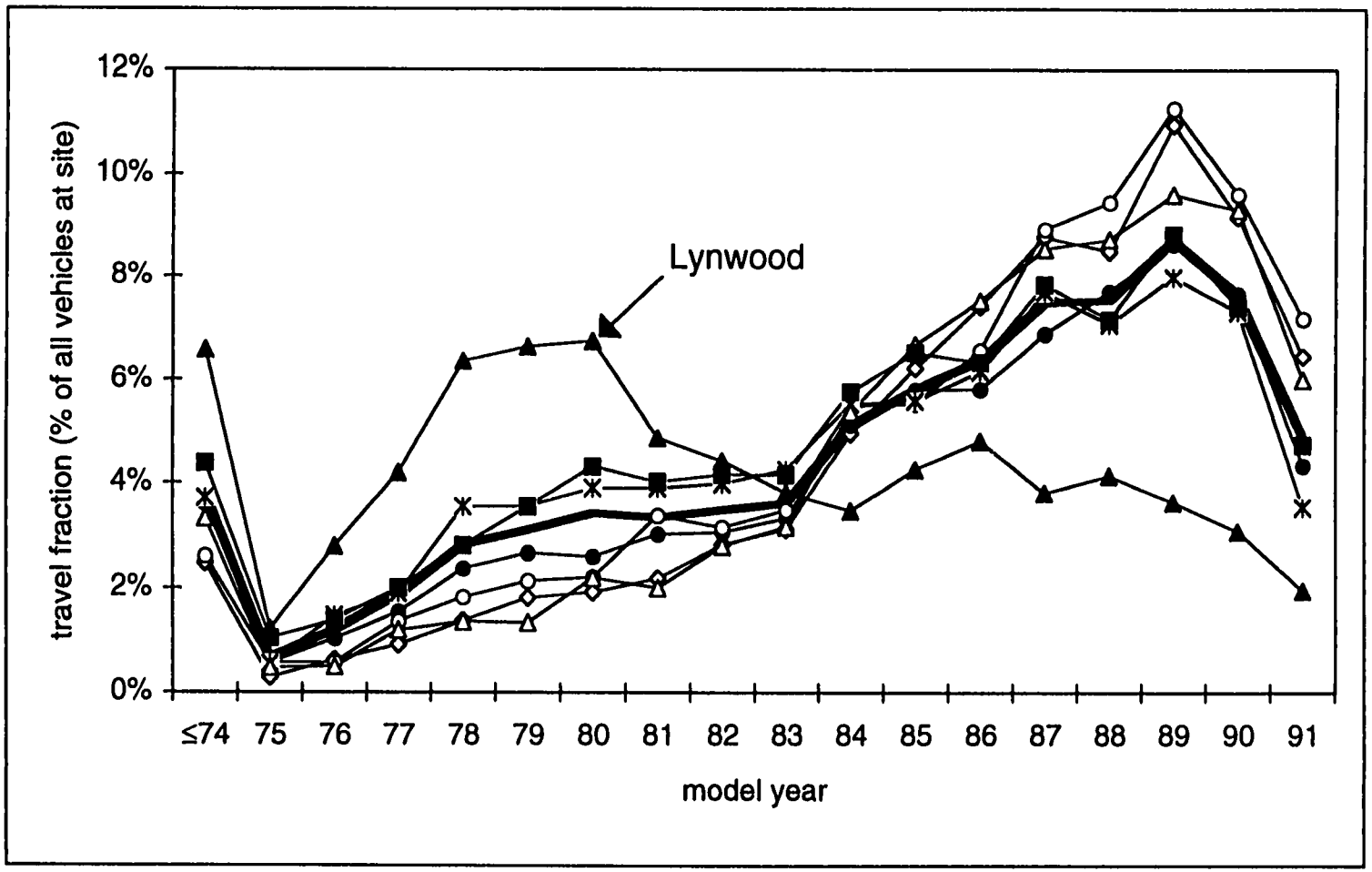

Figure 2.2. Observed age distributions for cars at each sampling site. The sites are identified as follows: Beach (open diamond), Broadway (open circle), El Segundo (open triangle), Lynwood (filled triangle), Peck (open square), Rosemead (filled circle), and Vermont (asterisk). The 7-site average distribution is plotted as a solid line.

Overall average emission factors for cars and trucks at the Rosemead site and for all seven sites combined are presented in Table 2.5. A correction factor was used to account for the bias of using only those remote sensing measurements which were matched to DMV registration records. Registration data were not available for out-of-state vehicles and for vehicles with unreadable or missing license plates. The correction factor was derived from Rosemead data, where the average CO concentration for 60,487 matched and unmatched vehicle measurements was 0.86%, whereas the average CO concentration for vehicles matched to DMV registration records (42,546 measurements) was 0.79% (Stedman et al., 1994). The class-average emission factors were therefore increased by a factor of 1.09.

Final emission inventory results for summer 1991 are presented in Table 2.5; corresponding predictions of CARB's MVEI 7F model are shown for comparison.[1] The fuel-based estimate of stabilized exhaust CO emitted by cars and light/medium-duty trucks is 2.3 times higher than the official emission inventory estimate of the MVEI 7F model. Fuel-based estimates are 2.2 and 2.6 times higher than MVEI 7F estimates for cars and trucks, respectively. Lower-bound inventory estimates — based on emission factors measured at the Rosemead site — are higher than MVEI 7F predictions by factors of 1.9 for cars and 2.3 for trucks. In Table 2.6, the fuel-based inventory of stabilized CO exhaust emissions is combined with MVEI 7F estimates of incremental start emissions and emissions from other vehicle types, such as heavy-duty vehicles. Total on-road vehicle CO emissions in the SoCAB were computed to be 7200 metric tons day^{-1}.

[1] MVEI 7F was California's official vehicle emission inventory model when the analysis in this chapter was completed. Comparison to MVEI 7G is included in Chapter 6.

Table 2.5. Stabilized CO exhaust emissions in the SoCAB, summer 1991.

	Emission factors[a]		Gasoline used	Fuel-based Inventory		MVEI 7F	Ratio of
	Rose-mead	7-site		Lower-bound[b]	Best-estimate[c]	Inventory	Fuel-based Best to MVEI 7F
	($g\ L^{-1}$ CO)		$\times 10^6$ ($L\ day^{-1}$)	($metric\ tons\ day^{-1}$)			
Cars	90	105±21[d]	37.8	3400	4000±800	1785	2.2±0.5
Trucks	104	120±35[d]	11.6	1200	1400±400	541	2.6±0.8
Totals	94	109±25[e]	49.4	4600	5400±1200	2326	2.3±0.5

(a) Emission factors from Tables 2.3 and 2.4 have been increased by a factor of 1.09 (see text).

(b) Calculated using Rosemead emission factors.

(c) Calculated using 7-site average emission factors.

(d) Uncertainty bounds calculated as ±20% of class-average emission factor for cars and ±30% of class-average emission factor for trucks. (See text for discussion of uncertainty).

(e) Total fleet-average emission factor and uncertainty bounds were calculated by weighting the emission factor and uncertainty for each vehicle class by the fractions of fuel used by each class.

Table 2.6. Estimated on-road vehicle CO emissions in the SoCAB, summer 1991.

	MVEI 7F Inventory				Fuel-Based Inventory		
	Starts[a]	Stabilized Exhaust	Total CO Emissions	Starts/ Total	Stabilized Exhaust	Total CO[b] Emissions	Starts/ Total
	($metric\ tons\ day^{-1}$)				($metric\ tons\ day^{-1}$)		
Cars	887	1785	2672	33%	4000	4900	18%
Trucks	263	541	803	33%	1400	1700	16%
HD+MC[c]	5	468	473	–	470	470	–
Diesel[d]	3	131	134	–	130	130	–
Total	1158	2925	4083	29%	6000	7200	16%

(a) Incremental cold + hot start emissions from MVEI 7F (CARB, 1993).

(b) Incorporates MVEI 7F estimates for incremental start emissions, heavy-duty gasoline-powered trucks, motorcycles, and all diesel vehicles so that total motor vehicle CO inventory can be calculated.

(c) Heavy-duty gasoline-powered trucks plus motorcycles. MVEI 7F provides no separate estimates for start emissions from HD gasoline-powered trucks.

(d) Diesel vehicles include cars, light-duty trucks, heavy-duty trucks, and urban buses.

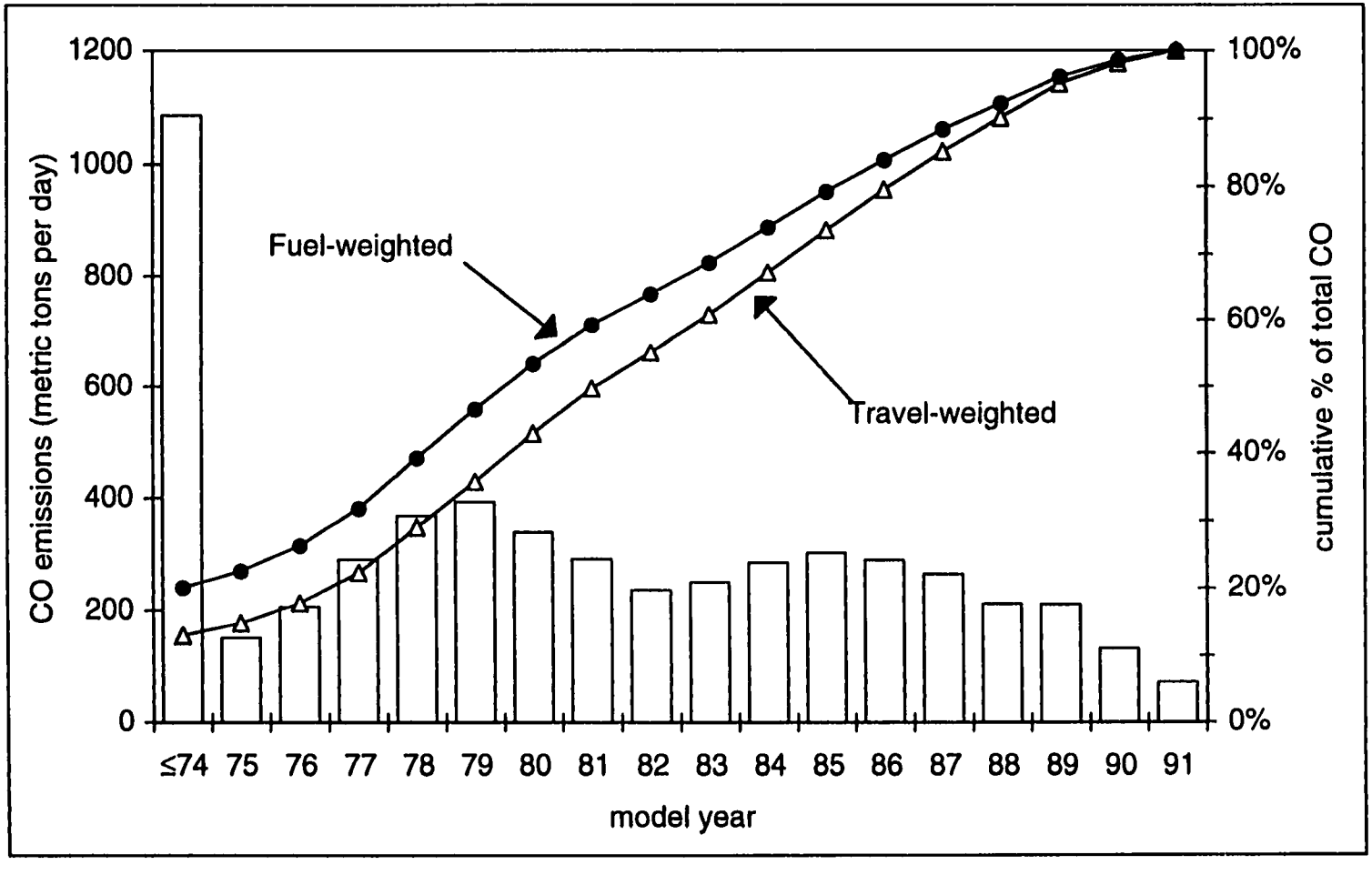

Figure 2.3. CO mass emissions from cars and trucks of each model year. Also shown is the cumulative contribution to total CO emissions as a function of vehicle age, using fuel-weighted and travel-weighted activity distributions.

Figure 2.3 shows the mass of CO emitted by cars of each model year. Cars which were ten or more years old (model year ≤ 1981) used ~30% of the fuel and contributed 59% of the stabilized exhaust CO from all cars. Similarly, trucks that were ten or more years old were responsible for 55% of the stabilized exhaust CO from all trucks. Despite the large contribution to total emissions from older vehicles, it should be noted that malfunctioning new vehicles can emit much more than well-tuned older vehicles (Lawson, 1995). Figure 2.3 also shows the cumulative percentage of total CO as a function of model year, calculated using both fuel-weighted and travel-weighted activity distributions. Since travel-weighted calculations ignore the upward trend in fuel economy between 1975 and 1990 vehicles, past analyses have understated the fraction of emissions contributed by older, less fuel-efficient vehicles.

2.5 DISCUSSION

2.5.1 Accuracy of Fuel-Based Inventory

The accuracy of a fuel-based emisssion inventory depends primarily on (1) how well the vehicles from which emission factors were measured represent the entire area under study, and (2) the accuracy of overall fuel use estimates and the apportionment of fuel use by vehicle type and model year.

The analysis in Chapter 6 indicates that both the age distribution and the profile of emissions by vehicle model year are strongly correlated to median income level in an area; emission factors and age distributions should thus be measured from samples of vehicles which are representative, vis-a-vis the income level of vehicle owners, of the overall vehicle population being studied. For the application presented in this chapter,

emission factors and age distributions were measured at seven sites distributed geographically throughout the South Coast Air Basin. Site-to-site differences in the percentage of foreign vs. domestic vehicles and in the vehicle age distribution suggest that the sampling sites represented a range of socioeconomic levels. It is uncertain, however, if the sites where vehicles were measured and the equal one-seventh weighting factors accurately represent the overall vehicle population in the SoCAB.

Of the seven sites, the vehicle fleet measured at Lynwood was most different than the others. The Lynwood site was located in a low-income neighborhood with an older-than-average vehicle fleet (see Figure 2.2). Emissions also increased with vehicle age more sharply at Lynwood than at the other sites, as shown in Figure 2.1. Since emission factors and age distributions from the seven sites were weighted equally to calculate fleet-average values, the population of vehicles at Lynwood was estimated to represent one-seventh of the SoCAB vehicle population. The importance of the weighting factor for Lynwood data was examined by recalculating fleet-average emission factors for cars and trucks, assuming that emission factors and age distributions measured at Lynwood represented only 4% of the entire SoCAB vehicle population. With this adjustment, fleet-average emission factors and corresponding inventory estimates were only 7% lower than the best-estimate values reported in Table 2.5. Thus, even if the fleet of vehicles at Lynwood represented a fraction of the SoCAB vehicle population much smaller than the initially assumed one-seventh (15%), the CO inventory would not differ substantially from the best-estimate values of Table 2.5.

Reduced fuel economy for CO high-emitters was not factored into the present inventory calculation. The presence of significant amounts of CO in vehicle exhaust

causes a reduction in the thermal efficiency of combustion (Heywood, 1988). As a result, high-emitting vehicles obtain lower fuel economy than similar vehicles which have lower CO emissions. Inclusion of fuel economy penalties for CO high-emitters would shift more of the fuel use to the high-emitters and result in higher calculated CO emissions, relative to the values presented in Table 2.5.

In Chapter 5, it will be shown that fuel-normalized CO emission factors are consistent across a range of positive loads and only slightly higher (<20%) during light decelerations. The emission factors used in this study were measured primarily from vehicles which were cruising, lightly accelerating, or lightly decelerating. At the Rosemead site, most vehicles were measured while cruising at moderate speeds on a level roadway; such moderate load driving produces the lowest CO emissions of any driving mode. One of the two remote sensors at the Vermont site measured vehicles as they were accelerating on a 5% uphill grade. Individual vehicles may enter fuel-enrichment mode and experience large increases in emssions levels during such high-load driving events. However, in Chapter 5 it will be shown that fleet-average CO emissions during loads which exceed those of the urban dynamometer driving schedule of the Federal Test Procedure (a benchmark test used for new vehicle emissions certification) are less than 10% higher than emission levels during moderate load driving. The effect of high-speed, high-load driving events of fleet-average emissions is not assessed in Chapter 5 because emissions data were unavailable for such driving events.

Statewide fuel use estimates are based on actual gasoline sales during summer 1991. Estimates of SoCAB gasoline use assume that fuel use per vehicle in the SoCAB is similar to fuel use per vehicle in other areas of the state. A study of vehicle odometer readings

recorded in California's inspection and maintenance (I/M) program betweem 1990 and 1993 (Horie and Thiele, 1994) found that travel rates for Los Angeles and Orange County vehicles were similar to the state average and travel rates for Riverside and San Bernardino vehicles were about 10% higher than the state average. As shown in Figure 2.4, the higher overall travel rates resulted from higher travel rates of newer vehicles in the outlying counties of San Bernardino and Riverside. This trend is consistent with the common practice that newer vehicles are used to commute longer distances. Since only 18% of SoCAB vehicles were registered in San Bernardino and Riverside counties, the 10% higher travel rates of these vehicles has only a 2% effect on the fraction of statewide fuel use apportioned to the SoCAB.

For this study, the fleet-average distribution of travel by vehicle age was estimated by equal weighting of the distributions observed at seven remote sensing sites. An independent estimate of travel by vehicle age was calculated by multiplying the travel rate data shown in Figure 2.4 by the number of registrations for each vehicle model year in July 1993 (Horie and Thiele, 1994); the result is presented in Figure 2.5(a). Figure 2.5(a) indicates that the estimated distribution of travel by model year (7-site) may overstate travel by newer vehicles.

2.5.2 Statistical Uncertainty of Inventory Estimates

Uncertainty in the fuel-based inventory results from uncertainty in the emission factors measured for each vehicle model year and from the weighting factors used to combine the emission factor data. In general, large numbers of measurements are required to ensure that average emission factors are measured accurately for each vehicle model year at each sampling site. For example, the large number of measurements at the Rosemead site

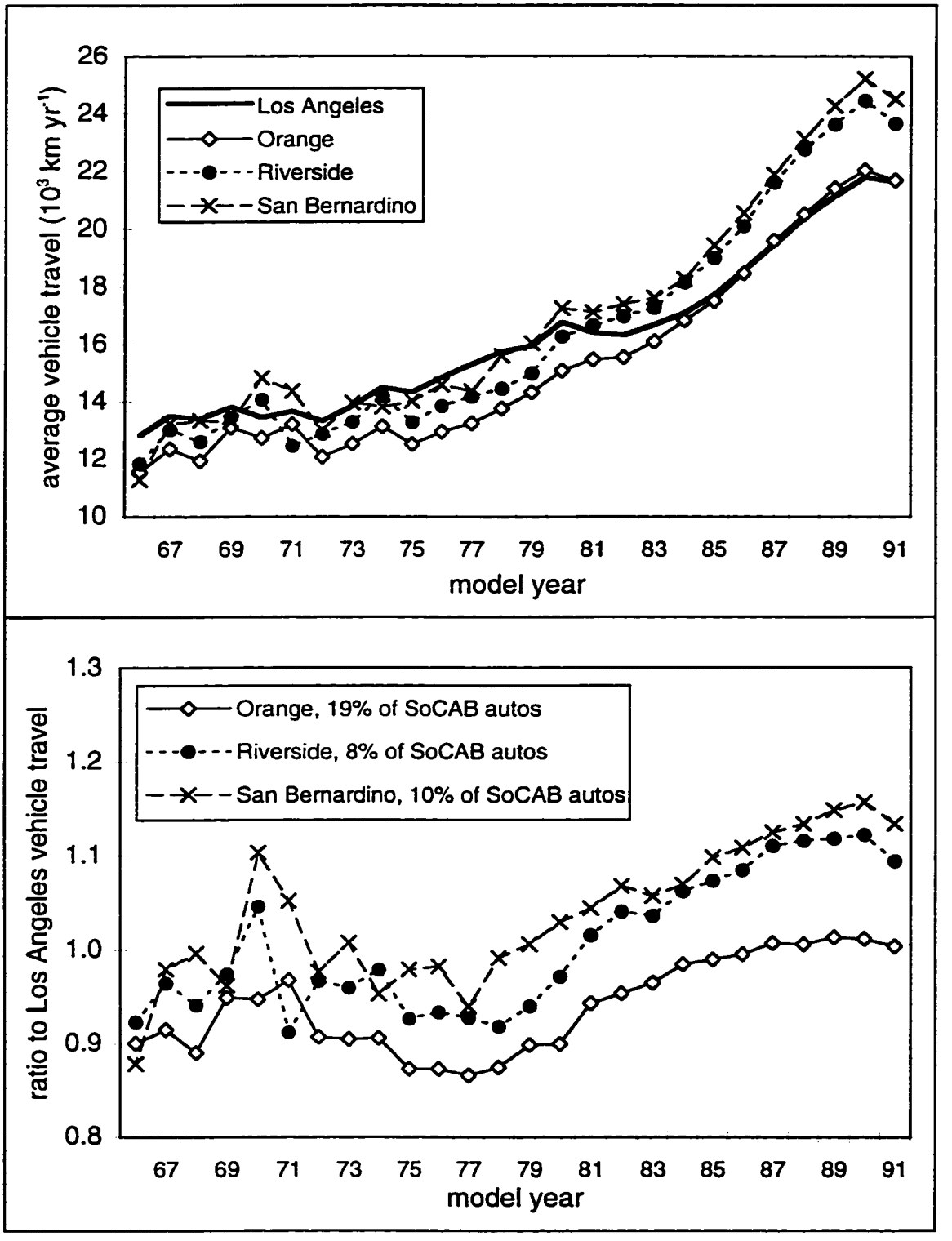

Figure 2.4. Travel accumulation rates for SoCAB vehicles from Horie and Thiele (1994) analysis of odometer readings recorded during California's inspection and maintenance program during 1990-1993.

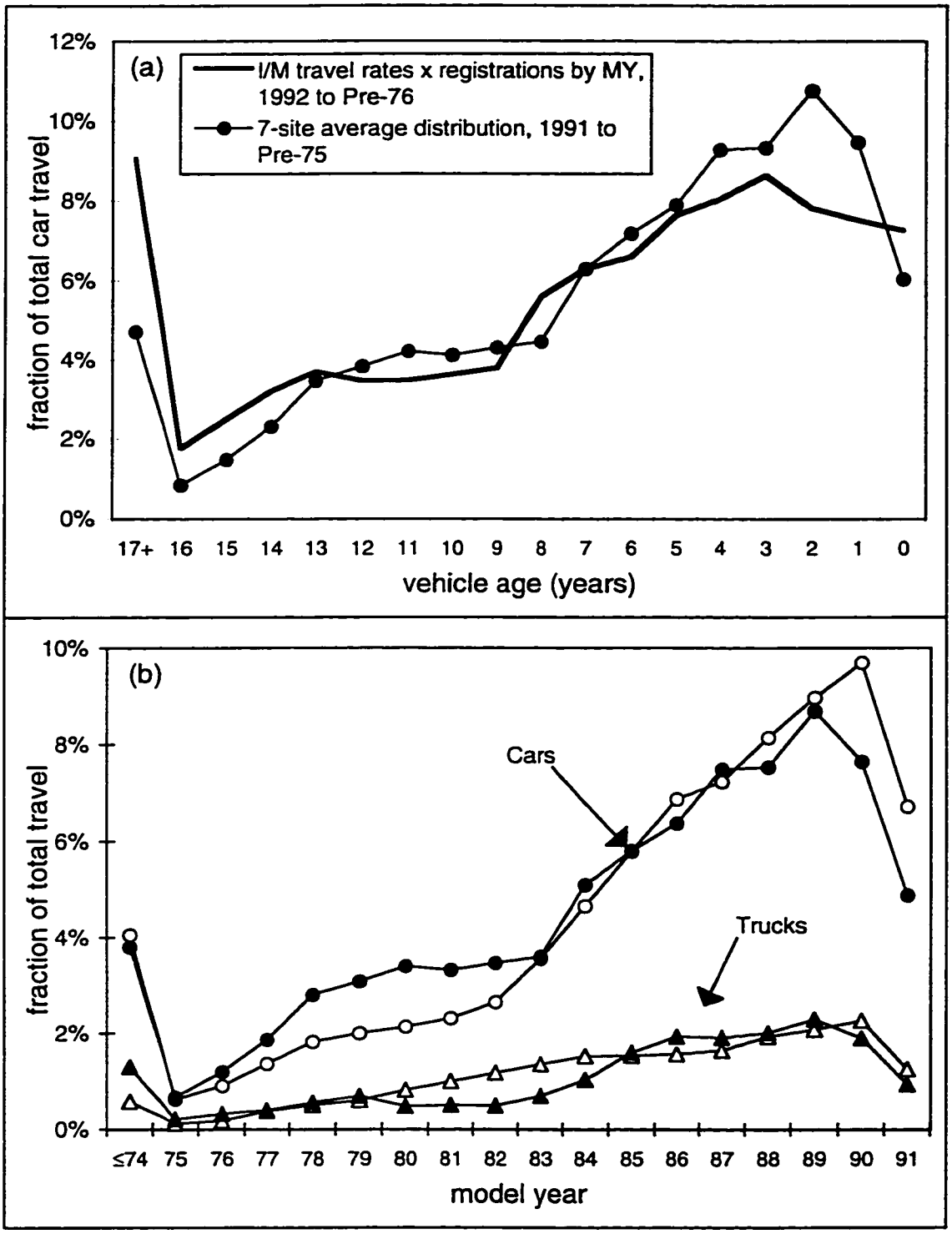

Figure 2.5. Distribution of travel by vehicle age. (a) Comparison between 7-site average and independent estimate calculated from vehicle registration records and travel rates from California's I/M program (Horie and Thiele, 1994).
(b) Comparison between 7-site average (solid) and MVEI 7F (open symbols).

ensured the precise calculation of emission factors for all vehicle model years at that site. High precision in the measurements at this site is indicated by the small standard errors associated with the model year specific emission factors presented in Tables 2.3-2.4. Smaller vehicle samples resulted in larger standard errors in emission factors at each of the other sites. Additional uncertainty results from weighting the data from individual sampling sites to calculate a basin-wide fleet-average emission factor.

Uncertainty bounds for the best-estimate inventory were estimated using the standard deviations of emission factors across the seven sites. The upper uncertainty bound was calculated using the mean plus one standard deviation as the emission factor for each car and truck model year. The lower uncertainty bound was calculated using the mean minus one standard deviation as the emission factor for each model year. Uncertainties associated with best-estimate values were thus calculated to be ±20% for cars and ±30% for trucks. These uncertainties were applied to the 7-site fleet-average emission factors and CO inventory estimates presented in Table 2.5.

2.5.3 Comparison Between Fuel-Based and MVEI 7F Methods

Consistent with the fuel-based activity apportionment, MVEI 7F assigns 43% of statewide car and truck travel to the SoCAB. The age distributions for cars and trucks used in MVEI 7F are similar to the 7-site average age distributions used in the present calculations, as shown in Figure 2.5(b). MVEI 7F activity data indicate that 80% of total car and light/medium-duty truck miles are driven by cars, consistent with the 81% travel fraction for cars observed on-road in the SoCAB and used in the fuel-based inventory. MVEI 7F reports fuel usage of 35.9×10^6 L day^{-1} for cars and 13.6×10^6 L day^{-1} for trucks. These values are consistent with the fuel use calcuations of the present study,

although MVEI 7F assigns a somewhat greater fraction of fuel use to trucks. When MVEI 7F fuel use and age distribution data were combined with fuel-based emission factors of the present study, calculated CO emissions were still 2.1 times higher than MVEI 7F predictions for cars and trucks combined. Therefore, differences between MVEI 7F model predictions and the fuel-based inventory presented here result mainly from differences in emission factors.

2.5.4 Additional CO Emissions

Stabilized exhaust emissions are shown in the context of total vehicular CO emissions in Table 2.6. In MVEI 7F, cold- and hot-start emissions are calculated from the difference between emission factors when vehicles are started (i.e., before the catalyst reaches operating temperature) and after the engine and emissions control equipment have reached stable operating conditions. Stabilized emissions are estimated assuming that all travel occurs after vehicles have reached stabilized conditions. Additional emissions which result from vehicle starting are termed incremental start emissions. Analogously, the fuel-based stabilized CO inventory considers that all fuel is used during stabilized vehicle operation and does not include incremental emissions associated with vehicle starting.

According to MVEI 7F, incremental start emissions comprised 33% of all summertime CO emissions from cars and light/medium duty trucks in summer 1991. The fuel-based inventory developed in this study indicates that stabilized exhaust emissions are much higher than suggested by MVEI 7F. This increase in stabilized emissions reduces the relative importance of incremental start emissions to only 16-18% of total summertime CO emissions from cars and trucks, as shown in Table 2.6. Therefore, MVEI 7F may overstate the importance of incremental start emissions. A fuel-based

approach to estimating real-world cold start emission factors is presented in the next chapter.

The present fuel-based inventory includes gasoline-powered light-duty cars, light-duty trucks, and medium-duty trucks. According to MVEI 7F, these vehicles were responsible for 80% of the stabilized exhaust CO emissions in the SoCAB. As shown in Table 2.6, motorcycles and heavy-duty gasoline-powered trucks contributed 16% and all diesel vehicles contributed only 4% of total vehicular CO emissions. Emissions associated with enrichment may be included to some extent in the present fuel-based inventory because some vehicles measured at the Vermont site were likely operating in enrichment mode. Enrichment is not included in the MVEI 7F estimates; however, results from the Auto/Oil program indicate that inclusion of off-cycle emissions would raise estimates of the exhaust CO inventory by about 9% (Schleyer et al., 1995).

2.5.5 Additional Applications

A fuel-based inventory can be calculated for any pollutant in any region for which representative emission factors can be measured; fuel use data are available for all 50 states in the U.S. Emission factor data are already available for many U.S. locations from tunnel and remote sensing studies. The use of remote sensors in Inspection and Maintenance programs is producing data for additional areas. Exhaust emissions of CO are measured accurately by remote sensors. The use of remote sensing HC measurements for inventory purposes is more complicated because conventional HC remote sensors sample at an infrared wavelength which is not absorbed equally, on a per-carbon basis, by all exhaust VOC. An approach for scaling IR remote sensor HC measurements to reflect total exhaust VOC emissions is demonstrated in Chapter 4. Newer remote sensors are

capable of measuring the NO/CO_2 ratio in vehicle exhaust (Zhang et al., 1996). Such instruments can provide on-road measurements of NO emissions analogous to the currently available CO data. Once the CO inventory is known, emissions of HC, NO_x, and additional pollutants such as formaldehyde and benzene, may also be estimated from emission factor ratios measured in roadway tunnels or from concentration ratios measured in ambient air.

2.6 CONCLUSIONS

A fuel-based methodology was developed and applied to calculate emissions of CO from cars and light/medium-duty trucks in the Los Angeles area. In the summer of 1991, stabilized exhaust CO emissions were calculated to be 4000±800 metric tons per day for cars and 1400±400 metric tons per day for trucks. These values were combined with incremental start and heavy-duty vehicle emissions estimates of the MVEI 7F model to estimate total on-road vehicle CO emissions of 7200 metric tons per day. Total car and truck stabilized exhaust emissions calculated using the fuel-based methodology were higher than predictions from the MVEI 7F model by a factor of 2.3. Lower-bound fuel-based inventory estimates indicate that MVEI 7F predictions were low by factors of at least 1.9 for cars, 2.3 for trucks, and 2.0 for both vehicle classes combined.

2.7 REFERENCES

AAMA (1993). *Motor Vehicle Facts & Figures '93*. American Automobile Maufacturers Association: Detroit, MI.

Asregado, R. (1995). *Personal Communication*. Emission Inventory Branch, Technical Support Division, California Air Resources Board, Sacramento, CA.

Bishop, G. A., J. R. Starkey, A. Ihlenfeldt, W. J. Williams and D. H. Stedman (1989). IR long-path photometry: a remote sensing tool for automobile emissions. *Anal. Chem.* **61**:671A-677A.

Caltrans (1995). *California motor vehicle stock, travel, and fuel forecast (MVSTAFF).* Transportation System Information Program, California Department of Transportation, Sacramento, CA.

CARB (1993). *Predicted California on-road motor vehicle emissions (BURDEN7F).* Mobile Source Emission Inventory Branch, California Air Resources Board, Sacramento, CA.

CARB (1995). *Methodology for estimating emissions from on-road motor vehicles, MVEI 7G.* Mobile Source Emission Inventory Branch, California Air Resources Board, Sacramento, CA. Volumes I-V.

CARB (1997). *Emission Inventory 1995.* Emission Inventory Branch, Technical Support Division, California Air Resources Board, El Monte, CA. Data accessed via the internet at www.arb.ca.gov.

Dept. of Finance (1992). *California Statistical Abstracts.* Financial and Economic Research Unit, California Department of Finance, Sacramento, CA.

EPA (1993). *MOBILE 5a.* United States Environmental Protection Agency, Office of Mobile Sources, Ann Arbor, MI.

EPA (1994). *National air pollutant emission trends, 1900 - 1993.* United States Environmental Protection Agency, Office of Air Quality Planning and Standards, Research Triangle Park, NC. EPA-454/R-93-032.

Fay, J. F., editor. (1993). *California Almanac.* Ronald J. Boehm, Pacific Data Resources: Santa Barbara, CA.

Gorse, R. A. (1984). On-road emission rates of carbon monoxide, nitrogen oxides, and gaseous hydrocarbons. *Environ. Sci. Technol.* **18**:500-507.

Guenther, P. L., D. H. Stedman, G. A. Bishop, S. P. Beaton, J. H. Bean and R. W. Quine (1995). A hydrocarbon detector for the remote sensing of vehicle exhaust emissions. *Rev. Sci. Instrum.* **66**:3024-3029.

Heywood, J. B. (1988). *Internal Combustion Engine Fundamentals.* McGraw-Hill Publishing Company: New York, NY.

Horie, Y. and M. Thiele (1994). *On-road motor vehicle activity data. Volume II - vehicle age distribution and mileage accumulation rate by county.* Valley Research Corporation, Northridge, CA. Prepared for California Air Resources Board Research Division, Sacramento, CA. Final Report, Contract No. A132-182.

Kelly, N. A. and P. J. Groblicki (1993). Real-world emissions from a modern production vehicle driven in Los Angeles. *J. Air Waste Manage. Assoc.* **43**:1351-1357.

Kirchstetter, T. W., B. C. Singer, R. A. Harley, G. R. Kendall and W. Chan (1996). Impact of oxygenated gasoline use on California light-duty vehicle emissions. *Environ. Sci. Technol.* **30**:661-670.

Lawson, D. (1995). 'Passing the test' - Human behavior and California's smog check program. *J. Air Waste Manage. Assoc.* **43**:1567-1575.

Macias, K. (1994). *Personal Communication*. Stationary Source Division, California Air Resources Board, Sacramento, CA.

Mintz, M., A. D. Vyas and L. A. Conley (1993). Differences between EPA-test and in-use fuel economy: are the correction factors correct? *Transportation Research Record* **1416**:124-130.

Murrell, J. D., K. H. Hellman and R. M. Heavenrich (1993). *Light-duty automobile technology and fuel economy trends through 1993*. U.S. Environmental Protection Agency. EPA/AA/TDG/93-01.

Pahl, R. H. and M. J. McNally (1990). Fuel blending and analysis for the Auto/Oil Air Quality Improvement Research Program. *SAE Tech. Pap. Ser.* **902098**.

Pierson, W. R., A. W. Gertler, N. F. Robinson, J. C. Sagebiel, B. Zielinska, G. A. Bishop, D. H. Stedman, et al. (1996). Real-world automotive emissions – summary of recent tunnel studies in the Fort McHenry and Tuscarora Mountain tunnels. *Atmos. Environ.* **30**:2233-2256.

Rogak, S., S. Green and U. Pott (1998). Use of a tracer gas for direct calibration of emission-factor measurements in a traffic tunnel. *J. Air Waste Manage. Assoc.* **48**:545-552.

Sawyer, R. F., R. A. Harley, S. H. Cadle, J. M. Norbeck, R. Slott and H. A. Bravo (1998). *Mobile source critical review: 1998 NARSTO assessment*. Report to Coordinating Research Council, Atlanta, GA and National Renewable Energy Laboratory, Golden, CO.

SCAQMD (1996). *Final 1997 air quality management plan*. South Coast Air Quality Management District, Diamond Bar, CA.

Schleyer, C. H., A. M. Dunker, J. L. Fieber, J. P. Cohen and A. K. Pollack (1995). Comparison of real-world emissions to MOBILE5a/EMFAC7F model predictions and resulting emission inventory changes - Auto/Oil Air Quality Improvement Research Program. *Fifth CRC On-Road Vehicle Emissions Workshop*, San Diego, CA, April 3-5, 1995. Coordinating Research Council, Atlanta, GA.

St. Denis, M. J., P. Cicero-Fernandez, A. M. Winer, J. W. Butler and G. Jesion (1994). Effects of in-use driving conditions and vehicle/engine operating parameters on "off-cycle" events: comparison with federal test procedure conditions. *J. Air Waste Manage. Assoc.* **44**:31-38.

Stedman, D. H. and G. Bishop (1994). *Personal Communication*. University of Denver, Denver, CO.

Stedman, D. H., G. Bishop, J. E. Peterson and P. L. Guenther (1991). *On-road CO remote sensing in the Los Angeles air basin*. Final Report to the California Air Resources Board, Contract No. A932-189.

Stedman, D. H., G. A. Bishop, S. P. Beaton, J. E. Peterson, P. L. Guenther, I. F. McVey and Y. Zhang (1994). *On-road remote sensing of CO and HC emissions in California*. Final Report to the California Air Resources Board, Contract No. A032-093.

Stephens, R. D. (1994). Remote sensing data and a potential model of vehicle exhaust emissions. *J. Air Waste Manage. Assoc.* **44**:1284-1292.

Stephens, R. D. and S. H. Cadle (1991). Remote sensing measurements of carbon monoxide emissions from on-road vehicles. *J. Air Waste Manage. Assoc.* **41**:39-46.

USDOT (1992). *Monthly motor fuel reported by states*. Federal Highway Administration, U.S. Department of Transportation, Washington, DC.

USDOT (1998). *Monthly fuel sales reported by states*. Federal Highway Administration, U.S. Department of Transportation, Washington, DC. Data accessed via the internet at www.fhwa.dot.gov.

Zhang, Y., D. H. Stedman, G. A. Bishop, S. P. Beaton, P. L. Guenther and I. F. McVey (1996). Enhancement of remote sensing for mobile source nitric oxide. *J. Air Waste Manage. Assoc.* **46**:25-29.

CHAPTER THREE

Cold Start Emissions

3.1 INTRODUCTION

Motor vehicle tailpipe emissions of carbon monoxide (CO), nitrogen oxides (NO_x), and hydrocarbons (HC) have been reduced substantially since the late 1960s by technological controls which reduce pollutant formation during combustion and remove pollutants from exhaust gases. Strict stoichiometric control of the air-fuel ratio results in lower levels of CO and HC production relative to fuel-rich operation, and lower levels of NO_x production relative to fuel-lean combustion. Stoichiometric air-fuel mixtures are also required for the treatment of exhaust gases by three-way catalytic converters, which simultaneously oxidize HC and CO to CO_2 and reduce NO to N_2. New vehicles, equipped with these and other emission controls, typically emit less than 5% of the pollutants emitted by pre-control vehicles (Calvert et al., 1993).

One limitation of current vehicle emission control systems is that they are ineffective for a short period after a vehicle is started. At start-up, the fuel-air mixture is intentionally enriched for several seconds or less to facilitate ignition and improve cold engine operation. This enrichment leads to increased production of CO and HC during

---

Derived with permission from Singer, B. C., Kirchstetter, T. W., Harley, R. A., Kendall, G. R. and J. M. Hesson (1999). A fuel-based approach to estimating motor vehicle cold start emissions. *J. Air Waste Manage. Assoc.* In Press.

combustion and limits the oxidation of these pollutants in the catalytic converter. In addition, automobile catalysts must reach temperatures above 200-400°C before significant pollutant conversion is achieved (Heywood, 1988; An et al., 1996). If a vehicle has been inactive for more than 30-60 minutes before being started, the unheated catalyst will be ineffective, or only partially effective, for some additional time after the initial fuel-enrichment period ends. Since the catalytic converter is heated by engine exhaust gases, catalyst warm-up occurs more rapidly when the engine operates under heavier loads and when the catalyst is positioned closer to the engine. Longer periods of vehicle inactivity and lower ambient air temperatures increase the heating required for the catalyst to reach effective operating temperatures, and thus prolong the period of elevated exhaust emission rates. When a vehicle is fully warmed-up and the engine and emissions controls have reached high temperatures, a vehicle is said to be in hot stabilized operating mode. The excess emissions that result from limited control system effectiveness during the period after a vehicle has been started are referred to as incremental start emissions.

According to current motor vehicle emission inventories, vehicle starts are responsible for a large fraction of total vehicle emissions. California's MVEI 7F model estimates that incremental start emissions contributed about one-third of the HC and CO, and one-fourth of the NO_x emitted from light-duty vehicles in the Los Angeles area during summer 1991 (CARB, 1993). In the winter, when ambient air temperatures are lower, vehicle starts are estimated to contribute an even larger fraction of total emissions. However, as discussed in Chapter 1, emissions estimates of MVEI 7F and earlier models are uncertain (Ingalls et al., 1989; Pierson et al., 1990; Fujita et al., 1992). In Chapter 2, remote sensing measurements of CO emissions from ~70,000 Los Angeles area vehicles

were combined with fuel sales data to show that MVEI 7F understated stabilized CO emissions by a factor of ~2 for summer 1991. If the stabilized CO inventory is increased by this factor with the incremental start emissions unchanged, the estimated contribution of start emissions is reduced to ~18%. In the newer MVEI 7G model, both stabilized exhaust and incremental start emissions estimates are higher than corresponding MVEI 7F values. According to MVEI 7G, incremental start emissions contributed 29% of CO emissions in the Los Angeles area during summer 1991 (CARB, 1996). At present, both the absolute magnitude and relative importance of incremental start emissions remain uncertain.

The objectives of this chapter were (1) to measure incremental cold start emission factors from a large sample of in-use vehicles under real-world conditions, and (2) to compare the measured emission factors with MVEI 7G model predictions.

3.2 APPROACH

Inventories of cold start emissions are calculated as the product of start emission factors, expressed as excess grams of each pollutant emitted per vehicle start, and the total number of starts per day for the vehicle fleet. Incremental start emission factors used by 7F and earlier versions of the MVEI model are derived from the dynamometer testing of recruited in-use vehicles on standardized cold start and hot stabilized driving cycles. Emissions are measured in travel-based (gram per mile) units and multiplied by the total distance driven during the tests. For MVEI 7G, start emission factors are derived from cold start dynamometer tests. Controlled dynamometer testing removes or reduces many variables, such as driver behavior, which can affect emissions. However, since dynamometer testing

is expensive and time-consuming, only limited numbers of vehicles are tested. Dynamometer testing also requires the voluntary participation of vehicle owners; this can result in sampling bias if owners of high-emitting vehicles are less willing to participate.

As an alternative to dynamometer studies, cold start emissions can be measured under real-world conditions by sampling the exhaust air in enclosed or underground parking garages (Ingalls et al., 1989). Parking garage studies are "real-world" because emissions are measured from vehicles as they are driven under everyday conditions. In garages used for workday parking, stabilized emissions can be measured as vehicles enter in the morning, and cold start emissions can be measured as vehicles start and exit in the afternoon. The incremental, or excess, emissions associated with vehicle starting are calculated by difference.

Vehicle emissions may be normalized to distance traveled by measuring the total distance driven by all vehicles inside the garage, and the air flow rates of the garage ventilation system (Ingalls et al., 1989). One problem with this approach is that travel-normalized emissions vary significantly with engine load. If vehicles spend more time idling during afternoon periods – when cars are started and allowed to warm up for a short time – than during morning periods, differences between morning and afternoon travel-normalized emission factors may not be due solely to cold start effects.

By carbon balance, vehicle emissions may also be normalized to fuel consumption, as follows:

$$E_P = \left(\frac{\Delta[P]}{\Delta[CO_2] + \Delta[CO] + \Delta[VOC]} \right) \times \left(\frac{w_c}{12} \rho_f \right) \times M_P \qquad (3.1)$$

where E_P is the pollutant P emission factor; delta values are background-corrected pollutant concentrations measured inside the garage, M_P is the molecular mass of pollutant P, w_c is the weight fraction of carbon in gasoline, and ρ_f the fuel density. Since emission factors are calculated by ratio to total carbon, air flow and driving distance measurements are not required, and uncertainties associated with these measurements are removed from emission factor calculations. Fuel-normalized emission factors are also more consistent as driving varies (see Chapter 5). As a result, changes in driving patterns between morning and afternoon periods should not bias the calculation of incremental start emission factors.

3.3 EXPERIMENTAL

Vehicle emissions were measured during March 1997 in a three-level underground parking garage at an office building in Oakland, CA. The first underground level of the garage accommodates visitor and company vehicles which enter and exit throughout the day. The bottom two levels (2 & 3) are used for employee parking. Most vehicles were parked on these levels before 9:00 and remained in the garage until after 16:00, providing a large sample of cold starting vehicles in the afternoon period. All vehicle activity and emissions measurements described in this study pertain only to levels 2 and 3 of the garage. Each parking space on these levels is assigned to an individual employee; as a result, vehicles proceed directly to their assigned spaces on these levels. The posted speed limit in the garage is 5 mph (8 km hr^{-1}).

Morning and afternoon sample periods were chosen to coincide with periods of maximum vehicle activity and the highest pollutant concentrations in the garage, generally

from 7:15-8:45 during morning periods, and 16:30-18:00 during evening periods. Exact sampling times varied slightly from day to day; dates and times of all sampling periods are provided in Table 3.1. Pollutant concentrations and vehicle activity were also monitored directly preceding and following the periods noted in Table 3.1.

The number of vehicles entering and exiting the garage was recorded during each ten minute interval for all sample periods. All vehicles entering the garage were assumed to be in hot stabilized mode. Arrival and departure times were matched for each vehicle to determine the length of time vehicles were parked before exiting the garage during the afternoon sampling period. The model year and fuel type of each vehicle was determined from vehicle registration records. Typical vehicle trip times during morning and afternoon periods were measured using a stopwatch. Timing of an arrival trip started as the vehicle turned the corner from the ramp to enter a level and ended when the vehicle was turned off. Departure trips extended from the first crank of the engine until the vehicle reached the exit ramp between levels 1 and 2 of the garage. Vehicle speeds were estimated by visual observations and by measuring the distance traveled during timed vehicle trips.

During sampling periods, clean ventilation air was supplied to the garage through a single plenum near the center of level 3; background pollutant concentrations were measured by inserting a sample line into this plenum. Polluted garage air was collected through ducts at the east end of levels 2 and 3, channeled into a central plenum, and discharged outdoors. Garage air was sampled at a point ~3 m above the junction of the exhaust air streams from levels 2 and 3. An additional clean air supply on level 2 and the exhaust ventilation system at the west end of the garage were turned off during all sample periods.

Table 3.1. Average pollutant concentrations measured in the garage exhaust air (Garage) and ventilation intake air (Bkg) during each sample period.

Date	Location	Time	CO_2 (ppm)	CO (ppm)	NO_x (ppb)	CH_4 (ppm)	NMHC (ppmC)
		Morning sample periods					
11-Mar	Garage	7:20-9:00	558	8.3	268	N/A[a]	N/A[a]
11-Mar	Bkg	7:20-9:00	411	0.8	88	N/A[a]	N/A[a]
12-Mar	Garage	7:10-9:00	558	7.4	273	2.37	3.65
12-Mar	Bkg	7:00-9:00	422	0.6	96	2.00	0.31
13-Mar	Garage	7:20-9:00	596	8.3	374	2.33	4.15
13-Mar	Bkg	7:12-9:02	450	1.8	172	2.13	0.56
17-Mar	Garage	7:20-8:50	566	8.7	239	2.12	4.07
17-Mar	Bkg	7:20-8:50	399	0.9	86	2.00	0.33
18-Mar	Garage	7:15-8:45	571	8.0	267	2.25	3.91
18-Mar	Bkg	7:00-9:00	429	1.0	119	2.12	0.39
19-Mar	Garage	7:10-8:50	606	7.8	349	2.33	3.96
19-Mar	Bkg	7:05-8:50	483	1.7	178	2.16	0.59
		Afternoon sample periods					
10-Mar	Garage	16:30-18:00	560	23.3	735	N/A[a]	N/A[a]
10-Mar	Bkg	16:30-18:00	404	1.1	99	N/A[a]	N/A[a]
11-Mar	Garage	16:30-18:00	578	28.2	782	2.22	5.55
11-Mar	Bkg	16:30-18:00	388	0.7	79	1.85	0.29
13-Mar	Garage	16:40-18:10	621	28.8	895	2.32	6.98
13-Mar	Bkg	16:15-18:00	384	0.6	76	2.00	0.27
17-Mar	Garage	16:30-18:00	560	22.7	588	2.20	4.64
17-Mar	Bkg	16:00-18:00	381	0.6	55	1.95	0.20
18-Mar	Garage	16:35-18:10	574	26.5	647	2.18	5.65
18-Mar	Bkg	16:15-18:00	384	1.0	60	1.95	0.28
19-Mar	Garage	16:40-18:10	592	25.5	674	2.18	5.75
19-Mar	Bkg	16:15-17:55	407	0.5	90	2.00	0.33

(a) Not available. Samples were not collected for this period.

Garage exhaust and clean ventilation air streams were monitored continuously for CO, CO_2, and NO_x. CO_2 concentrations were measured using Thermo Environmental Instruments (TECO; Franklin, MA) model 41H gas filter correlation spectrometers. NO_x concentrations were measured using TECO model 42 chemiluminescent analyzers. CO in garage exhaust was measured with a TECO model 48 gas filter correlation spectrometer; background CO was measured with a Langan Databear electrochemical CO analyzer (Langan Instruments, San Francisco, CA). Continuous monitoring data were averaged and recorded for each 5-minute period between 6:30-9:30 and 15:30-18:30.

Total and speciated HC concentrations were measured by collecting integrated 90-minute air samples in 6-liter stainless steel canisters using XonTech model 910A continuous flow samplers. Background and garage air samples were analyzed by GC-FID at the Bay Area Air Quality Management District laboratory in San Francisco using the technique described in Kirchstetter et al. (1996). Carbonyl samples were collected in parallel with HC canister samples using DNPH-impregnated silica cartridges. The cartridges were eluted with acetonitrile immediately following each sample period and the liquid samples were capped and stored in a refrigerator for ~3 months prior to analysis; the extracted samples were at room temperature for ~3 weeks during this period. Carbonyl samples were analyzed by HPLC to quantify concentrations of individual aldehydes and ketones (Fung and Grosjean, 1981; Fung, 1997).

3.4 RESULTS

3.4.1 Vehicle Activity

A summary of vehicle counts during morning and afternoon sampling periods is provided in Table 3.2. Vehicles entering during the 5-10 minutes directly preceding emissions sampling are included because these vehicles contributed to pollutant concentrations measured in the garage in the early part of each sample period. Morning vehicle activity was steady from 7:00 until 7:40, increased between 7:40 and 8:00, gradually declined until 8:30, then was steady again until the end of the sample period. During afternoon periods, ~40% of the vehicles exited between 16:30 and 16:50; vehicle traffic then declined gradually through the remainder of each afternoon sample period. Light-duty trucks, minivans, and sport-utility vehicles constituted 25-35% of the vehicle fleet sampled in each period. Almost all of the vehicles sampled had gasoline engines; less than 1% of the vehicles in the garage were diesel-powered. Each day, 80-90% of vehicles sampled during the afternoon were also present during the morning sample period; the remaining vehicles

Table 3.2. Vehicle counts during morning and afternoon sample periods.

		AM: 7:10-8:50			PM: 16:20-18:00		
Date:	Day	IN	OUT	% stab[a]	IN	OUT	% stab[a]
10-Mar	Mon	-	-	-	7	110	6%
11-Mar	Tue	128	8	94%	9	120	7%
12-Mar	Wed	123	10	92%	8	137	6%
13-Mar	Thu	-	-	-	8	128	6%
17-Mar	Mon	126	7	95%	5	121	4%
18-Mar	Tue	121	15	89%	7	133	5%
19-Mar	Wed	129	9	93%	11	130	8%
Mean		125	10	93%	8	126	6%

(a) Fraction of vehicles operating in hot stabilized mode.

entered the garage either before 7:10 or after 8:50. As shown in Table 3.2, on average 93% of morning vehicles and 6% of afternoon vehicles were operating in hot stabilized mode. About one third of the vehicles *exiting* the garage in the morning had been in the garage for less than one hour.

Soak time distributions for vehicles exiting 16:20-18:00 on the afternoons of March 17-19 are shown in Figure 3.1. This figure indicates that 70-80% of vehicles exiting the garage during afternoon periods were parked for 8 or more hours, and fewer than 5% were parked in the garage for less than 2 hours. The age distribution of vehicles parked in the garage during the three-day period is presented in Figure 3.2, along with the age distributions used by MVEI 7G for 1997 San Francisco Bay Area emission inventory calculations. MVEI 7G uses slightly different age distributions to calculate fleet-average start and stabilized exhaust emissions; both profiles are shown in Figure 3.2. The age distribution of vehicles parked in the garage is similar to the age distributions used by MVEI 7G. The garage sample includes fewer vehicles from the most recent (1995-97) and oldest (pre-1983) model years, and a higher fraction of 1984-93 model year vehicles.

Driving in the garage consisted mainly of low-speed operation at ~15-25 km hr^{-1}. Exit times for vehicles parked on level 2 ranged from 15 to 125 s, with 90% of the vehicles exiting within ~60 s. A mean exit time of 41±3 s was calculated from 43 observed trips (vehicles starting from all areas of level 2). Since the layout of the two levels is almost identical, it was assumed that vehicles parked on level 3 followed the same exit pattern as those parked on level 2. Vehicles parked on the lowest level drove through level 2 en route to the garage exit in 28±1 s. These vehicles spent an additional ~10 s on the ramp between levels 2 and 3. Therefore, vehicles exiting from level 3 were in the

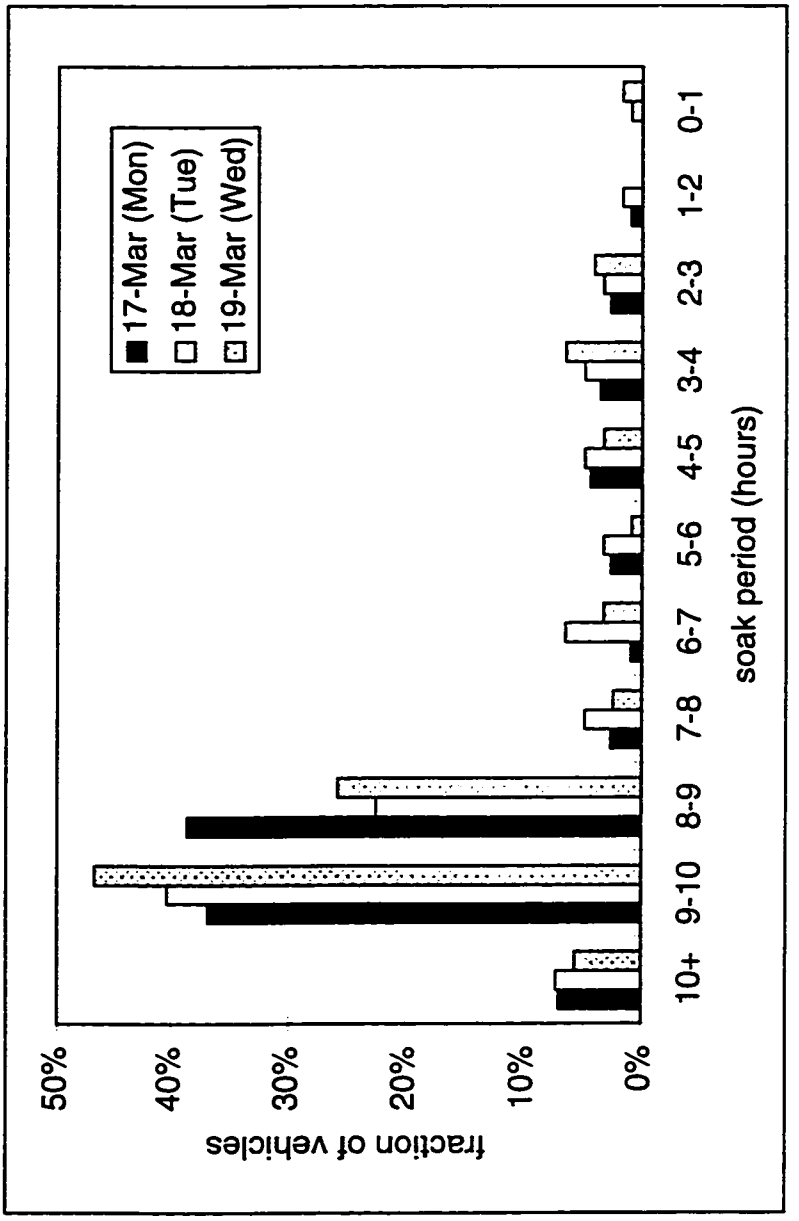

Figure 3.1. Distribution of soak times for vehicles parked in the garage. Soak time refers to the amount of time a vehicle was parked in the garage.

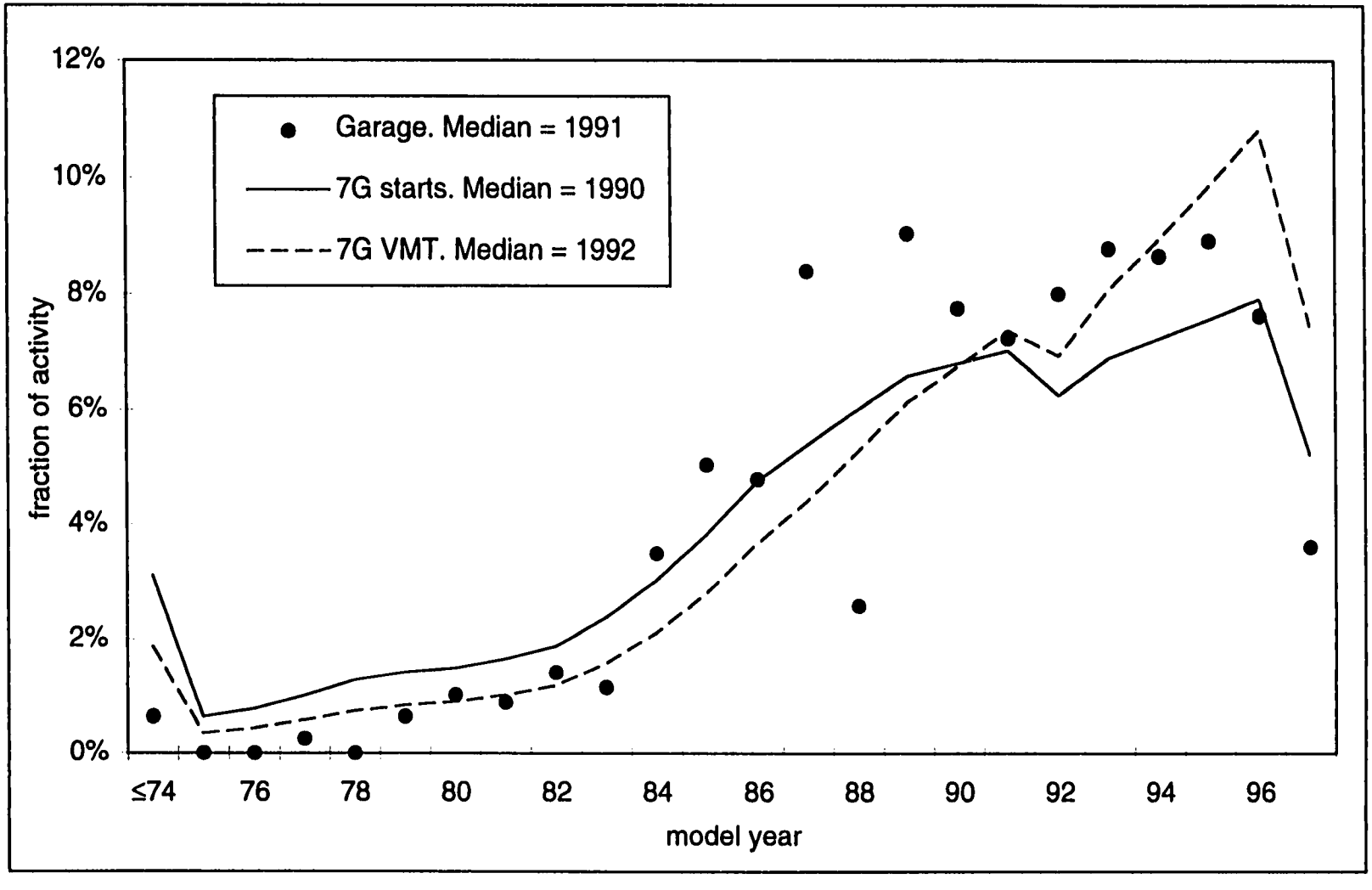

Figure 3.2. Age distributions of vehicles parked in the garage and for the overall Bay Area fleet, as estimated in the MVEI 7G model.

garage for ~80 s on average following ignition. In the morning, vehicles reached their assigned parking spaces in 29±2 s after arriving on their assigned level. During morning periods, vehicles parking on level 3 spent 25±1 s driving through level 2 and an additional ~10 s on the ramp between levels 2 and 3. Since speeds were similar and no significant traffic back-ups were observed during any morning or afternoon period, these observations confirm that, on average, vehicles spent an additional ~10-15 s in idle during afternoon periods.

3.4.2 Pollutant Concentrations

Average pollutant concentrations measured during each sample period are presented in Table 3.1. In this table, methane and non-methane hydrocarbon (NMHC) concentrations are reported separately. Except for methane, all pollutant levels were much higher in garage exhaust air than in background air. Background pollutant concentrations were similar for most morning and afternoon periods, except on the mornings of March 13 and 19, when background concentrations of CO_2, CO, NO_x, and NMHC were elevated. CO_2 levels inside the garage were similar during morning and afternoon periods. However, after accounting for differences between morning and afternoon background CO_2 levels, ΔCO_2 values were higher during afternoon periods (190±26 ppm) compared to morning periods (144±14 ppm). Since ventilation settings and vehicle counts were similar during morning and afternoon periods, the higher ΔCO_2 suggests that more fuel was burned per vehicle in the afternoon. This may be attributed to two factors: increased fuel consumption rate during the period of fuel enrichment at ignition, and the longer vehicle trip times during afternoon periods as compared to morning periods. Garage CO and NO_x

levels were much higher in afternoon periods as a result of increased emissions of these pollutants during cold start. In contrast, NMHC concentrations in the garage were similar during morning and afternoon periods. While exhaust NMHC emissions were expected to be higher during afternoon periods due to cold start, morning NMHC samples included hot soak evaporative emissions in addition to exhaust emissions.

The composition of volatile organic compound (VOC; includes both hydrocarbons and carbonyls) emissions measured during morning and afternoon periods is presented in Table 3.3. The morning profile represents a mix of stabilized running and hot soak evaporative emissions. The afternoon profile represents cold start running emissions for the garage fleet. The composition of stabilized running VOC emissions measured at the nearby Caldecott tunnel during August 1996 (Kirchstetter, 1998) is also presented in Table 3.3. Running emissions are composed primarily of tailpipe exhaust, but include evaporative losses. Overall, the garage cold start and tunnel stabilized running profiles are similar. The weight fractions of most compounds are similar in the two profiles, and the same compounds (methane, 2-methylbutane, ethene, toluene, xylene, and MTBE) are most abundant in both profiles. The lower methane and higher acetylene fractions in the cold start profile are consistent with the reduced catalyst activity expected during cold start (Jackson, 1978; Black et al., 1980; Lonneman et al., 1986). However, the acetylene fraction measured in garage cold start sampling is still much lower than that measured from fleets of non-catalyst vehicles (Lonneman et al., 1974; Jackson, 1978; Harley et al., 1992). Higher abundances of 2-methylbutane and n-butane in garage cold start samples likely result from the increased presence of these compounds in higher vapor pressure gasoline sold during winter months as compared to the summertime gasoline in use during

Table 3.3. Measured VOC speciation profiles (wt % VOC).

Species	Morning Hot soak + stabilized running[a]	Afternoon Cold start running[a,b]	Caldecott '96 Stabilized running
methane	5.99±2.86	5.37±1.31	9.09±1.25
ethane	0.30±0.17	0.52±0.03	0.92±0.28
propane	0.29±0.06	0.61±0,08	0.12±0.04
n-butane	6.79±1.41	3.18±0.72	1.12±0.13
n-pentane	2.63±0.10	1.83±0.16	2.27±0.18
n-hexane	1.31±0.06	1.33±0.05	1.16±0.10
n-heptane	0.96±0.10	1.02±0.03	0.79±0.09
n-octane	0.62±0.08	0.70±0.04	0.35±0.14
n-nonane	0.20±0.05	0.17±0.02	0.19±0.08
2-methylpropane	1.19±0.34	0.42±0.21	0.28±0.04
2-methylbutane	10.11±0.73	5.91±0.91	8.95±0.80
2-methylpentane	5.32±0.45	4.21±0.18	2.87±0.37
3-methylpentane	3.17±0.23	2.50±0.05	1.70±0.13
2-methylhexane	0.40±0.04	0.42±0.04	0.98±0.09
3-methylhexane	1.08±0.13	1.14±0.08	1.10±0.08
C8+ monosub. alkanes	1.30±0.29	1.48±0.07	0.92±0.10
2,2-dimethylbutane	1.77±0.17	1.19±0.08	0.78±0.06
2,3-dimethylbutane[c]	1.75±0.12	1.13±0.06	0.79±0.31
dimethylpentanes	0.41±0.03	0.37±0.05	0.82±0.07
dimethylhexanes	0.23±0.04	0.27±0.06	0.78±0.28
dimethylheptanes	0.24±0.11	0.26±0.08	0.57±0.10
dimethyloctanes	0.27±0.22	0.22±0.06	0.18±0.02
2,2,4-trimethylpentane	2.11±0.13	2.01±0.07	2.42±0.18
2,3,4-trimethylpentane	1.00±0.07	0.94±0.04	0.81±0.09
cyclopentane[c]	0.46±0.03	0.30±0.02	0.21±0.08
cyclohexane	0.49±0.05	0.48±0.04	0.84±0.07
methylcyclopentane	2.92±0.16	2.68±0.07	2.38±0.14
methylcyclohexane	0.54±0.04	0.56±0.19	0.78±0.32
other C5-C9 alkanes	0.41±0.10	0.57±0.18	0.17±0.07
C10+ alkanes	0.47±0.14	0.22±0.06	0.64±0.15
ethene	2.03±0.71	6.02±0.35	5.67±1.04
propene	1.21±0.19	3.20±0.18	3.33±0.43
1-butene/isobutene	1.37±0.32	2.75±0.38	3.43±0.37
c/t-2-butene	0.70±0.14	0.64±0.07	0.64±0.14
1,3-butadiene[d]	0.24±0.05	0.73±0.02	0.45±0.10
1-pentene	0.24±0.17	0.21±0.05	0.13±0.03
c/t-2-pentene	0.39±0.04	0.29±0.05	0.37±0.06
other C5 alkenes	1.00±0.31	0.84±0.15	1.03±0.24

Table 3.3. continued.

Species	Morning Hot soak + stabilized running[a]	Afternoon Cold start running[a,b]	Caldecott '96 Stabilized running
C6+ alkenes	0.75±0.03	0.78±0.08	1.29±0.25
acetylene	1.06±0.11	3.66±0.28	2.64±0.25
benzene	1.44±0.12	2.30±0.11	3.03±0.27
toluene	7.76±0.62	9.20±0.31	7.70±0.32
ethylbenzene	1.12±0.19	1.36±0.04	1.12±0.05
styrene	0.06±0.01	0.19±0.01	0.28±0.04
m/p-xylene	4.75±0.43	5.80±0.22	4.57±0.25
o-xylene	1.96±0.40	2.09±0.07	1.56±0.07
iso- & n-propylbenzene	0.30±0.07	0.31±0.03	0.31±0.04
m/p-ethyltoluene	0.64±0.11	0.77±0.06	1.86±0.08
o-ethyltoluene	0.40±0.14	0.49±0.06	0.33±0.04
1,2,4-trimethylbenzene	1.91±0.34	2.08±0.21	1.50±0.12
1,2,3-trimethylbenzene	0.31±0.15	0.38±0.15	0.22±0.01
1,3,5-trimethylbenzene	0.55±0.20	0.53±0.11	0.00±0.00
diethylbenzenes	0.97±0.50	0.96±0.33	0.38±0.10
other C10+ aromatics	1.07±0.38	1.02±0.26	0.71±0.19
MTBE	8.10±8.31	5.66±0.58	4.96±0.66
formaldehyde	0.41±0.06	0.75±0.01	1.98±0.31
acetaldehyde	0.13±0.02	0.38±0.04	0.33±0.03
other carbonyls	0.51±0.09	0.96±0.19	1.53±0.24
unidentified	3.87±2.16	3.61±2.14	3.36±2.05

(a) Mean ± 1 standard deviation of the compound weight percent from 5 sample periods.

(b) Based on analysis of canister samples collected during afternoon periods, when 93% of the vehicles were operating in cold start mode.

(c) 2,3-dimethylbutane coeluted with cyclopentane. The peak was resolved to 79% 2,3-dimethylbutane and 21% cyclopentane.

(d) The number shown here is a lower limit; 1,3-butadiene was not stable in the stainless steel canisters.

the Caldecott tunnel study. By contrast, the weight fractions of methylpentanes and n-pentane are higher in the VOC profile measured at the Caldecott tunnel during summer 1996. The cold start profile indicates a higher ratio of C_7+ aromatics to benzene compared to stabilized emissions. The increased C_7+ aromatics to benzene ratio suggests a larger fraction of unburned fuel in the cold start profile. The combined weight fractions of formaldehyde and acetaldehyde are much lower during cold start than during stabilized driving. This difference results from reduced aldehyde production during the fuel-rich period following ignition, and because combustion products are reduced relative to unburned fuel in the cold start profile.

Morning VOC emissions include larger fractions of fuel components such as n-butane, n-pentane, 2-methylpropane, and 2-methylbutane, and smaller fractions of combustion-derived compounds such as ethene, propene, and formaldehyde. These differences are consistent with the presence of hot soak evaporative emissions during morning sampling periods.

Morning NMHC emissions were apportioned to stabilized running and hot soak evaporative contributions using the chemical tracer approach described below:

$$f_{st} = \frac{w_{i,g}}{w_{i,st}} \tag{3.2}$$

where f_{st} represents the fraction of garage NMHC attributable to stabilized running emissions, $w_{i,g}$ is the weight fraction of species i in garage NMHC emissions and $w_{i,st}$ is the weight fraction of species i in stabilized running emissions measured at the Caldecott tunnel in summer 1996 (Kirchstetter, 1998). This chemical tracer approach was used only with the combustion-derived species ethane, ethene, acetylene, and propene that are

present in exhaust but absent from evaporative emissions. Results of the apportionment are summarized in Table 3.4, which shows that 33-40% of morning NMHC were attributed to stabilized running emissions; the balance was attributed to hot soak evaporative emissions.

Emission factors were calculated for each sample period using eq 3.1 and the time-averaged pollutant concentrations from Table 3.1; these emissions factors are shown in Table 3.5. California Phase 2 reformulated gasoline properties ρ_f=743 g L^{-1} and w_c=0.85 were determined from an analysis of gasoline purchased from all of the major suppliers in the Bay Area during summer 1996 (Kirchstetter, 1998). By convention, NO_x emission factors were calculated using a molecular mass of 46 g mol^{-1}. HC emissions were calculated using a molecular mass of 14 g mol^{-1} C. Emissions of each pollutant were very consistent from day to day, which is expected since many of the same vehicles were measured each day.

Table 3.4. Apportionment of hydrocarbon emissions to exhaust and evaporative sources.

Tracer species	wt % NMHC[a]	Exhaust contribution to total NMHC[b]				
		12-Mar	13-Mar	17-Mar	18-Mar	19-Mar
Ethene	6.5	42%	13%[c]	36%	41%	36%
Acetylene	3.0	38%	44%	34%	38%	34%
Ethane	1.1	43%	39%	34%	42%	36%
Propene	3.8	35%	32%	29%	34%	29%
Mean		40%	38%[c]	33%	39%	34%

(a) Weight fraction of species in hot stabilized exhaust emissions measured at Caldecott tunnel in Summer, 1996. From Kirchstetter (1998).

(b) Fraction of total parking garage NMHC emissions attributed to tailpipe exhaust, estimated using a tracer species and eq 3.2.

(c) The weight fraction of ethene in VOC measured on March 13 was significantly lower than for all other sampling days; the exhaust contribution to NMHC on this day was calculated using the average results from acetylene, ethane, and propene as exhaust tracers.

Emission factors from morning and afternoon sample periods were extrapolated by linear regression to 0% and 100% hot stabilized driving. The resulting cold start and hot stabilized emission factors, shown in Table 3.5, are only slightly different than the emission factors measured during afternoon and morning periods. Cold start emission estimates were further adjusted to account for differences between emission levels averaged over the full cold start period and those of the first 60 s (i.e., the period measured in the parking garage), as described in the next section.

Table 3.5. Exhaust emission factors in morning and afternoon sample periods.

Date	CO ($g\ L^{-1}$)	NO_x ($g\ L^{-1}$)	NMHC ($g\ L^{-1}$)	Stabilized fraction[a]
	Morning sample periods			
11-Mar	70	2.7	N/A	94%
12-Mar	68	2.9	6.6	93%
13-Mar	61	3.1	6.4	N/A
17-Mar	64	2.1	5.1	95%
18-Mar	67	2.3	6.6	89%
19-Mar	68	3.1	6.3	94%
	Afternoon sample periods			
10-Mar	178	8.4	N/A	6%
11-Mar	181	7.6	17.3	7%
13-Mar	152	7.3	18.1	6%
17-Mar	158	6.3	15.9	5%
18-Mar	169	6.4	17.9	5%
19-Mar	170	6.5	18.5	7%
AM mean[b]	66±3	2.7±0.4	6.1±0.5	(93±2)%
PM mean[b]	168±11	7.1±0.8	17.5±1.0	(6±1)%
Stabilized[c]	59±5	2.3±0.3	5.0±0.4	100%
Cold start[c]	175±4	7.4±0.3	18.3±0.3	0%
Full cold start[d]	119±8	10.2±1.3	13.0±0.7	

(a) Fraction of active vehicles in hot stabilized operating mode.
(b) Mean ± standard error of morning and afternoon emission factors.
(c) Results of linear regression analysis (see text).
(d) Cold start emission factors adjusted to reflect the average emissions over the full cold start period, estimated to last for ~ 200 s (see text).

3.5 DISCUSSION

To interpret and use the emissions measurements from the parking garage, more information is required about vehicle operation during cold start. First, it is important to quantify the time period over which high cold start emissions levels fall to the lower levels characteristic of stabilized operation. With this knowledge, the cold start emission factors measured in the garage can be related to emissions during the full cold start period. Second, since one of the objectives of this study is to compare garage results with the gram per start emission factors of MVEI 7G, an estimate of the average fuel used during start mode is required (recall that emission factors measured in the garage were expressed in g L^{-1} units). The ensuing discussion of cold start emissions, and the estimation of fuel use during cold start, are based on analyses of available dynamometer emissions data.

3.5.1 Fuel use during cold start

The average second-by-second emissions of twenty 1993-94 model year light-duty vehicles measured during the cold start portion of the Federal Test Procedure (FTP) (Haskew et al., 1994) are plotted in Figure 3.3. The fuel-normalized emission factors presented in Figure 3.3 were calculated using eq 3.1 and exhaust pollutant concentrations measured during each second of the dynamometer test. Although these were not in-use vehicles, their catalytic converters were aged to simulate 50,000-160,000 km of driving. Prior to testing, vehicles were conditioned for a minimum of 12 hours at an ambient temperature of ~20 °C. In Figure 3.4, catalyst temperature is plotted against time and cumulative fuel use for three of the vehicles; recall that the catalyst must reach operating temperatures of 200-400 °C before significant pollutant conversion occurs.

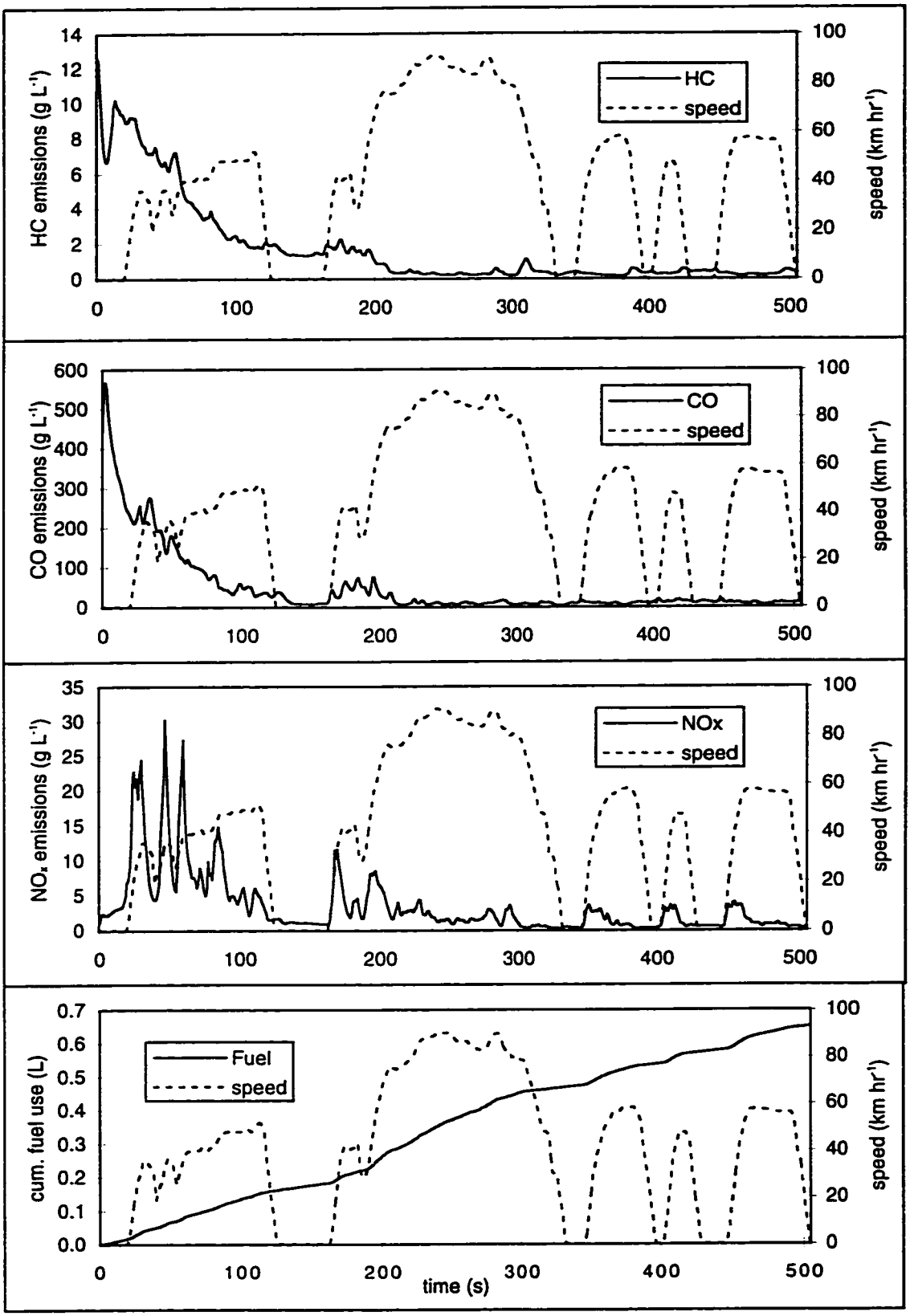

Figure 3.3. Average second-by-second emissions of 20 1993-94 model year vehicles tested on FTP cold start cycle. Data from testing described in Haskew et al. (1994).

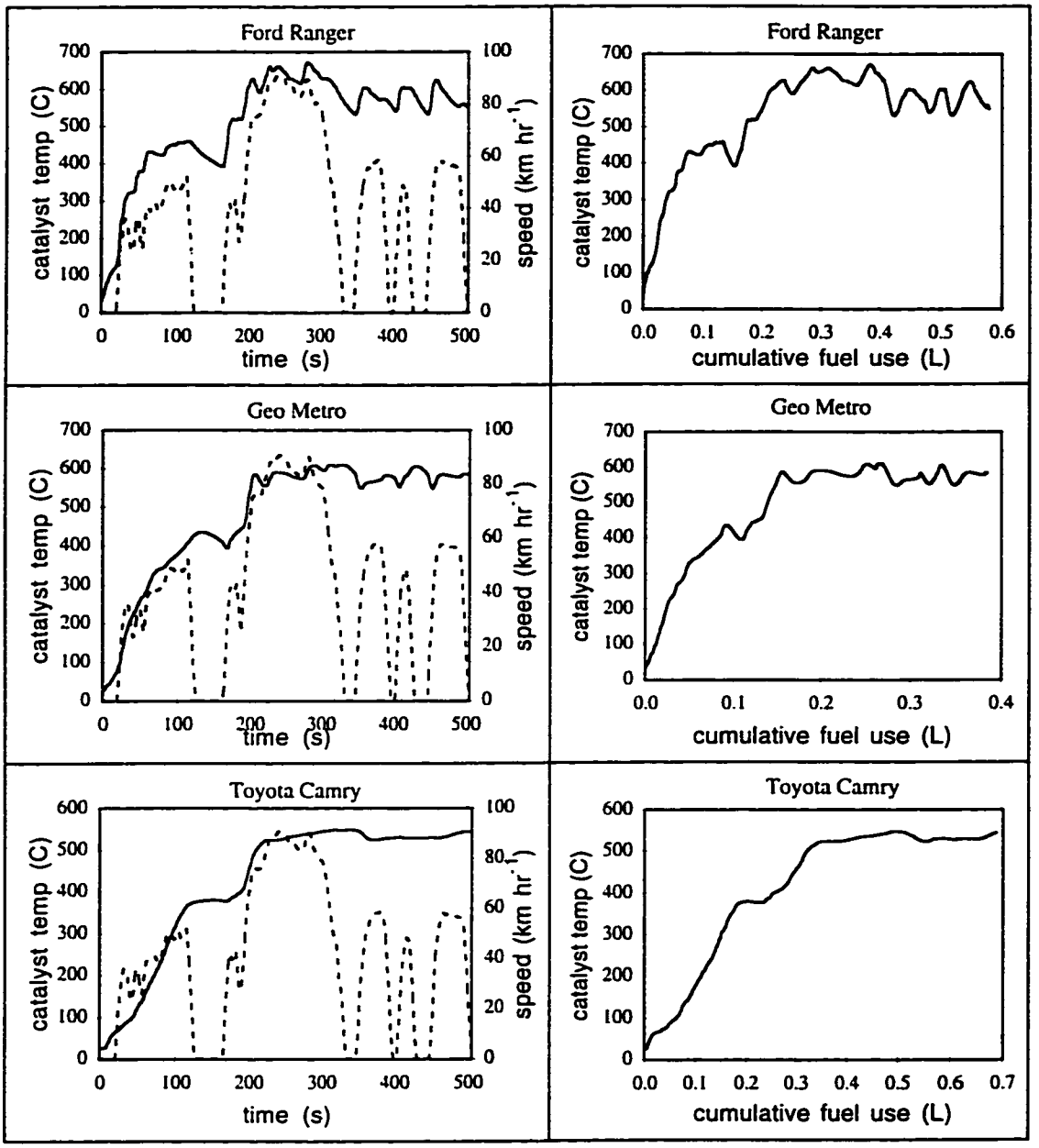

Figure 3.4. Second-by-second FTP data described in Haskew et al. (1994) which shows that heating of the catalyst to operating temperatures of 200-400 C is roughly linearly related to both fuel use and elapsed time.

The FTP cold start emissions profiles shown in Figure 3.3 begin with sharp HC and CO peaks which result from fuel enrichment at ignition. NO_x emissions remain relatively low during this period (0-20 s) even though the catalyst is ineffective. CO and HC emissions drop quickly through the first 80-100 s, as the catalyst warms rapidly. Catalyst temperature, HC and CO emissions then remain approximately constant through the extended idle period beginning at ~125 s. Within 200-220 s, the vehicles' catalysts have reached stable high temperatures and emissions of HC and CO drop to their stabilized values, as shown in Figures 3.3-3.4. In contrast to the smoother CO and HC profiles, NO_x emissions are characterized by sharp peaks at each acceleration event. These peaks are highest during the first 80-100 s, moderate during the acceleration to >80 km hr^{-1} (165-210 s), then roughly constant in magnitude after about 210 s.

Figure 3.3 shows that while emissions are much higher during cold start driving than after vehicles have warmed to stabilized operation, there is no single emissions level that persists throughout the cold start period. It is therefore important to identify clearly the period over which cold start emissions are averaged.

Figure 3.4 shows that in the FTP cycle, heating of the catalyst to effective operating temperatures is approximately linearly related to both elapsed time and cumulative fuel use. Results from a recent Environmental Protection Agency (EPA) study (Enns and Brzezinski, 1997) comparing incremental start emissions during the first 298 s of the CARB LA92 (Unified) cycle and the EPA ST01 cycle suggest that the relationship between catalyst warm-up and fuel use may be independent of the test cycle. The speed vs. time trace of the two cycles are plotted in Figure 3.5a; Figures 3.5b-3.5c show the HC and CO emissions vs. fuel use for a 1984 Oldsmobile driven through the two cycles.

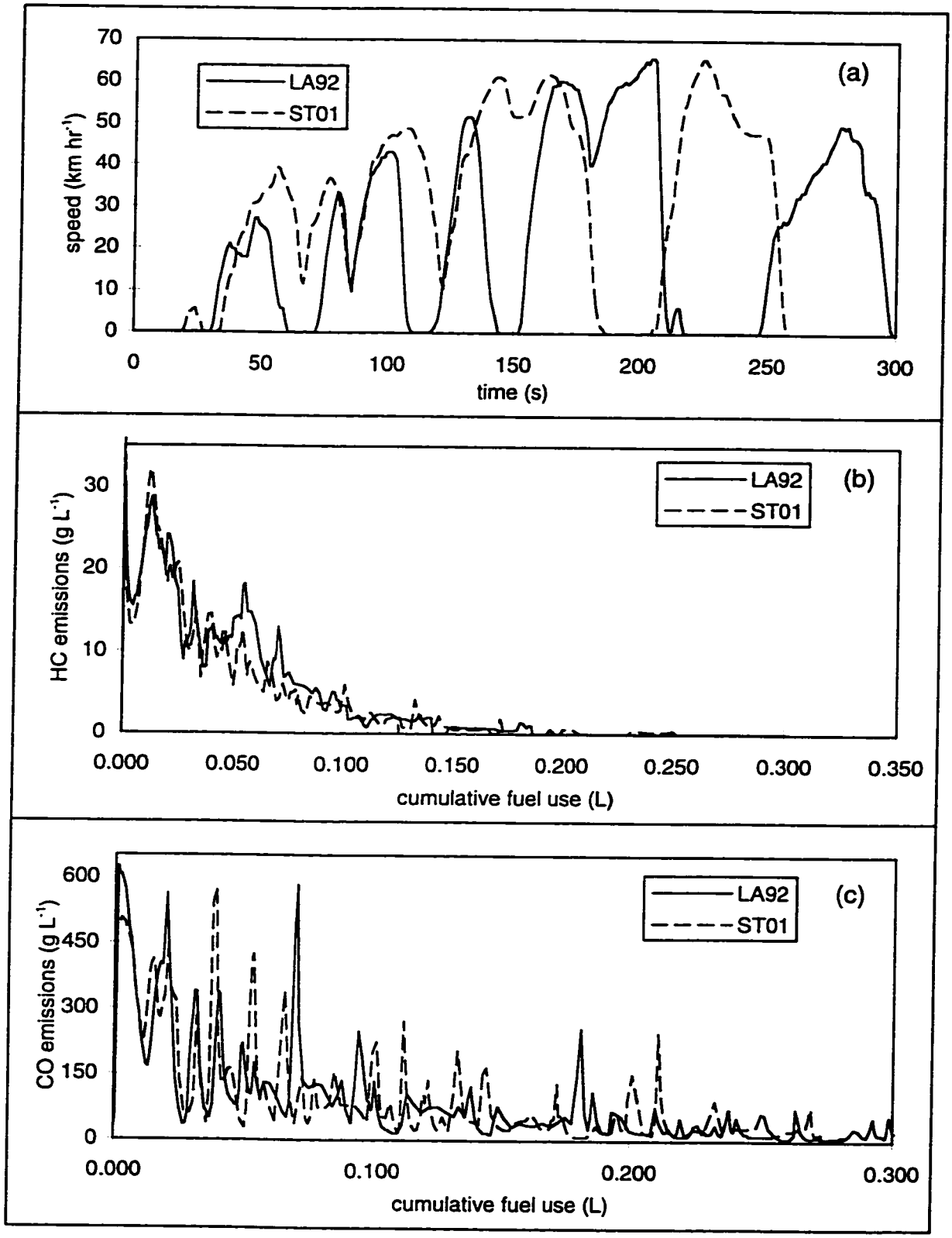

Figure 3.5. Cold start data for a 1994 Oldsmobile Achieva tested on EPA ST01 and CARB LA92 cycles. Data from testing described in Enns et al. (1997).

Reductions in HC and CO emissions indicate increasing catalyst effectiveness as cumulative fuel use increases. By the time that ~0.15 L of gasoline have been consumed in each test, HC and CO emissions have reached their stabilized levels. While the emissions vs. fuel use relationships are similar for the two cycles, it must be noted that the early portions of the two driving cycles are also similar. Each cycle begins with ~30 s of idle, followed by an acceleration to ~25-40 km hr^{-1} and a deceleration event; Figures 3.5b-3.5c show that by the end of this period, emissions have reached very low levels, indicating that much of the catalyst heating has already occurred. Testing of additional vehicles on driving cycles with shorter initial idle periods and different speed traces is needed to examine further the relationship between catalyst heating and fuel use.

3.5.2 Calculation of gram/start emission factors

The preceding discussion shows that the cold start period may be characterized by the amount of fuel which must be consumed before stabilized engine and catalyst operating temperatures are reached. If this fuel use is multiplied by the average g L^{-1} emission factor for the same period, an estimate of the total grams of pollutant emitted per start may be calculated. Real-world cold start and hot stabilized emission factors were measured in the parking garage and are presented in Table 3.5. Fuel use was estimated by analyzing a subset of emissions data from California's 12th light-duty vehicle surveillance program (Devesh, 1994). The ongoing surveillance program recruits for emissions testing a sample of California in-use vehicles; results of the testing provide the basis for emission factors used in the MVEI model. In the present study, second-by-second emissions data were analyzed for 82 in-use vehicles tested on the LA92 driving cycle during 1992. The mean and median model year of the vehicle sample was 1987, the mean odometer reading

was 86,000 miles, and ~25% of the vehicles were light-duty trucks. Neither catalyst temperature nor catalyst efficiency were measured during the program; the end of cold start was therefore inferred from the emissions data.

The use of emissions data from surveillance program vehicles requires some explanation. As discussed in the first two chapters, the vehicle fleet which is successfully recruited to the surveillance program does not appear to be entirely representative of the overall in-use fleet. Average emissions of the surveillance program test fleet are lower, on average, than emissions of the in-use fleet. For the current study, surveillance program data are used to determine the average amount of time that vehicles spend in cold start mode. The duration of cold start depends upon the heating of the catalyst and oxygen sensor to operating temperatures, and is therefore most relevant for vehicles with properly-functioning emissions controls. In contrast to fleet-average stabilized emission levels which are most influenced by high-emitting vehicles, the average cold start period is determined by the characteristics of properly-functioning vehicles.

Figure 3.6 shows the average HC, CO, and NO_x emission factors of the 82 vehicles during each of the first 850 s of the LA92 driving cycle. A cumulative plot of average second-by-second fuel use is also included in this figure. In contrast to the FTP cold start test, the early portion of the LA92 cycle includes harder accelerations and more high-speed driving; as a result, emissions data for the LA92 cycle fluctuate more than for the FTP (compare Figures 3.3 and 3.6). Nevertheless, Figure 3.6 shows that, on average, cold start effects ended after ~200 s of operation for the surveillance program vehicles; during this period, average fuel use was ~0.26 L.

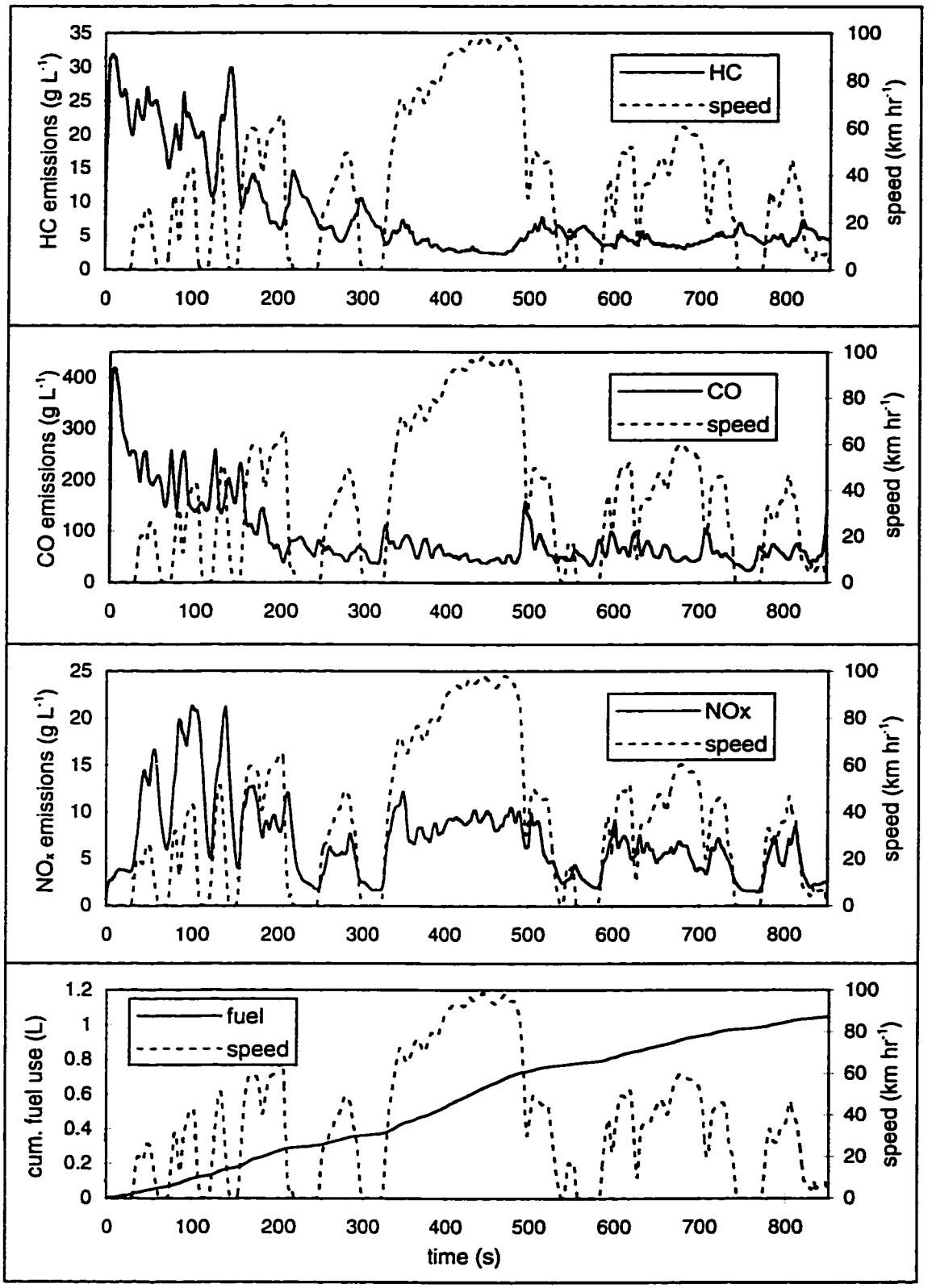

Figure 3.6. Average second-by-second emissions of 82 light-duty vehicles tested on CARB LA92 cycle. Data from testing described in Devesh et al. (1994).

To verify that most of the cold start effects had occurred within the first 200 s, stabilized emission factors were estimated from a later portion of the driving cycle (550-850 s) which has a speed vs. time trace similar to the first part of the LA92 test. Average emissions during this period were 59 g L^{-1} CO, 4.4 g L^{-1} HC, and 5.2 g L^{-1} NO_x. These stabilized emissions levels are lower than emissions during the 200 s cold start period by factors of 3, 4, and 2 for CO, HC, and NO_x, respectively. Total excess mass emissions, M, for the cold start portion of the cycle were calculated using the following formula:

$$M = \sum_{i=1}^{300} (E_i - E_s) f_i \tag{3.3}$$

where E_i and f_i represent the average instantaneous g L^{-1} emissions and fuel use of all 82 vehicles measured during each of the first 300 s and E_s was the average stabilized emission level (in g L^{-1} units) measured during the period 550-850 s. Using this approach, it was verified that 94% of excess HC, 100% of excess CO, and 96% of excess NO_x emissions occured during the first 200 s of operation for the surveillance program vehicle fleet.

The argument that cold start duration is determined by the properly-functioning vehicles in a fleet is supported by repeating the above analysis for the "clean" fleet of vehicles whose emissions are shown in Figure 3.3. For these vehicles, ~0.26 L of fuel was used and most of the cold start effects occurred within the first 200 s. Average cold start duration for the surveillance program fleet – which includes some, but perhaps not enough high-emitters to represent the in-use fleet – was identical to the average cold start duration of a fleet which included no high-emitters. It is thus assumed that average cold start duration for the in-use fleet is well approximated by the same value.

Emission factors measured in the parking garage corresponded to the first ~40 s and ~80 s of operation for vehicles parked on levels 2 and 3, respectively. For the

surveillance program vehicles, average emissions during the full 200 s cold start period were lower than emissions averaged over the first 60 s (corresponding to the average period over which vehicles were measured in the garage) by factors of 0.71 for HC and 0.68 for CO; average NO_x emissions during the full 200 s were *higher* than during the first 60 s by a factor of 1.39. Cold start emission factors measured in the garage were scaled by these factors to calculate emission factors representative of the full 200 s cold start period; these are shown at the bottom of Table 3.5. Ideally, the scaling would be based upon the average amount of fuel used by vehicles during the time they were operated in the garage, rather than the time of vehicle operation. Incremental start emission factors were calculated as the difference between full cold start emission levels and the stabilized emission levels presented in Table 3.5. Incremental start emission factors (in g L^{-1} units) were then combined with the estimated cold start fuel consumption of 0.26 L to calculate exhaust emission factors of 2.1 g NMHC, 16 g CO, and 2.1 g NO_x per vehicle start.

3.5.3 Comparison to MVEI 7G

Figure 3.7 compares the gram per start emission factors derived from parking garage measurements to MVEI 7G model estimates for a catalyst-equipped fleet of 70% cars and 30% light-duty trucks. The MVEI 7G model was run for summer 1997 conditions to reflect the ambient air temperatures of ~20 °C at which vehicles soaked in the garage. The distribution of soak times measured in the garage was also specified for the model runs. MVEI 7G cold start emission factors are higher than those derived from parking garage measurements by factors of 1.8 for NMHC and 2.8 for CO, whereas MVEI 7G NO_x emission factors are comparable to those derived from parking garage measurements. This

suggests that incremental cold start NMHC and CO emissions may be overstated in current emission inventories.

3.6 CONCLUSIONS

This study demonstrated the use of an underground parking garage for the measurement of cold start emissions from large samples of in-use vehicles. Cold start emission factors of 18.3±1.0 g L^{-1} NMHC, 175±12 g L^{-1} CO, and 7.4±0.9 g L^{-1} NO_x were measured during the first ~40-80 s of vehicle operation in a parking garage in Oakland, California during March, 1997. Average fuel consumption during start mode was estimated to be ~0.26 L, based on an analysis of second-by-second emissions data from California's light-duty vehicle surveillance program. Incremental start emission factors of 2.1 g/start NMHC, 16 g/start CO, and 2.1 g/start NO_x were derived from the fuel use estimates and the emissions measured in the garage. These emission factor estimates are lower than MVEI 7G estimates by 45% for NMHC, 65% for CO, and 12% for NO_x. It appears that both the absolute magnitude and relative importance of cold start CO and HC emissions may be overstated in current vehicle emission inventories.

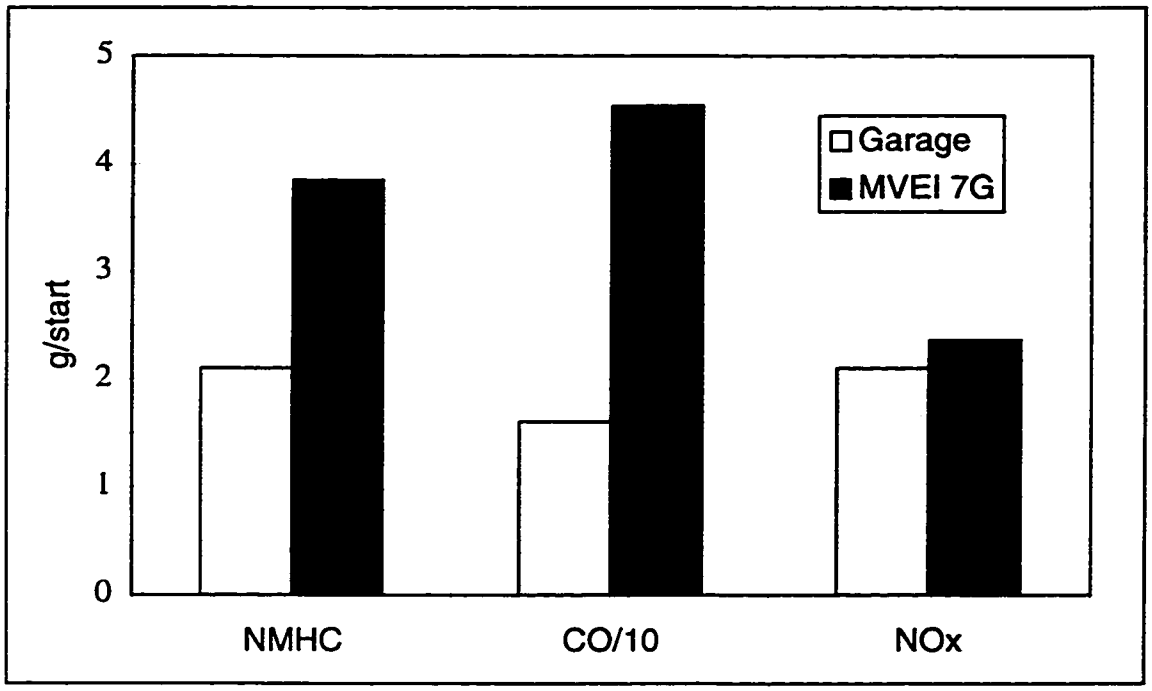

Figure 3.7. Comparison between incremental start emission factors calculated from garage measurements and those predicted by the MVEI 7G model.

3.7 REFERENCES

An, F., M. Barth, G. Scora and T. Younglove (1996). Catalyst cold-start characterization and modeling. *Sixth CRC On-Road Vehicle Emissions Workshop*, San Diego, CA, March 16-18, 1996. Coordinating Research Council, Atlanta, GA.

Black, F. M., L. E. High and J. M. Lang (1980). Composition of automobile evaporative and tailpipe hydrocarbon emissions. *J. Air Pollut. Control Assoc.* **30**:1216-1221.

Calvert, J. G., J. B. Heywood, R. F. Sawyer and J. H. Seinfeld (1993). Achieving acceptable air quality: some reflections on controlling vehicle emissions. *Science.* **261**:37-45.

CARB (1993). *Predicted California on-road motor vehicle emissions (BURDEN7F).* Mobile Source Emission Inventory Branch, California Air Resources Board, Sacramento, CA.

CARB (1996). *MVEI 7G, Version 1.0.* Technical Support Division, Mobile Source Emission Inventory Branch, California Air Resources Board, Sacramento, CA.

Devesh, S. (1994). *Test report of the light-duty vehicle surveillance program, series 12 (LDVSP 12).* Mobile Source Division, California Air Resources Board, El Monte, CA. MS-94-04.

Enns, P. and D. Brzezinski (1997). *Comparison of start emissions in the LA92 and ST01 test cycles.* Assessment and Modeling Division, Office of Mobile Sources, U.S. EPA, Ann Arbor, MI. M6.STE.001.

Fujita, E. M., B. E. Croes, C. L. Bennett, D. R. Lawson, F. W. Lurmann and H. H. Main (1992). Comparison of emission inventory and ambient concentration ratios of CO, NMOG, and NO_x in California's South Coast Air Basin. *J. Air Waste Manage. Assoc.* **42**:264-276.

Fung, K. (1997). *Personal Communication.* Atmospheric Assessment Associates, Inc., Calabasas, CA.

Fung, K. and D. Grosjean (1981). Determination of nanogram amounts of carbonyls as 2,4-dinitrophenylhydrazones by high-performance liquid chromatography. *Anal. Chem.* **53**:168-171.

Harley, R. A., M. P. Hannigan and G. R. Cass (1992). Respeciation of organic gas emissions and the detection of excess unburned gasoline in the atmosphere. *Environ. Sci. Technol.* **26**:2395-2408.

Haskew, H. M., K. Cullen, T. F. Liberty and W. K. Langhorst (1994). The execution of a cooperative industry/government exhaust emission test program. *1994 Convergence*

International Congress on Transportation Electronics, Dearborn, MI, SAE 94C016. Society of Automotive Engineers, Warrendale, PA.

Heywood, J. B. (1988). *Internal Combustion Engine Fundamentals*. McGraw-Hill Publishing Company: New York, NY.

Ingalls, M. N., L. R. Smith and R. E. Kirksey (1989). *Measurement of on-road vehicle emission factors in the California South Coast air basin. Volume I: regulated emissions*. Southwest Research Institute, San Antonio, TX.

Jackson, M. W. (1978). Effect of catalytic emission control on exhaust hydrocarbon composition and reactivity. *SAE Tech. Pap. Ser.* **780624**.

Kirchstetter, T. (1998). *Impact of reformulated fuels of motor vehicle emissions*. Ph.D. Dissertation, Department of Civil and Environmental Engineering, University of California, Berkeley, CA.

Kirchstetter, T. W., B. C. Singer, R. A. Harley, G. R. Kendall and W. Chan (1996). Impact of oxygenated gasoline use on California light-duty vehicle emissions. *Environ. Sci. Technol.* **30**:661-670.

Lonneman, W. A., S. L. Kopczynski, P. E. Darley and F. D. Sutterfield (1974). Hydrocarbon composition of urban air pollution. *Environ. Sci. Technol.* **8**:229-236.

Lonneman, W. A., R. L. Seila and S. A. Meeks (1986). Non-methane organic composition in the Lincoln tunnel. *Environ. Sci. Technol.* **20**:790-796.

Pierson, W. R., A. W. Gertler and R. L. Bradow (1990). Comparison of the SCAQS tunnel study with other on-road vehicle emission data. *J. Air Waste Manage. Assoc.* **40**:1495-1504.

CHAPTER FOUR

Scaling of Infrared Hydrocarbon Measurements

4.1 INTRODUCTION

The study of on-road motor vehicle emissions has been enhanced in recent years by the development of roadside long-path infrared spectrometers, commonly referred to as remote sensors (Bishop et al., 1989; Bishop and Stedman, 1990; Lawson et al., 1990; Stephens and Cadle, 1991; Stephens, 1994). Remote sensors measure the relative exhaust concentrations of carbon monoxide (CO), hydrocarbons (HC), and carbon dioxide (CO_2) as an infrared beam is projected across a roadway and through the tailpipe exhaust plume of each passing vehicle. By carbon balance, the CO/CO_2 and HC/CO_2 ratios measured by a remote sensor can be converted to fuel-normalized mass emission rates, e.g. gram of pollutant emitted per liter of fuel burned. Chapter 2 demonstrated how the emission factors measured with remote sensors can be combined with fuel sales data to calculate CO emission inventories at the air-basin or regional level. In principle, fuel-based inventories may be calculated for pollutants other than CO if representative emissions

---

Derived with permission from Singer, B.C., Harley R.A., Littlejohn, D., Ho, J., and Vo, T. (1998). Scaling of infrared remote sensor hydrocarbon measurements for motor vehicle emission inventory calculations. *Environ. Sci Technol.* 32: 3241-3248. ©1998 American Chemical Society.

data are available. The fuel-based inventory technique has not been applied to estimate total volatile organic compound (VOC) emissions because of concerns that infrared sensors understate VOC concentrations in motor vehicle exhaust (Stephens et al., 1996).

Remote sensors measure HC concentrations based on energy absorption within a narrow infrared band centered at a frequency of 2940 cm^{-1}, corresponding to a wavelength of 3.4 μm (Guenther et al., 1995). The absorption spectrum of an interference filter similar to those used in the University of Denver remote sensors is shown in Figure 4.1 (3.4 μm filter). Absorption in this region of the infrared is associated with vibrational frequencies, or stretching, of carbon-hydrogen bonds. The C-H bonds of paraffinic carbons absorb strongly within the range of wavelengths passing through the filter, whereas the C-H bonds of olefinic and aromatic carbons absorb at slightly higher frequencies: in the ranges of 3010-3040 cm^{-1} and 3075-3095 cm^{-1} for olefins, and at 3030 cm^{-1} for aromatics (Bellamy, 1958). When calibrated with an alkane such as propane or hexane, an infrared detector with a 3.4 μm filter will therefore understate total HC concentrations relative to FID measurements of mixtures containing alkenes and aromatics. In contrast, it has long been known that the response per carbon atom of a flame ionization detector is approximately the same for all HC (Harris, 1991).

The response of a non-dispersive infrared (NDIR) analyzer to individual organic compounds present in vehicle exhaust was first reported by Jackson (1966). Using a hexane detector (i.e. a filter that passes infrared radiation between 3.3 and 3.5 μm, where hexane absorbs strongly), Jackson observed a measurement response close to 1.0 for

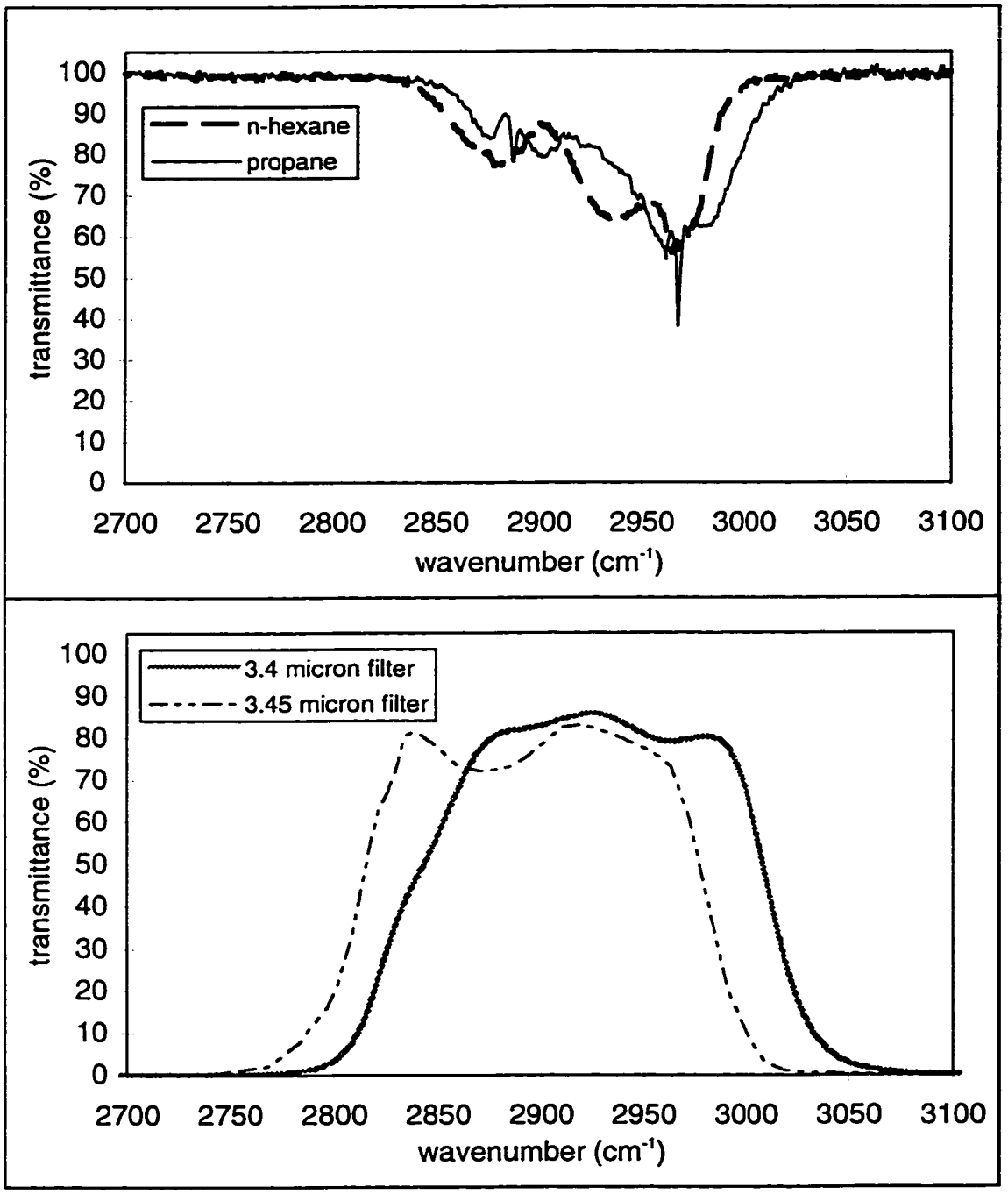

Figure 4.1. Infrared transmission profiles of propane, n-hexane, and filters used in infrared HC analyzers. Note that the magnitude of absorption will vary with concentration and path length.

several alkanes, alkene responses ranging from 0.09 for ethene to 0.61 for 1-hexene, and near-zero response for benzene and toluene. Stephens et al. (1996) measured concentrations of individual organic compounds using high- and low-range commercial NDIR analyzers mounted on-board a test vehicle, a General Motors (GM) remote sensor with a 3.4 μm filter, an older version of the Denver University remote sensor with a 3.3 μm filter, and an FID. The ratio of infrared sensor to FID reading was termed the response factor for each compound. Table 4.1 lists the individual organic compound response factors measured by Stephens et al. using a Horiba MEXA-324GE NDIR analyzer and the GM remote sensor. The relative responses of alkanes, alkenes, and aromatics measured by Stephens et al. were consistent with those measured by Jackson. Stephens et al. used the same suite of instruments to measure exhaust VOC concentrations for two modern technology vehicles operated in a series of simulated failure modes. The authors noted that the exhaust VOC concentrations measured by NDIR would need to be scaled up by factors ranging from 1.5 to 4.4 to be consistent with FID measurements (Stephens et al., 1996).

The objective of the work presented in this chapter was to develop and demonstrate an approach for scaling infrared remote sensor measurements to represent total exhaust VOC emissions. Scaling factors presented in this study can be used to adjust fleet-average emissions measured by infrared HC remote sensors to calculate fleet-average VOC emission factors for motor vehicle emission inventory calculations.

Table 4.1. IR/FID response factors measured by Stephens et al. (1996).

Compound	On-board NDIR analyzer	GM remote sensor (3.4 μm filter)	Denver Univ. remote sensor (3.3 μm filter)
Methane	0.15±0.003	0.26±0.043	0.35±0.044
Propane	1.01-1.09	0.94-1.08	0.91-1.02
n-Butane	1.11±0.015	0.99±0.061	0.94±0.033
Iso-octane	0.85±0.022	0.76±0.091	0.70±0.060
MTBE	0.89±0.016[a]	0.77±0.137[a]	0.86±0.033[a]
Ethene	0.05±0.001	0.08±0.030	0.10±0.008
Propene	0.29±0.004	0.29±0.024	0.31±0.037
Iso-butene	0.51±0.007	0.46±0.034	0.44±0.039
Toluene	0.08±0.005	0.07±0.047	0.11±0.031
o-Xylene	0.14±0.002	0.21±0.236	0.13±0.057

(a) MTBE values reported by Stephens et al. (1996) do not account for partial response when MTBE is measured by FID.

4.2 APPROACH

Infrared response factors were measured for 31 individual organic compounds which together account for >60% of fleet-composite motor vehicle exhaust VOC emissions, as measured on-road (Kirchstetter, 1998). Special attention was given to branched alkanes, cycloalkanes, and C_9 aromatics whose response factors have not been reported previously. These measurements were used to calculate coefficients for a linear regression model which relates infrared absorption to the number and types of C-H bonds in a molecule. The regression model was used to predict response factors for additional exhaust VOC constituents. Since vehicle exhaust contains more than 150 identifiable, individual organic compounds — most of which are present at levels below 0.5% of total VOC mass — each individual compound was assigned to one of 20 response factor

groups. Compounds were grouped by structural characteristics which affect infrared absorption, and by their model-predicted response factors. Several important exhaust components, including methane, ethane, ethene, propene, isobutene, acetylene, benzene, toluene, and MTBE, were treated explicitly as individual species.

Group response factors (RF_g) were combined with speciated VOC measurements to predict response factors (RF_m) for vehicle exhaust mixtures as follows:

$$RF_m = \sum_g \left(RF_g \times c_g \right) = \sum_g \left(RF_g \times w_g \right) \tag{4.1}$$

where c_g is the fraction of total organic carbon contributed by all of the organic compounds assigned to group g, and w_g is the weight fraction of total VOC contributed by the organic compounds in group g. Use of w_g versus c_g in eq 4.1 gives similar results because weight fractions and carbon fractions are nearly identical for individual vehicle exhaust hydrocarbons. Strictly speaking, however, eq 4.1 should be applied using carbon fractions (c_g) since NDIR/FID response factors are based on carbon counts.

The accuracy of eq 4.1 was verified experimentally by collecting simultaneous IR and FID measurements of total VOC concentrations in real vehicle exhaust samples. Speciated VOC profiles measured from the same exhaust samples were used to predict, with eq 4.1, the IR/FID ratio measured for each sample. VOC speciation profiles measured in recent tunnel studies were then used to calculate overall IR/FID response factors for on-road vehicle fleets using conventional and reformulated gasolines. Inverting these response factors yields FID/IR ratios which can be used to scale infrared HC remote sensor measurements to correspond to FID-based measurements. The approach is

demonstrated for a "fleet" of 20 high-emitting vehicles recruited from an Orange County, CA roadway (Cadle et al., 1996).

4.3 EXPERIMENTAL

4.3.1 Measurement of Individual Compound Infrared Response Factors

Infrared response factors were determined by measuring with FID and an infrared spectrometer the concentrations of individual organic compounds in prepared air samples. Samples of HC-free air and a 167 ppmv (500 ppmC) propane standard were also measured to obtain baseline readings and a span calibration point for each instrument. Individual compounds chosen for testing include those that contribute significantly to motor vehicle exhaust VOC emissions, and others that are structurally representative of major classes of VOC found in vehicle exhaust. A complete list of the organic compounds tested is presented in Table 4.2.

Air samples containing single organic compounds were prepared by volatilizing ~5 μL of pure liquid, or by mixing 5-15 mL of pure gas, into 20-liter Tedlar bags filled with 10-18 L of ultrapure hydrocarbon-free air (<0.01 ppmC, Scott-Marrin, Riverside, CA). Liquids were injected by syringe through a septum while the Tedlar bags were more than half full, but still filling with ultrapure air. Gaseous species were injected by gas-tight syringe while the bags were filling with ultrapure air. Each bag was then kneaded for several minutes to promote mixing and set aside for ~1 hr before being sampled. VOC

Table 4.2. Measured IR/FID response factors for individual organic compounds.

Compound	Measured response 3.4 μm filter[a]	Measured response 3.45 μm filter[b]
Methane	0.21±0.02	0.30
Ethane	0.89±0.03	0.81
Propane	1.00	1.00
n-Pentane	0.983±0.002	-
n-Hexane	-	1.11
n-Octane	0.91	-
2-Methylbutane	0.90	0.99
2-Methylpentane	0.89±0.02	0.99
2-Methylhexane	0.89±0.02	-
2-Methylheptane	0.88±0.02	-
2,3-Dimethylbutane	0.858±0.005	-
2,4-Dimethylpentane	0.811±0.002	-
2,4-Dimethylhexane	0.82	-
2,5-Dimethylhexane	-	0.99
2,2,4-Trimethylpentane	0.74±0.04	0.90
Cyclopentane	0.93	1.06
Cyclohexane	0.95	1.15
Methylcyclopentane	0.91	1.02
Methylcyclohexane	0.94	1.13
Ethene	0.085±0.008	0.04
Propene	0.37±0.02	0.30
Isobutene	0.53±0.02	0.48
1-Pentene	0.67	-
1-Hexene	-	0.70
Benzene	0.01	-
Toluene	0.10±0.02	0.15
p-Xylene	0.20±0.02	0.27
Ethylbenzene	0.22	-
1,2,4-Trimethylbenzene	0.30	0.43
n-Propylbenzene	0.27±0.02	-
MTBE[c]	0.69	0.72

(a) Filter similar to those used in Denver Univ. remote sensors, shown in Figure 4.1.

(b) Filter used in Horiba PIR-2000 NDIR analyzer, shown in Figure 4.1.

(c) Measured IR/FID response of MTBE was multiplied by 0.86. See text and Hoekman (1992).

concentrations were in the range of 350-650 ppmC for most samples. Compounds which were expected to show less infrared absorption were mixed to higher concentrations (in the ranges of 750-850 ppmC for toluene and xylene, and 850-1200 ppmC for methane). Higher concentrations resulted in increased absolute infrared absorption, and more precise IR measurements for these weakly-absorbing compounds. The actual concentration of VOC in each sample was determined by FID. The stability of organic compound concentrations in the bags was verified by repeating the measurements for several of the samples over a 4-hour period.

The optics of an on-road remote sensor were simulated using a Nicolet Magna 760 FTIR spectrometer with the 3.4 μm filter shown in Figure 4.1. The infrared beam was reflected 8 times through a 530 cm^3 multiple path White cell for a total path length of 240 cm. The beam then passed through the 3.4 μm filter, which is centered at the same location, but has a slightly narrower bandpass than those used in the newer Denver University HC remote sensors (Guenther et al., 1995; Bishop, 1997). To mimic a remote sensor detector which measures total transmitted energy, the FTIR transmittance versus wavenumber plot for each sample was integrated from 2700 to 3100 cm^{-1}. This range includes all energy transmitted by the 3.4 μm filter, as shown in Figure 4.1. Absorbance, $A = \log (I_o/I_s)$, was calculated as the ratio of energy transmitted when the cell was filled with hydrocarbon-free air (I_o) to the energy transmitted when the cell was filled with a sample (I_s). Since path length remained constant, the Beer-Lambert Law indicates that the

measured absorbance should have been linearly proportional to the concentration of absorbing species in each sample.

For each sample, the White cell was evacuated to 0.03 atm pressure, then filled with sample air from the Tedlar bag three times before any measurements were made. On the fourth filling, the IR spectrum was recorded. The cell was then evacuated and filled, and the spectra recorded, twice more for each sample. Each sample intensity I_s was calculated as the average of the three integrated intensities measured for each compound. The reference intensity I_o was obtained by performing the same procedure for a sample containing only ultrapure air. A calibration point was obtained by repeating the procedure with the propane-in-air standard. Following the IR measurement, the organic vapor concentration in each sample was measured by FID. Since each sample contained only a single compound of known identity, an external pump was used to bypass the column and introduce sample air directly to the flame ionization detector of a Hewlett-Packard 5880A gas chromatograph. The sample flow rate to the FID was held constant and monitored continuously. The FID signal was zero-corrected using ultrapure air and calibrated using the propane standard. The linearity of both instruments over the range of experimental conditions described above was verified by measuring a series of n-pentane samples ranging in concentration from 296-1114 ppmC.

4.3.2 Measurement of VOC Exhaust Speciation for Individual Vehicles

In an ongoing surveillance program to measure in-use motor vehicle emissions, the California Air Resources Board (CARB) recruits and tests in-use vehicles on a series of

prescribed dynamometer driving cycles (Devesh, 1994). Nine high-emitting vehicles recruited to the program during the winter of 1996-97 were tested on the following four standard driving cycles: the Urban Dynamometer Driving Schedule, CARB's LA92 (Unified) cycle, the stop-and-go New York City Cycle, and a high-speed highway driving cycle developed by CARB (SCF58). Collectively, these cycles span a wide range of driving conditions. The concentration of total VOC in the diluted exhaust from each vehicle test was measured by the dynamometer bench FID and a Horiba PIR2000 NDIR analyzer calibrated with n-hexane. On a per-carbon basis, the response of the NDIR analyzer to propane was measured to be 0.9 times the response to n-hexane. Since the HC channel of remote sensors is calibrated using propane, all of CARB's NDIR measurements were divided by 6 to convert from hexane equivalents to C_1 equivalents, then multiplied by 0.9 to be consistent with instruments calibrated with propane. A portion of each exhaust sample was collected in a 1 L Tedlar bag and analyzed by GC-FID to determine speciated VOC concentrations. All vehicle testing and speciated VOC analyses were performed at CARB facilities in El Monte, CA.

The interference filter used in the Horiba PIR2000 analyzer has a similar bandwidth, but is centered at a slightly higher wavelength (3.45μm) than the 3.4 μm filter for which response factors were measured; the absorption spectrum of each filter is shown in Figure 4.1. Using a slightly modified experimental procedure, IR/FID response factors appropriate to the 3.45 μm filter were measured for many of the organic compounds listed in Table 4.2. The operating software of the FTIR allowed for a digital

representation of the 3.45 μm filter to be used in place of a physical filter. Absorption spectra of the filter and organic compound samples were combined by adding absorbance as a function of wavenumber. The result of this calculation is equivalent to the spectrum measured when a physical filter and organic compound air sample are measured in series. Other procedural differences included the use of nitrogen as dilution gas in place of ultrapure air, and FID measurement using a 0.32 mm x 20 m GasPro GSC column on the HP 5880A GC-FID. To verify the equivalence of this modified approach to the original test procedure, response factors were remeasured for selected compounds using the 3.4 μm filter and the modified approach described in this paragraph.

4.4 RESULTS AND DISCUSSION

4.4.1 Individual Compound Response Factors

Measured IR/FID response factors for the individual organic compounds tested in this study are presented in Table 4.2. The IR/FID response of MTBE was multiplied by 0.86 to account for the partial response when MTBE is measured by an FID calibrated for propane (Hoekman, 1992). The response factor of acetylene was not measured in the current study because C-H absorption for this compound occurs at 3300 cm^{-1} (Bellamy, 1958), which is outside the bandpass region of the 3.4 μm filter shown in Figure 4.1. Accordingly, a response factor of zero was assumed for acetylene.

Inspection of Table 4.2 shows that as alkanes become more highly branched, their response factors drop, while increasing the number of alkyl substituents on an aromatic

ring increases the infrared response. Together, Tables 4.1 and 4.2 show that the individual compound response factors measured for the two filters in this study are generally consistent with each other and with those previously measured by Stephens et al. (1996).

One notable difference is that, other than for ethane and the C_2-C_4 alkenes, response factors measured using the 3.45 μm filter were significantly higher than those measured for the same compounds using the 3.4 μm filter. This may be understood from Figure 4.1, which shows the absorption properties of propane, hexane, and the two interference filters. Much of the energy absorption by propane occurs at wavelengths which do not pass through the 3.45 μm filter, whereas most of the hexane absorption occurs within the range of this filter. As a result, more energy will be absorbed (per carbon atom) by hexane than by propane when a 3.45 μm filter is used. If an infrared spectrometer with 3.45 μm filter is calibrated with a standard propane mixture, a sample containing n-hexane at the same carbon concentration (ppmC) will absorb more energy and a higher concentration will be reported. Since the other C_5+ alkanes listed in Table 4.2 absorb over a wavelength range similar to that of n-hexane, their 3.45 μm filter response factors are higher than those measured with the 3.4 μm filter. Ethane absorption occurs in a lower wavelength range relative to propane and hexane. The 3.45 μm filter thus captures less of ethane's absorption, and ethane's response factor drops relative to propane and hexane.

The measured 3.4 μm response factors listed in Table 4.2 were used to calculate coefficients for a linear regression model relating the number and types of C-H bonds to

infrared absorption per carbon atom for each compound. Physically, this model is based on the understanding that each C-H bond is responsible for absorbing a portion of the total infrared energy absorbed by the molecule. Mathematically, the model is described by eq 4.2:

$$RF_i = \frac{a_1 n_1 + a_2 n_2 + a_3 n_3 + a_4 n_{olef} + a_5 n_{arom}}{n_C} \qquad (4.2)$$

where RF_i is the response factor for compound i; n_1, n_2, and n_3 are the number of C-H bonds associated with primary, secondary, and tertiary paraffinic carbon atoms; n_{olef} and n_{arom} are the number of C-H bonds associated with olefinic and aromatic carbon atoms; n_C is the total number of carbon atoms per molecule; and the unknown coefficients a_i are determined by linear regression.

Results of the regression analysis shown in Table 4.3 indicate that each trio of primary C-H bonds and each pair of secondary C-H bonds absorbs an amount of infrared energy which indicates the presence of approximately one carbon atom. This is consistent with the observation that straight-chain alkanes have response factors close to 1. In contrast, each tertiary C-H bond indicates the presence of only about one-half of a carbon atom; when combined with the fact that quaternary carbon atoms do not have C-H bonds and are thus not counted by the IR technique described, this explains the observed reduction in response factors for more highly branched alkanes. The small value of a_4 is expected because olefinic C-H bonds show little absorption in the wavelength range of the filter. The near-zero value of a_5 indicates that aromatic C-H bonds do not contribute to infrared absorption in the 3.4 μm filter window.

Table 4.3. Coefficients for predicting individual HC IR/FID response factors.

C-H bond type	coefficient[a]	value[b]
Primary alkane	a_1	0.31 ± 0.01
Secondary alkane	a_2	0.48 ± 0.01
Tertiary alkane	a_3	0.49 ± 0.09
Alkene	a_4	0.08 ± 0.04
Aromatic	a_5	-0.04 ± 0.02

(a) Coefficients appearing in eq 4.2 used to predict individual compound response factors.
(b) Coefficient estimate ± 1 standard error as determined by multiple linear regression using the measured IR/FID response factors for the 3.4 μm filter shown in Table 4.2.

Eq 4.2 was used to predict response factors for all of the compounds listed in Table 4.2. As shown in Figure 4.2, these predictions correspond closely (r^2 = 0.99) to the individual compound response factors measured with the 3.4 μm filter. This is not surprising since the model coefficients were calculated from these experimental data. It is important to note, however, that the model accurately describes absorption at 3.4 μm for the full range of organic compounds listed in Table 4.2. Stephens et al. (1994) proposed a similar linear model which was not normalized to the total number of carbon atoms in a molecule. As a result, regression coefficients calculated by Stephens et al. do not have the same physical significance as those described above.

4.4.2 Response to Organic Compound Mixtures

Twenty lumped species groups were used to represent the absorption characteristics of all individual VOC found in vehicle exhaust; the corresponding group response factors for both the 3.4 and 3.45 μm filters are listed in Table 4.4. Uncertainty in the group response factors shown in Table 4.4 was estimated from uncertainty in the response factors

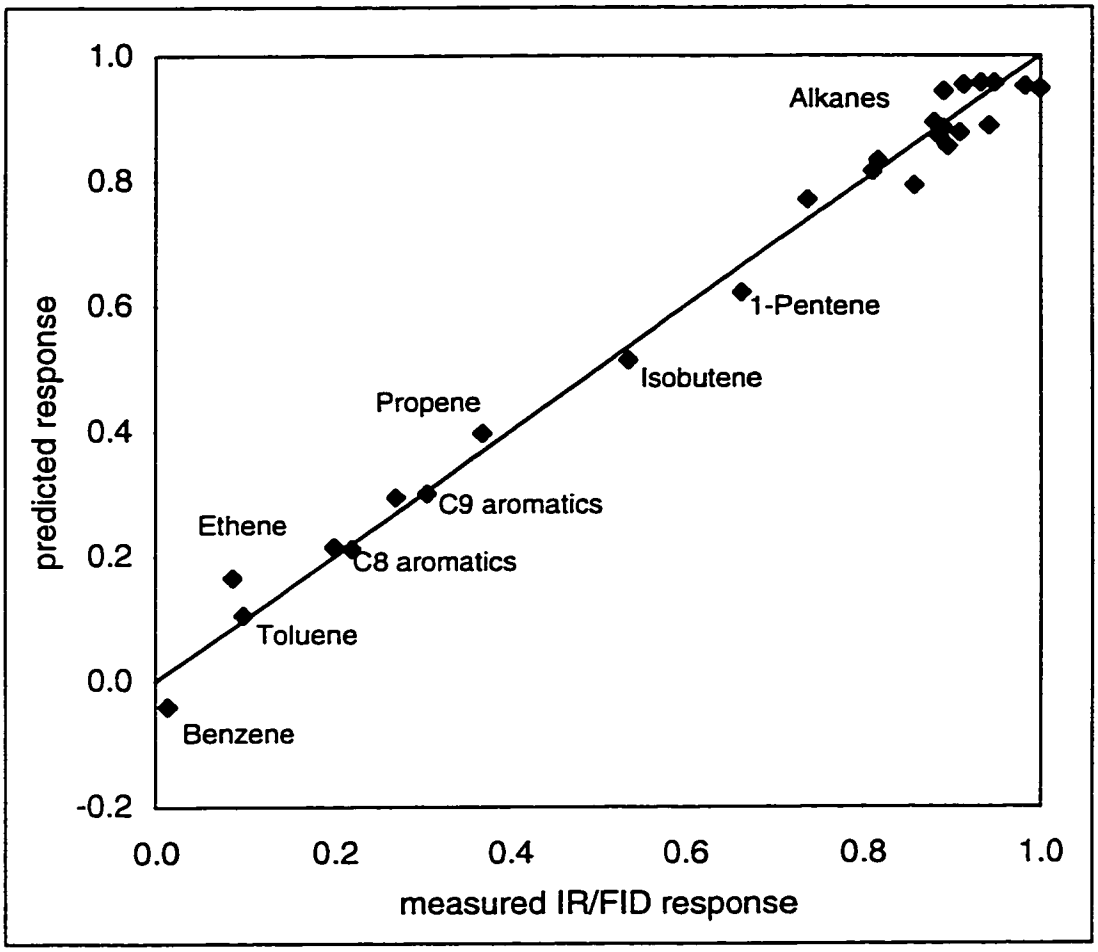

Figure 4.2. Predicted vs. measured response factors at 3.4 μm for the individual organic compounds listed in Table 4.2. Predictions calculated using eq 4.2 and coefficients of Table 4.3.

measured for individual compounds, and from variability among response factors for individual compounds assigned to each group. The regression model described above was used to predict the response of compounds whose response factors were not measured directly. These predictions were used to estimate the response factor for C_{10} or larger (C_{10}+) aromatics, to confirm that all C_5+ alkenes could be grouped together, and to assign to groups the minor exhaust constituents listed in the footnotes to Table 4.4. A response factor of 0.60 ± 0.15 (3.4 μm filter) was assigned to the unidentified fraction of total VOC because this group was expected to consist of branched C_{10}+ alkanes and/or C_{10}+ aromatics; the large uncertainty bounds on this response factor account for the possibility that the mass is composed entirely of alkanes *or* aromatics. Formaldehyde, which typically accounts for ~1-2% of exhaust VOC mass emissions (Hoekman, 1992; Kirchstetter, 1998), does not respond to FID measurement and was thus not included in the analysis.

Using eq 4.1, the 3.45 μm group response factors shown in Table 4.4 were combined with measured VOC speciation profiles to predict exhaust mixture response factors for the CARB surveillance program vehicles. Predicted response factors are plotted in Figure 4.3 against corresponding measured values (i.e., the ratio of NDIR to FID measurements of exhaust VOC concentrations). Figure 4.3 shows that if the composition of VOC in vehicle exhaust is known, infrared response can be predicted accurately. Predicted exhaust response factors correlate 1:1 to measured NDIR/FID ratios with an r^2 of 0.93.

Table 4.4. Organic compound grouping scheme and response factors for use with eq 4.1.

Compound group	Response for 3.4 μm filter	Response for 3.45 μm filter
Methane	0.21±0.02	0.30
Ethane	0.89±0.03	0.81
C_3-C_5 n-alkanes	0.98±0.01	1.00
C_6+ n-alkanes	0.91±0.03	1.11
Monosubstituted alkanes	0.89±0.02	0.99
Dimethylpropane/butanes	0.86±0.02	0.99
Other disubstituted alkanes	0.81±0.02	0.99
Trisubstituted alkanes	0.74±0.04	0.90
Cycloalkanes	0.93±0.03	1.09
MTBE	0.69±0.05	0.72
Ethene[a]	0.09±0.01	0.04
Propene[b]	0.37±0.02	0.30
Isobutene[c]	0.54±0.02	0.48
Other alkenes	0.67±0.05	0.70
Acetylene	0	0
Benzene[d]	0.01±0.01	0.01
Toluene	0.10±0.02	0.15
C_8 aromatics	0.21±0.02	0.27
C_9 aromatics	0.30±0.03	0.43
C_{10}+ aromatics	0.37±0.05	0.56
Unidentified	0.60±0.15	0.70

(a) Lumped group includes 1,3-butadiene, 1,2-propadiene, 1-buten-3-yne (see text).

(b) Lumped group includes 1,2-butadiene, 1-propyne, 2-methyl-1,3-butadiene.

(c) Lumped group includes 1-butyne, 2-butyne.

(d) Lumped group includes styrene, naphthalene.

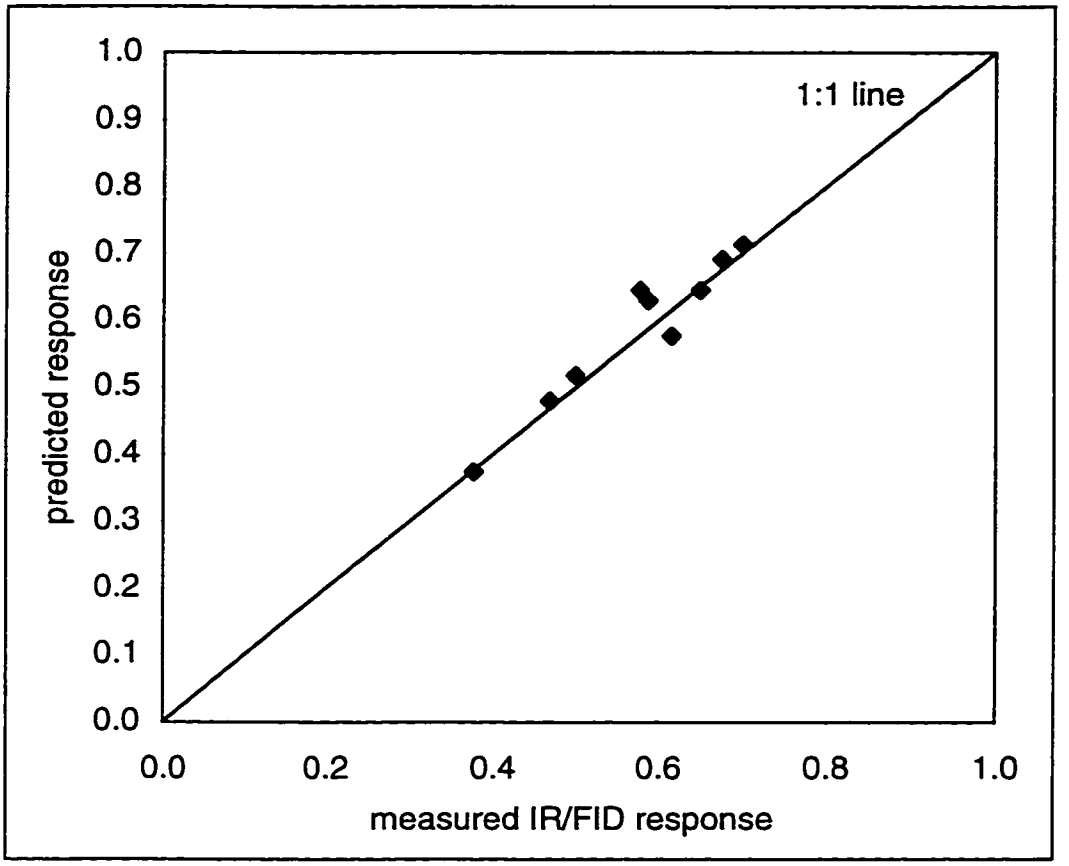

Figure 4.3. Comparison of exhaust mixture response factors predicted using eq 4.1 wtih NDIR/FID ratios measured from CARB surveillance program vehicles. Mixture response factors were calculated using the 3.45 μm group response factors listed in Table 4.4. NDIR/FID ratios were measured using an infrared analyzer with a 3.45 μm filter and a FID.

Figure 4.3 includes data from only 9 of the 36 dynamometer tests performed on CARB surveillance program vehicles. Despite a screening process which was intended to identify high-emitting vehicles, measured exhaust VOC concentrations in all but 12 of the 36 tests were below 10% of the full scale NDIR setting of 3000 ppm. The ratio of predicted to measured IR response for these tests decreased and was much more variable as exhaust VOC concentration decreased. The bias was 15-30% for measured VOC concentrations between 5 and 9% of full scale, but was much larger (10-90%) for vehicles with exhaust VOC concentrations below 5% of full scale on the NDIR analyzer. Since there was no consistent change in exhaust VOC speciation that could be correlated to this trend, it was determined that infrared measurements below 10% of full scale were biased, and therefore were not used to calculate NDIR/FID ratios. Three additional tests were rejected because the total VOC identified and quantified during speciated analysis was less than 85% of the total measured by the dynamometer bench FID.

4.4.3 Fleet-Average Infrared Response Factors

The exact scaling of individual HC remote sensor measurements is infeasible in real-world sampling scenarios because the composition of VOC in each exhaust plume is unknown. It is often possible, however, to measure the composite VOC speciation profile for an on-road fleet similar to the fleet being measured by remote sensing. The measured VOC profile can be used to calculate a fleet-average IR/FID response factor; infrared remote sensor measurements can then be scaled by the inverse of this factor. Fleet-composite VOC speciation profiles are most readily measured in roadway tunnels. Speciated VOC

profiles measured in roadway tunnels represent the average speciation, weighted by VOC mass emission rate, of all vehicles traveling through the tunnel during sampling. A tunnel-derived scaling factor will produce accurate estimates of total fleet VOC emissions if the composite VOC profile of the fleet being measured by remote sensing resembles the VOC profile measured in the tunnel, as demonstrated below.

As part of a separate study of on-road vehicle emissions (Cadle et al., 1996), twenty in-use vehicles were recruited from an Orange County, CA roadway based on high HC remote sensor readings. Total and speciated exhaust VOC emissions were measured for each vehicle by dynamometer testing. Table 4.5 includes a brief description of each vehicle along with the exhaust VOC concentration measured from the vehicle in an as-received state (i.e. without repairs). IR/FID response factors were calculated using eq 4.1, the 3.4 μm group response factors shown in Table 4.4, and the exhaust speciation profile measured for each vehicle (Mulawa and Cadle, 1997). As shown in Table 4.5, 70% of the vehicles had response factors in the range of 0.45-0.55, and all but one of the response factors were between 0.40 and 0.60. The VOC concentration that would have been reported by infrared measurement of each exhaust sample was calculated as the product of the response factor and total VOC concentration for each vehicle. Since it has been shown experimentally that infrared response factors can be predicted accurately if VOC speciation is known (Figure 4.3), the calculated infrared readings will be discussed as if infrared measurements had actually been made. Assuming that emissions are proportional to exhaust VOC concentrations, the last row of Table 4.5 indicates that IR measurements

Table 4.5. Comparison of IR and FID estimates of exhaust VOC concentrations for 20 in-use Orange County, CA vehicles.

Vehicle Description	Vehicle #	Exhaust VOC conc.[a] (ppmC)	Calculated IR/FID response[b]	Estimated VOC by IR[c] (ppmC)	Scaled IR estimate[d] (ppmC)
1985 Plymouth Voyager	134	28	0.50	14	26
1987 Volkswagen Jetta	136	58	0.46	27	51
1988 Jeep Wrangler	9	75	0.48	36	69
1985 Toyota Corolla	13	117	0.43	51	97
1988 Nissan Sentra	68	118	0.52	62	118
1988 Suzuki Samurai	122	130	0.52	67	128
1983 Chevrolet Caprice	35	171	0.48	81	155
1976 Ford Pinto	6	211	0.43	91	173
1975 Mercedes 280C	16	262	0.40	104	199
1984 GMC S-15 Sierra	108	307	0.53	163	312
1987 Mercury Sable	127	420	0.45	189	360
1985 Oldsmobile Tornado	23	467	0.67	311	593
1987 Ford Taurus	89	504	0.51	258	493
1986 Chevrolet Blazer	59	519	0.53	277	529
1987 Ford Taurus	123	546	0.45	245	467
1985 Volkswagen Golf	138	701	0.46	321	612
1987 Chevrolet Blazer	97	987	0.58	574	1095
1975 Nissan 280Z	51	1610	0.47	758	1447
1985 Chev. S-10 Blazer	99	1706	0.59	1003	1914
1987 Dodge Dakota	91	3441	0.54	1856	3541
Totals[e]		12379		6489	12379

(a) As measured by FID; does not include formaldehyde.

(b) Calculated using eq 4.1, the measured exhaust VOC speciation for each vehicle, and the 3.4 μm filter response factors of Table 4.4.

(c) Calculated as the product of response factor and exhaust VOC concentration measured by FID for each vehicle.

(d) IR-based estimate of true VOC emissions: predicted infrared reading divided by fleet-average IR/FID response factor of 0.52 (see text).

(e) Exhaust concentrations are assumed to be proportional to emission rates expressed as gram of HC emitted per unit volume of fuel burned. The total concentration is therefore assumed to be proportional to total emissions.

would understate total VOC emissions by 48% for these 20 vehicles.

A composite VOC speciation profile for all 20 vehicles was calculated as the emissions-weighted average of the measured speciation profiles of the individual vehicles. Using this composite speciation profile together with eq 4.1 and the group response factors shown in Table 4.4, a fleet-average response factor of 0.52 was calculated. The inverse of this value (1.92) was used to scale up the calculated infrared measurement for each vehicle. Note that the same fleet response factor is calculated from the ratio of summed infrared to summed FID measurements shown at the bottom of Table 4.5. Table 4.5 shows two important results of this analysis: (1) the scaled emission estimate for each vehicle is much more accurate than the unscaled infrared measurement; and (2) the sum of the individual scaled estimates matches exactly the total measured VOC. This equality occurs because the fleet-average response factor was calculated from a composite VOC speciation profile which matches exactly the composite speciation of the vehicle sample.

4.4.4 Scaling Factors for Typical On-Road Fleets and Fuels

Typical fleet-average IR/FID response factors were calculated using VOC speciation profiles measured in roadway tunnel studies (Sagebiel et al., 1995; Gertler et al., 1997; Kirchstetter, 1998). Table 4.6 lists the tunnel locations, the fuel in use at the time of study, and the calculated response factors. Methane emissions were reported for the Caldecott tunnel only, where methane accounted for about 10% of total VOC mass (Kirchstetter, 1998). This same methane fraction was assumed when calculating IR/FID response factors for the other light-duty vehicle fleets. The heavy-duty vehicle fleet

observed at the Fort McHenry tunnel (Sagebiel et al., 1995) was comprised of >70% diesel-powered vehicles. As a result, VOC emissions from this fleet included significant contributions from high molecular weight alkanes that are not found in gasoline engine exhaust. A response factor of 0.85 ± 0.05 (3.4 μm filter) was assigned to C_{11}+ n-alkanes

Table 4.6. IR/FID response factors calculated using VOC speciation profiles measured in roadway tunnels[a].

Year	Tunnel[a]	Location	Fleet[b]	Fuel	RF_m[c] 3.4 μm filter	RF_m[c] 3.45 μm filter
1992	Ft. McHenry	Baltimore, MD	HD	>70% diesel	0.49±0.04	0.58
1992	Tuscarora	PA Turnpike	LD	Gasoline[d]	0.44±0.02[e]	0.50[e]
1992	Ft. McHenry	Baltimore, MD	LD	Gasoline[d]	0.45±0.02[e]	0.52[e]
1994	Caldecott	Oakland, CA	LD	Gasoline[f]	0.44±0.03	0.50
1995	Caldecott	Oakland, CA	LD	Gasoline[f]	0.47±0.03	0.55
1995	Deck Park	Phoenix, AZ	LD	Fed. RFG[g]	0.51±0.03[e]	0.59[e]
1995	Van Nuys	Los Angeles, CA	LD	Fed. RFG[g]	0.49±0.03[e]	0.57[e]
1995	Callahan	Boston, MA	LD	Fed. RFG[g]	0.53±0.03[e]	0.60[e]
1996	Caldecott	Oakland, CA	LD	CA RFG[h]	0.51±0.03	0.58
Scaling factor for vehicles using conventional gasoline					2.2±0.1	1.9
Scaling factor for vehicles using reformulated gasolines					2.0±0.1	1.7

(a) See Sagebiel et al. (1995), Gertler et al. (1997), and Kirchstetter (1998).

(b) Predominant vehicle type sampled: LD = light-duty; HD = heavy-duty.

(c) RF_m = mixture response factor calculated using measured exhaust VOC speciation profile, group response factors shown in Table 4.4, and eq 4.1.

(d) Conventional gasoline.

(e) Calculated response assumes 10% methane weight fraction (see text for details).

(f) California Phase 1 reformulated gasoline. Properties similar to conventional gasoline except for: summer RVP limit of 7.8 psi, complete removal of lead, and requirement for detergent additives.

(g) Federal reformulated gasoline.

(h) California Phase 2 reformulated gasoline.

based on the observation that n-alkane response decreases as carbon number increases; this trend is shown in Table 4.3 and discussed in Stephens et al. (1996). Unidentified branched alkanes measured from the heavy-duty fleet at the Fort McHenry tunnel were split equally and assigned to the di- and tri-substituted alkane groups shown in Table 4.4. Following the measurements of Clark et al. (1995, 1996) which show that diesel engines emit very low levels of methane, the non-methane organic compound emissions profile reported from measurements in the Fort McHenry tunnel (Sagebiel et al., 1995) was used without adjustment to estimate infrared response for heavy-duty vehicles.

Table 4.6 shows that for the 3.4 μm filter, light-duty fleet response factors range from 0.44 to 0.47 for vehicles using conventional gasoline, and from 0.49 to 0.53 for vehicles using either California or Federal reformulated gasolines. Fleet response factors for the 3.45 μm filter are higher by about 13%. These results indicate that fleet-average infrared response is most sensitive to filter bandpass and fuel composition, but varies less by geographic area or across the range of driving conditions in the tunnels studied. The higher response factors associated with reformulated gasolines may be explained by changes in the exhaust VOC emissions of vehicles burning these fuels. Specifically, reductions in the aromatic content of gasoline leads to exhaust mixtures that absorb more 3.4 μm infrared radiation per unit mass of VOC emitted. This result is expected given the low IR/FID response factors measured for individual aromatic hydrocarbons (see Table 4.2), compared to the higher response factors for branched alkanes, cycloalkanes, and

MTBE that are blended into reformulated gasoline in increased amounts when aromatic levels are lowered.

Application of the fleet-average response factors presented in Table 4.6 is demonstrated using emissions data collected from the 20 Orange County, CA vehicles discussed previously. This "fleet" includes a relatively small number of vehicles which have average VOC emissions comparable to those measured from much larger samples of on-road vehicles (Kirchstetter, 1998).

The scaling factor of 2.0 calculated from the VOC speciation profile measured in the Van Nuys tunnel was chosen as most appropriate because the tunnel is located in the same metropolitan area as the vehicles tested, and because VOC sampling occurred at the tunnel during the same year as the individual vehicle testing. The average scaling factor for vehicle fleets using Federal reformulated gasoline also could have been used. When each of the infrared measurements listed in Table 4.5 is multiplied by the scaling factor of 2.0, the accuracy of individual vehicle VOC emissions estimates is improved substantially compared to the unscaled infrared data; this is shown in Figure 4.4. Unscaled infrared measurements understate tailpipe VOC concentrations by 33-60%, whereas most of the scaled infrared estimates fall within the range of ±15% of true VOC concentrations. Overall, the scaled infrared estimates overstate VOC emissions from this fleet by 4%; this small bias reflects the difference between the scaling factor derived from Van Nuys tunnel measurements (2.0), and the factor calculated explicitly for the twenty Orange County vehicles (1.92).

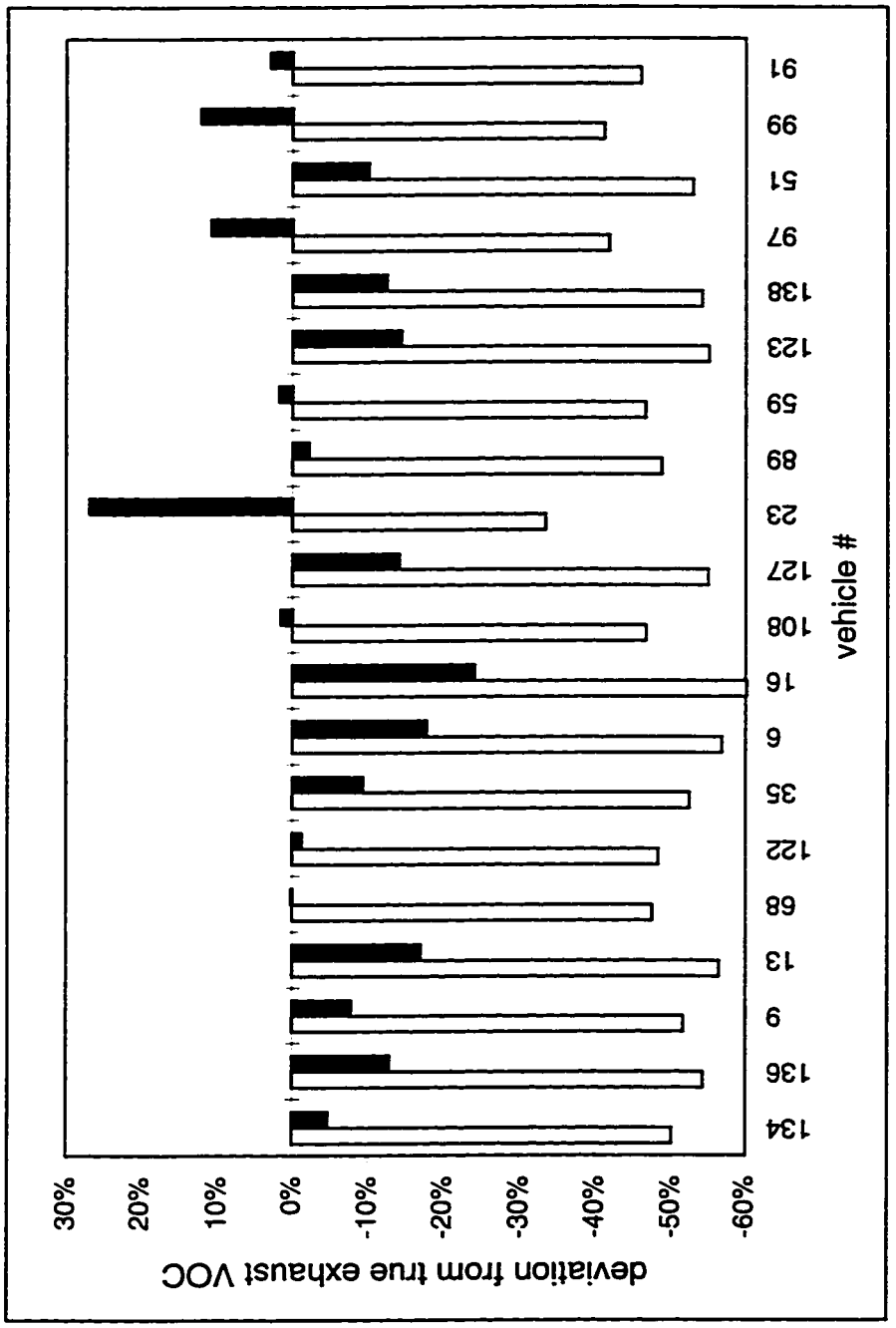

Figure 4.4. Results of using simulated IR readings to estimate true exhaust VOC concentrations for 20 in-use vehicles from Orange County, CA. Light bars show unadjusted IR readings consistently understating true VOC concentrations. Dark bars show that adjusted IR readings are within ±15% of true VOC for most of the vehicles.

4.4.5 Uncertainty

The reported uncertainty of each fleet-average response factor shown in Table 4.6 accounts only for the uncertainties in underlying group response factors for the 3.4 μm filter (shown in Table 4.4). The uncertainties in scaling factors for each fuel, shown at the bottom of Table 4.6, are also based on the group response factor uncertainties. The variability in response factors (RF_m) across the relevant on-road studies for each fuel is less than the uncertainty resulting from the group response factors.

From the earlier discussion and results, it is clear that infrared response depends upon the exact transmission range of the interference filter. The magnitude of this effect may be inferred from the 13% difference between response factors calculated for 3.4 and 3.45 μm filters (last two columns of Table 4.6). This difference is consistent with the observation that exhaust mixture IR/FID response factors predicted with the 3.4 μm group response factors were 11% lower than those measured for CARB surveillance program vehicles with the 3.45 μm filter. Individual filters with the same nominal band center may in reality have slightly different bandpass ranges; however, the effect of these differences on mixture response should be smaller than the difference between the 3.4 and 3.45 μm filters. Whenever possible, the exact transmission range of an infrared filter should be determined before selecting an appropriate scaling factor. Bandpass range variability is bounded by the need to capture the large peak of most alkanes (similar to the absorption profile of hexane, as shown in Figure 4.1) while avoiding interference of water vapor above 3000 cm^{-1} (Guenther et al., 1995).

Two other sources of uncertainty exist when using remote sensor measurements to quantify on-road vehicle emissions. First, and most important, is the accuracy of the remote sensor. Previous assessments show that HC remote sensors can accurately measure dry gas mixtures of propane (or hexane), CO, CO_2, and air (Stedman et al., 1994; Pedrosa et al., 1995). This work thus assumes that remote sensors would yield accurate results if exhaust VOC emissions were composed entirely of propane. A second source of uncertainty – remote sensor measurement precision – would also have to be considered if in-use emissions levels of *individual* vehicles were to be estimated from single remote sensor measurements. Addressing this issue, Bishop et al. (1996) have shown that emissions of high-emitting vehicles vary from test to test regardless of the analytical technique or test duration; the authors thus caution against using any single measurement to assess individual high-emitting vehicle performance. The individual vehicle test results of Figure 4.4 should be viewed in this light, with the additional understanding that infrared remote sensors facilitate repeat measurements of large numbers of individual in-use vehicles. Most important to the objectives of this study, the precision of individual measurements is less of an issue when remote sensors are used to estimate fleet-average emissions.

4.4.6 Motor Vehicle Emission Inventory Calculations

The objective of this work was to develop an approach for scaling infrared remote sensor measurements for quantitative fleet emissions assessment. Measurements of fleet-composite VOC speciation throughout the U.S. indicate that measurements from HC

remote sensors equipped with 3.4 μm filters should be multiplied by a factor of about 2 when calculating fleet-average emission factors for motor vehicle emission inventory calculations. The exact scaling factor is slightly higher (2.2±0.1) for vehicles using conventional gasoline, and slightly lower (2.0±0.1) for vehicle fleets using either California or Federal reformulated gasoline. Alternatively, a local fleet scaling factor can be calculated if on-road measurements of the composite exhaust VOC profile are available. The appropriate scaling factor can be applied to data sets containing tens of thousands of remote sensor measurements in the same manner that the scaling factor calculated from Van Nuys tunnel data was applied to the simulated infrared exhaust measurements of Orange County vehicles. The scaled remote sensor measurements can then be used to calculate fleet-average exhaust VOC emission factors which can be used in fuel-based emission inventory calculations. This approach is applied in Chapter 6 to calculate a stabilized exhaust VOC inventory for the Los Angeles, CA area in summer 1998.

4.5 REFERENCES

Bellamy, L. J. (1958). *The Infra-red Spectra of Complex Molecules*. John Wiley & Sons, Inc.: New York, NY.

Bishop, G. A. (1997). *Personal Communication*. University of Denver, Denver, Colorado.

Bishop, G. A., J. R. Starkey, A. Ihlenfeldt, W. J. Williams and D. H. Stedman (1989). IR long-path photometry: a remote sensing tool for automobile emissions. *Anal. Chem.* **61**:671A-677A.

Bishop, G. A. and D. H. Stedman (1990). On-road carbon monoxide emission measurement comparisons for the 1988-1989 Colorado oxy-fuels program. *Environ. Sci. Technol.* **24**:843-847.

Bishop, G. A., D. H. Stedman and L. Ashbaugh (1996). Motor vehicle emissions variability. *J. Air Waste Manage. Assoc.* **46**:667-675.

Cadle, S. H., P. A. Mulawa, J. Ball, C. Donase, A. Weibel, J. Sagebiel, K. T. Knapp, et al. (1996). Particulate and speciated HC emission rates from in-use vehicles recruited in Orange County, CA. *Sixth CRC On-Road Vehicle Emissions Workshop*, San Diego, CA, March 16-18, 1996. Coordinating Research Council, Atlanta, GA.

Clark, N. N., C. M. Atkinson, D. L. McKain, R. D. Nine and L. El-Gazzar (1996). Speciation of hydrocarbon emissions from a medium duty diesel engine. *SAE Tech. Pap. Ser.* **960322**.

Clark, N. N., C. J. Gadapati, K. Kelly, C. L. White, D. W. Lyons, W. Wang, M. Gautum, et al. (1995). Comparative emissions from natural gas and diesel buses. *SAE Tech. Pap. Ser.* **952746**.

Devesh, S. (1994). *Test report of the light-duty vehicle surveillance program, series 12 (LDVSP 12)*. Mobile Source Division, California Air Resources Board, El Monte, CA. MS-94-04.

Gertler, A. W., J. C. Sagebiel, D. N. Wittorff, W. R. Pierson, W. A. Dippel, D. Freeman and L. Sheetz (1997). *Vehicle emissions in five urban tunnels*. Desert Research Institute, Reno, NV. Report to the Coordinating Research Council, Atlanta, GA. Project No. E-5.

Guenther, P. L., D. H. Stedman, G. A. Bishop, S. P. Beaton, J. H. Bean and R. W. Quine (1995). A hydrocarbon detector for the remote sensing of vehicle exhaust emissions. *Rev. Sci. Instrum.* **66**:3024-3029.

Harris, D. C. (1991). *Quantitative Chemical Analysis*. W.H. Freeman and Company: New York, NY.

Hoekman, S. K. (1992). Speciated measurements and calculated reactivities of vehicle exhaust emissions from conventional and reformulated gasolines. *Environ. Sci. Technol.* **26**:1206-1216.

Jackson, M. W. (1966). Analysis for exhaust gas hydrocarbons — nondispersive infrared versus flame-ionization. *J. Air Pollut. Control Assoc.* **11**:697-702.

Kirchstetter, T. (1998). *Impact of reformulated fuels on motor vehicle emissions*. Ph.D. Dissertation, Department of Civil and Environmental Engineering, University of California, Berkeley, CA.

Lawson, D. R., P. J. Groblicki, D. H. Stedman, G. A. Bishop and P. L. Guenther (1990). Emissions from in-use motor vehicles in Los Angeles: a pilot study of remote sensing and the inspection and maintenance program. *J. Air Waste Manage. Assoc.* **40**:1096-1105.

Mulawa, P. A. and S. H. Cadle (1997). *Personal Communication*. General Motors NAO Research and Development Center, Warren, MI.

Pedrosa, J., R. Benjaminson and M. Yang (1995). *Technical assessment of on-road emissions measurement systems*. California Bureau of Automotive Repair, Engineering & Technical Research Branch, Sacramento, CA.

Sagebiel, J. C., B. Zielinska, W. R. Pierson and A. W. Gertler (1995). Real-world emissions and calculated reactivities of organic species from motor vehicles. *Atmos. Environ.* **30**:2287-2296.

Stedman, D. H., G. A. Bishop, S. P. Beaton, J. E. Peterson, P. L. Guenther, I. F. McVey and Y. Zhang (1994). *On-road remote sensing of CO and HC emissions in California*. Final Report to the California Air Resources Board, Contract No. A032-093.

Stephens, R. D. (1994). Remote sensing data and a potential model of vehicle exhaust emissions. *J. Air Waste Manage. Assoc.* **44**:1284-1292.

Stephens, R. D. and S. H. Cadle (1991). Remote sensing measurements of carbon monoxide emissions from on-road vehicles. *J. Air Waste Manage. Assoc.* **41**:39-46.

Stephens, R. D., P. A. Mulawa, M. T. Giles, K. G. Kennedy, P. J. Groblicki, S. H. Cadle, J. W. Duncan, et al. (1994). *An experimental evaluation of remote sensing based hydrocarbon measurements: a comparison of FID measurements*. Report to the Coordinating Research Council, Atlanta, GA. Contract VE-11-4.

Stephens, R. D., P. A. Mulawa, M. T. Giles, K. G. Kennedy, P. J. Groblicki, S. H. Cadle and K. T. Knapp (1996). An experimental evaluation of remote sensing-based hydrocarbon measurements: a comparison to FID measurements. *J. Air Waste Manage. Assoc.* **46**:148-158.

CHAPTER FIVE

Effects of Driving Mode on Emission Factors

5.1 INTRODUCTION

Emission factors expressed per km of travel are greatly influenced by driving mode. California's EMFAC model (the emission factor component of the MVEI model) represents this dependence using emissions data measured during twelve transient driving cycles which range in average speed from 3 to 65 mph (5 to 104 km h^{-1}) (CARB, 1995). The higher speed cycles include more moderate and high speed cruise driving, while the lower average speed cycles include more stop-and-go driving. Modal emissions relationships for MVEI 7G, derived from testing of 746 vehicles (CARB, 1995), are shown for the light-duty fleet in Figure 5.1a. The plot was created by weighting emission factors for each technology group by the prevalence of that group in the on-road fleet for summer 1997 (according to MVEI 7G), then calculating the ratio of emissions at each average speed to emissions at 45 mph (72 km h^{-1}). The plot indicates that emissions of carbon monoxide (CO) and reactive organic gases (ROG) change little between average speeds of 40-55 mph (64-88 km h^{-1}), but increase sharply during higher and lower speed cycles. Nitrogen oxides (NO_x) emissions appear to vary less over a wide range of driving

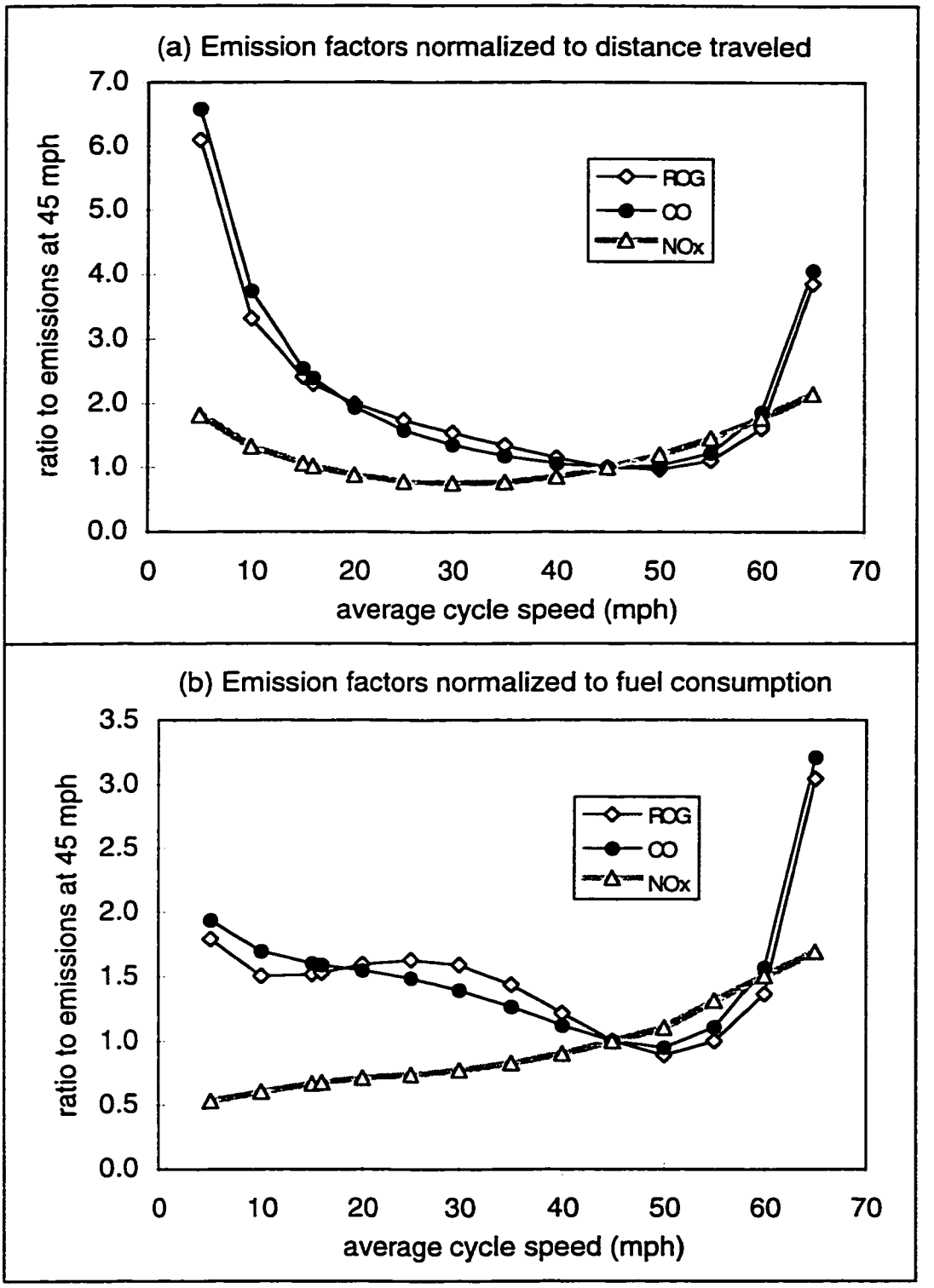

Figure 5.1. Dependence of exhaust emission factors on driving conditions as predicted by California's EMFAC 7G model. Plots are based on model output for the San Francisco Bay Area in summer 1997.

cycles. The large increases in ROG and CO emissions during lower average speed driving cycles result in part because these cycles include a much higher percentage of time in idle; since no travel occurs during idle, travel-normalized emission factors are very sensitive to the amount of time a vehicle spends in idle. NO_x emissions are known to be load-dependent (Heywood, 1988); the overall lower loads reduce the effect of increased idle time on NO_x emissions during lower average speed cycles.

Figure 5.1b shows that emission factors normalized to fuel consumption vary less as a function of driving mode. ROG and CO emissions vary by less than a factor of 2 over all but the highest average speed cycle. This plot was created using the EMFAC-predicted CO_2 emission factor for each average speed, together with the carbon balance equation described below (eq 5.4). Limited available on-road evidence also indicates that on a fleet-average basis, changes in driving mode affect fuel-normalized emission factors much less than travel-normalized emission factors. Pierson et al. (1996) measured emission factors for uphill and downhill driving on the 3.8% grade in the Ft. McHenry tunnel. When normalized to travel, uphill-to-downhill emissions ratios were 1.5, 1.9, and 2.2 for non-methane hydrocarbons (NMHC), CO, and NO_x respectively. By contrast, uphill-to-downhill emissions ratios were 0.95 for NMHC, 1.2 for CO, and 1.4 for NO_x when emissions were normalized to fuel consumption.

In recent years, remote sensors have been used to measure the on-road emissions of hundreds of thousands of vehicles in connection with vehicle inspection and maintenance (I/M) programs in Arizona, California, Texas, and other states (Lawson et al., 1990; Stedman and Bishop, 1990; Lyons and Stedman, 1991; Klausmeier et al., 1995; Brown et

al., 1996; Cox et al., 1996; Kite et al., 1997; O'Connor et al., 1997; Walsh and Gertler, 1997). Remote sensor site selection criteria for these studies have included the following: single lane roadway, minimal number of vehicles in cold start mode, minimal driving at loads higher than those encountered in the urban driving cycle of the Federal Test Procedure (FTP), and a predominance of "loaded" mode driving. Cold start operation and driving at loads higher than those included in the FTP are avoided because otherwise low-emitting vehicles may have much higher emissions under these conditions (Cullen and Liberty, 1996; Goodwin and Ross, 1996). An emissions screening program in Ontario, Canada includes remote sensing of each vehicle in deceleration, cruise, and acceleration modes, but measurements are made only when a vehicle is brought to a centralized testing facility (Petherick, 1997). In principle, on-road remote emissions data from I/M screening programs could also be used to calculate fuel-based emission inventories. It must still be determined, however, whether fuel-normalized emissions vary within the range of loaded driving modes which are used for I/M screening, and how emission levels during these loaded modes compare to emissions during other driving modes.

The objectives of this study were (1) to quantify how fuel-based fleet-average emission factors change with driving mode; and (2) to estimate how loaded mode emissions measured during typical on-road remote sensing configurations relate to emissions averaged over all, or at least most, on-road driving.

5.2 ANALYTICAL APPROACH

5.2.1 Overview

This study relies on analysis of remote sensing, dynamometer, and no-load idle emissions data. The data were analyzed to determine the dependence of fleet-average fuel-normalized emission factors on vehicle operating mode. The fraction of total fuel used in each driving mode was also estimated. This section describes the data used and analyses performed.

5.2.2 Characterization of Driving Modes

Numerous approaches have been used to characterize driving patterns and to differentiate between different driving modes. These include groupings by speed and acceleration, and various methods of calculating physical loads, or power requirements. Emissions data measured by remote sensing in Arizona were examined as a function of measured speed, measured acceleration, and two separate load metrics. The first load metric, specific power [$m^2\ s^{-3}$] was calculated with eq 5.1:

$$P_s = 2(a + g\sin\theta)V \qquad (5.1)$$

where a, V, and θ are the measured acceleration [$m\ s^{-2}$], velocity [$m\ s^{-1}$], and roadway angle [°], and $g = 9.81\ m\ s^{-2}$ is gravitational acceleration. Roadway angle was calculated as the arctangent of the roadway grade. The inclusion of the g sin θ term captures the effect of roadway grade on engine load.

The second metric, referred to here as *road load*, is an estimate of the power required to propel a vehicle at a specific speed and acceleration. Road load, P_b [kW], was calculated using eq 5.2:

$$P_b = \left(Ma + MgC_R + 0.5\rho_a C_D A V^2 + Mg\sin\theta\right)\frac{V}{1000} \qquad (5.2)$$

where M is vehicle mass [kg], C_R is the coefficient of rolling resistance, C_D is the coefficient of drag, A is frontal area [m^2], and $\rho_a = 1.2$ kg m^{-3} is air density. The terms in parentheses represent the forces required to overcome inertia, rolling resistance, air drag, and gravity. Average 1993 passenger vehicle characteristics (Ross, 1994) of $M = 1500$ kg, $C_R = 0.010$, and $C_D A = 0.7$ m^2 were used together with the roadway grade reported for each site in Table 5.1 to calculate a typical vehicle load based on measured vehicle speed and acceleration. The term *road load* is used in place of the more conventional *brake power* to emphasize that it reflects the load encountered by a typical newer vehicle at the measured speed, acceleration, and roadway grade rather than the exact power requirement of each individual vehicle.

The road load approach provides an estimate of the overall physical load encountered by vehicles at the observed speed and acceleration. Specific power is, in effect, a simplified form of the road load equation which does not account for aerodynamic drag and rolling resistance. Road load represents the power required to propel the vehicle and does not include engine friction, which varies with displacement and engine speed (Ross, 1994). A typical value of engine friction at idle for a mid-sized engine from the early 1990s is ~7 kW (Ross, 1994). Road loads below -5 to -10 kW

indicate braking, and result when the deceleration rate is faster than would be caused by the combined forces of air drag, rolling resistance, gravity, and engine friction.

5.2.3 Loaded Mode Emissions

The variability of emissions over a range of positive vehicle loads and during braking was determined from analysis of remote emissions measurements made in the Phoeniz, AZ area in 1996 and 1997. Vehicle emissions were measured by Hughes Santa Barbara Research Center (SBRC) (Hughes Environmental Systems, 1994-5; Brown et al., 1996; Cox et al., 1996); the focus of the program was to identify high-emitters for the Arizona I/M program. CO and HC emissions were measured using infrared remote emissions sensors (Jack, 1996). Vehicle speed was measured with pneumatic strips on the roadway at points before and after each vehicle passed a sensor; acceleration was calculated using the measured distance between two speed sensors (Jack, 1996). One limitation of these data is that the individual vehicle acceleration measurements are thought to be precise to only ~1.5 km h^{-1} s^{-1} (~1 mph s^{-1}) (Rendahl, 1998). Measurement sites were selected to minimize the number of vehicles sampled during cold start conditions or while driving under very high loads. Basic information about each site, including cross-streets, roadway grade, and predominant driving mode was provided by the contractor (Hughes Environmental Systems, 1994-5). The full set of remote sensing measurements collected through mid-1997 was obtained directly from Hughes SBRC (Brown, 1997) and is being used here by permission of the Arizona Department of Environmental Quality (Grubbe, 1998).

The analysis focused on data from a single section of the metropolitan Phoenix area; the goal of this focus was to reduce the influence that neighborhood to neighborhood changes in fleet composition might have on the emissions measured at each site. The sites selected for analysis are listed in Table 5.1. They include three sets of on- and off-ramps to US highway 60 which are within about 5 km of one another. As described later, five of the sites featured mostly moderate load driving; the sixth site featured a 7% uphill grade which enabled the measurement of vehicles under higher load conditions. Each site was sampled on multiple days using several different remote sensing units, or vans. CO emissions reported by five of the units were generally in very good agreement, while the sixth van consistently reported CO emissions about twice those measured by the other units. Vans 1, 4, and 5 consistently measured similar HC emissions levels, but vans 3 and 6 reported HC emissions which were about 30% higher and van 2 reported HC emissions which were about 70% higher on average than the other three vans. All emissions data

Table 5.1. Phoenix, AZ remote sensing measurement sites used for modal analysis.

Location	Grade	# of van-days	# of vehicles sampled	mean ± 1 std. dev. speed ($m\ s^{-1}$)	accel ($m\ s^{-2}$)
Alma School on-ramp to US-60 WB	Flat	12	22,785	19±3	0.1±0.6
Dobson on-ramp to US-60 EB	-3%	10	31,164	20±3	0.2±0.6
McClintock on-ramp to US-60 WB	Flat	2	5,718	18±3	0.1±0.6
US-60 EB off-ramp to Alma School	2%[a]	14	44,572	17±5	-0.3±0.7
US-60 EB off-ramp to Dobson	7%	24	61,716	21±3	-0.1±0.7
US-60 EB off-ramp to McClintock	Flat	4	8,196	20±4	-0.2±0.6

(a) Described in Hughes Environmental Systems (1994-5) as "uphill". Grade was estimated at 2%.

were grouped and analyzed by sampling unit so that van-to-van calibration differences wouldn't obscure any dependence of emissions on speed, acceleration, and/or load.

The data were also analyzed by van-site-day combination to remove any variability which could have resulted from day-to-day differences in the calibration of each unit. For each van-site-day combination, vehicle emissions measurements were grouped according to calculated vehicle road load into one of six bins. The nominal bins were <-10, 0, 10, 20, 30, and ≥40 kW; the central bins represented all road loads within ± 5 kW of the nominal values and the outer bins represented all loads of <-5 kW and ≥35 kW. The lowest bin corresponds roughly to braking conditions. The highest load bin was chosen to ensure that a large number of vehicle measurements would be included in the calculated average emission factor for that bin. The average emission factor for each load was then divided by the average emission factor for vehicles measured at 10 kW road load.

As a point of reference, a road load of ~10 kW is produced when a typical newer vehicle cruises at 90 km h^{-1} on a level roadway; a road load of ~30 kW is produced when the same vehicle is driven at a constant speed of 90 km h^{-1} on a 5.5% uphill grade. The computed ratios thus compare emissions during a range of load levels to emissions during moderate road load.

5.2.4 Emissions at Idle

The relationship between emissions at idle and emissions during loaded modes was examined using data from California's I/M Pilot program (Patel et al., 1996). The program was designed to compare a constant-load test (the ASM test described below) to

a transient 240-second dynamometer driving cycle (IM240) in terms of their ability to identify and aid in the repair of high-emitting vehicles. Vehicles were recruited from a target group selected to be representative of the California vehicle fleet. Excluding those vehicles which were excused from the program for a variety of reasons, the capture rate of targeted vehicles was >60%. A complete description of vehicle procurement and the representativeness of the vehicle sample is provided elsewhere (Patel et al., 1996).

The I/M Pilot program vehicles were tested on the IM240 transient driving cycle, two acceleration simulation mode (ASM) constant-load dynamometer tests, and with a standard tailpipe emissions probe during no-load idle conditions. The constant-load dynamometer tests were the ASM-5015, during which the dynamometer is set at 50% of a maximum load based on vehicle weight (Patel et al., 1996) and the vehicle is driven at 15 mph (24 km h^{-1}); and the ASM-2525, during which the vehicle is driven at 25 mph (40 km h^{-1}) under 25% load (Patel et al., 1996). Emissions of CO, HC, and CO_2 were measured during the ASM and idle tests using a BAR-90 infrared-based emissions analyzer (Patel et al., 1996). Complete CO, HC, and CO_2 data for the two ASM and idle emissions tests were obtained for 574 of the 642 vehicles included in the I/M Pilot Program; CO and HC, but not CO_2, exhaust concentration data for both ASM and the idle emissions tests were available for an additional 44 vehicles. Mean fuel-normalized emission factors were calculated for the 574 vehicle sample and mean exhaust concentrations were calculated for the 618 vehicle sample. IM240 emissions data were not used for this analysis because the IM240 cycle includes a range of driving conditions, whereas the use of only the ASM and idle tests allow for direct comparison of emissions

during idle to emissions during constant load driving. Note also that unadjusted HC concentrations measured by the infrared absorption analyzers used in the ASM and idle tests cannot be compared directly to HC concentrations measured during the IM240 test using a flame ionization detector (see Chapter 4).

5.2.5 Fuel Use

To determine how emissions measured during a single driving mode relate to emissions during a wide range of on-road driving conditions, it was necessary to estimate the distribution of fuel use by driving mode. This was accomplished using the empirical fuel consumption model described by Ross and An (An and Ross, 1993; Ross and An, 1993) together with CARB's Unified driving cycle. The Unified cycle was developed to represent the distribution of on-road driving observed with chase cars in Los Angeles in 1992 (Gammariello and Long, 1993); however, the inability of the chase cars to follow the most aggressive drivers resulted in a cycle which probably underrepresents very high load driving. Ross and An showed that fuel energy input is linearly related to brake power output with an offset equal to the energy required to overcome engine friction at idle (referred to here as K_{ef}); as mentioned earlier, this offset is on the order of 7 kW for typical mid-sized 1990s passenger cars. The dimensionless slope of the fuel energy input P_f [kW] to brake power output P_b [kW] relationship is ~2.4 (Ross and An, 1993); this yields eq 5.3:

$$P_f = K_{ef} + 2.4P_b \tag{5.3}$$

The speed and acceleration data from a Unified cycle dynamometer test was used, together with typical 1993 model year vehicle rolling resistance and air drag coefficients discussed previously, to calculate the road load for each second of the cycle. The fuel energy requirement at each second was calculated using eq 5.3. with the condition that $P_b = 0$ for all calculated road loads ≤ 0. Each second of the Unified cycle was assigned to one of the driving modes shown in Table 5.2; the load cutpoints were chosen to be consistent with the remote sensing analyses outlined above. The amount of fuel energy used in each mode was calculated by summing the fuel energy used during all seconds assigned to the mode.

Table 5.2. Emissions measured in California's I/M Pilot Project (mean±1 std. error).

Pollutant	# vehicles	Mean ± 1 std. error emissions			Idle to loaded-mode emissions ratios.	
		No-load Idle	ASM 2525[a]	ASM 5015[a]	Idle/ 2525	Idle/ 5015
CO (g/kg)[b]	574	73±6	89±8	91±8	0.82	0.80
CO (%)[c]	618	0.55±0.05	0.67±0.06	0.69±0.06	0.82	0.80
HC (g/kg)[b]	574	2.4±0.3	4.0±0.6	4.9±0.8	0.60	0.49
HC (ppm)[c]	618	52±6	94±13	107±14	0.55	0.48

(a) The acceleration simulation mode is a constant load dynamometer emissions test. Refer to the text and Patel et al. (1996) for additional details.

(b) Fuel-normalized emissions were calculated from the measured exhaust concentrations of CO_2, CO, and HC using eq 5.4.

(c) CO_2 data were unavailable for a subset of the vehicle emissions tests. HC and CO exhaust concentration data were available for a larger number of vehicles.

5.2.6 Calculation of Emission Factors

Fuel-normalized emission factors were calculated by carbon balance from the measured exhaust concentrations of pollutant P (either HC or CO), CO_2, CO, and HC (as hexane):

$$E_P = \frac{[P]}{[CO_2]+[CO]+6[HC]} \cdot \frac{w_c M_P}{12} \tag{5.4}$$

where E_P is the HC or CO emission factor in units of g of pollutant emitted per kg fuel consumed; w_c is the fraction of gasoline mass contributed by carbon atoms, M_P is the molecular mass of pollutant P, and 12 is the molecular mass of a single carbon atom. The factor of 6 converts from hexane equivalents to C_1 equivalents.

As discussed in the previous chapter, HC mass emissions levels calculated from infrared measurements do not reflect the total HC mass that would be calculated from flame ionization detector measurements. The difference results because the infrared technique does not respond equally to all classes of HC. Large changes in exhaust composition between driving modes could affect the fraction of total HC reported by infrared remote sensors, and therefore the apparent relative HC emissions at various loads. Similar HC speciation has been observed at roadway tunnels with somewhat different driving patterns; this suggests that infrared analyzers may be used to compare HC emissions over different driving conditions (see Chapter 4). However, the relationship between driving mode and HC speciation remains poorly understood.

5.3 RESULTS AND DISCUSSION

5.3.1 Loaded-Mode Emissions

Fuel-normalized HC and CO emissions are shown as a function of road load, specific power, acceleration and speed in Figures 5.2-5.5, respectively. Each figure also includes the number of emissions measurements for each value of the independent variable. The dependence of emissions on driving mode shown in these figures is consistent across all sampling units, despite variations in absolute emission levels reported by individual remote sensors.

Figure 5.2 shows that fuel-normalized emissions of both HC and CO were relatively stable over a range of positive road loads, but higher for the zero and negative road loads which correspond to deceleration and braking events. The scatter in emissions data for road loads below about -20 kW results from the smaller sample sizes used to calculate average emission factors for these road load levels. Overall, HC emissions appear to have a greater load dependence than CO emissions. HC emissions decreased gradually as road load decreased from 60 to 10 kW, increased sharply as road load decreased from 10 to -10 kW, and remained high for the more negative road loads. CO emissions were consistent for road loads greater than 10 kW, increased gradually as road load decreased to -10 kW, and were consistent for all negative values of road load.

Emission levels at high values of calculated road load are difficult to assess because (a) most of the remote sensing sites were selected to minimize the measurement of vehicles during high load driving conditions and (b) many of the higher calculated road

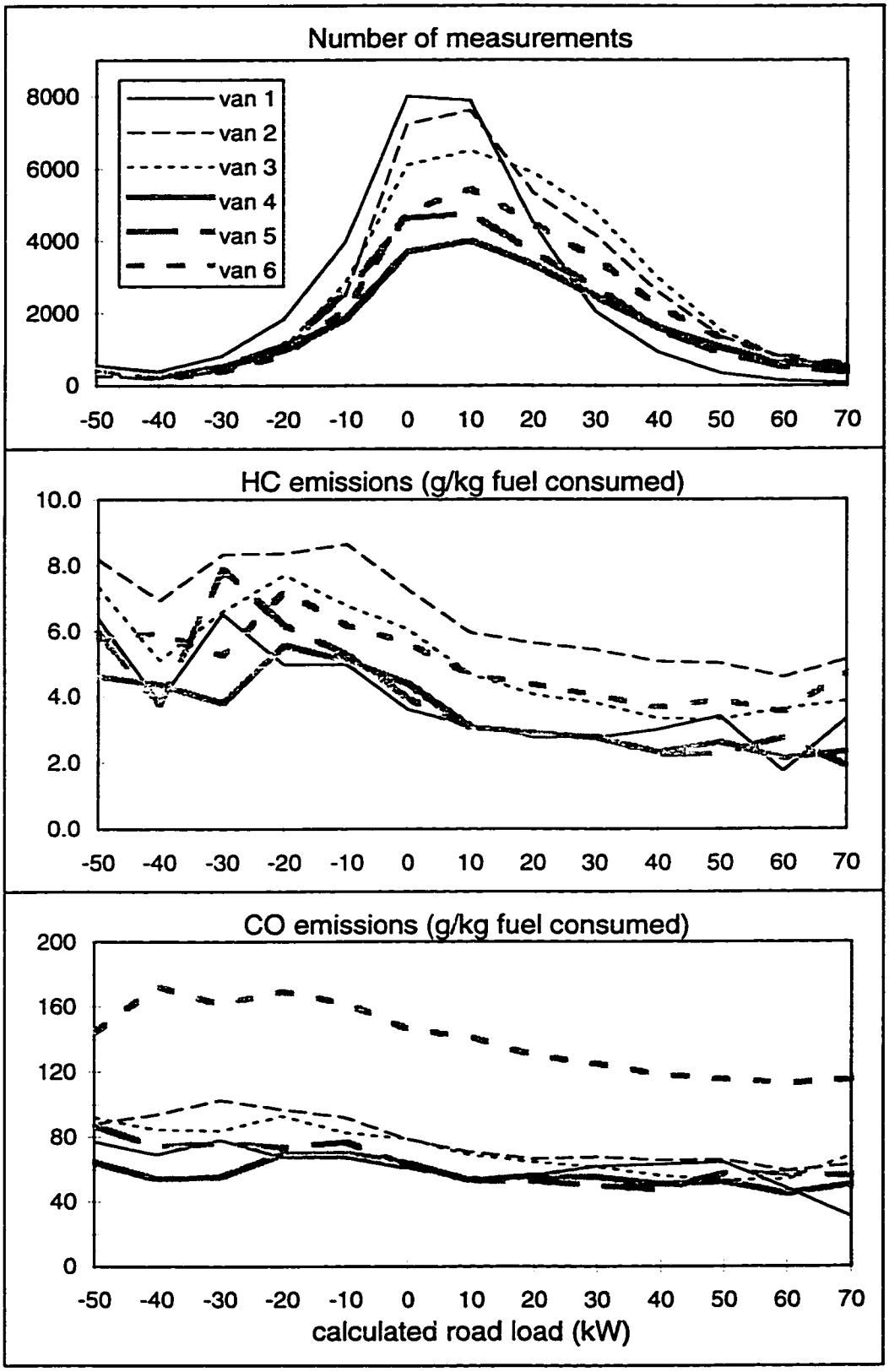

Figue 5.2. Dependence of fuel-normalized HC and CO emission factors on calculated road load, as measured by remote sensing in Phoenix, AZ.

loads may result from imprecision in the acceleration measurements. For example, a 1 mph s^{-1} error in an acceleration measurement at a measured speed of 45 mph yields a 14 kW overestimate of road load. Emissions data from accelerating vehicles at the Dobson off-ramp (7% uphill grade) appear to indicate that fleet-average CO and HC emissions do not increase substantially at loads much higher than those encountered during the FTP or even the Unified cycle. This conclusion should be considered as uncertain and the assessment of emissions at very high loads should be determined at sites which are more suited to promote very high load driving (e.g. uphill freeway on-ramps).

The fact that emissions do not appear to change substantially between moderate and high values of road load – on either the positive or negative side – indicates that the most important distinction is between loaded and non-loaded modes, rather than the exact level of load (except, perhaps, for very high load driving). The gradual shift in emissions between positive and negative road loads may result from imprecision in the individual vehicle acceleration measurements.

Figure 5.3 shows the same modal emissions trend when load is expressed in terms of specific power. HC and CO emissions were relatively consistent for all positive values of specific power (corresponding to positive acceleration), and for all negative values of specific power (corresponding to deceleration).

Figure 5.4 shows that much of the observed load effect can be explained by variations in acceleration; the acceleration shown in this figure includes gravitational acceleration associated with driving on hills. As with the trend observed in Fig. 5.3, HC and CO emissions were consistent over a range of positive accelerations and over a range

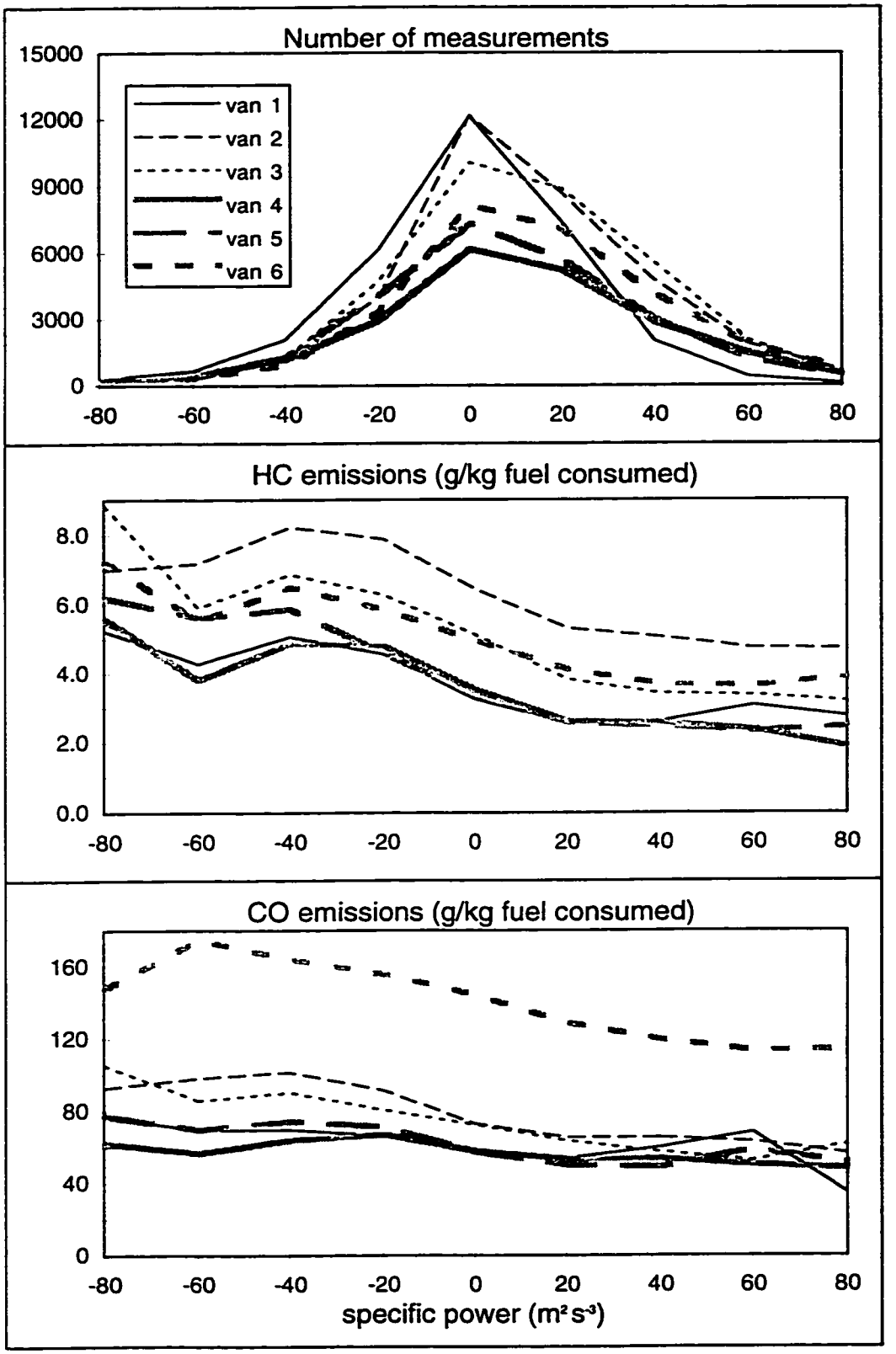

Figure 5.3. Dependence of fuel-normalized HC and CO emission factors on specific power, as measured by remote sensing in Phoenix, AZ.

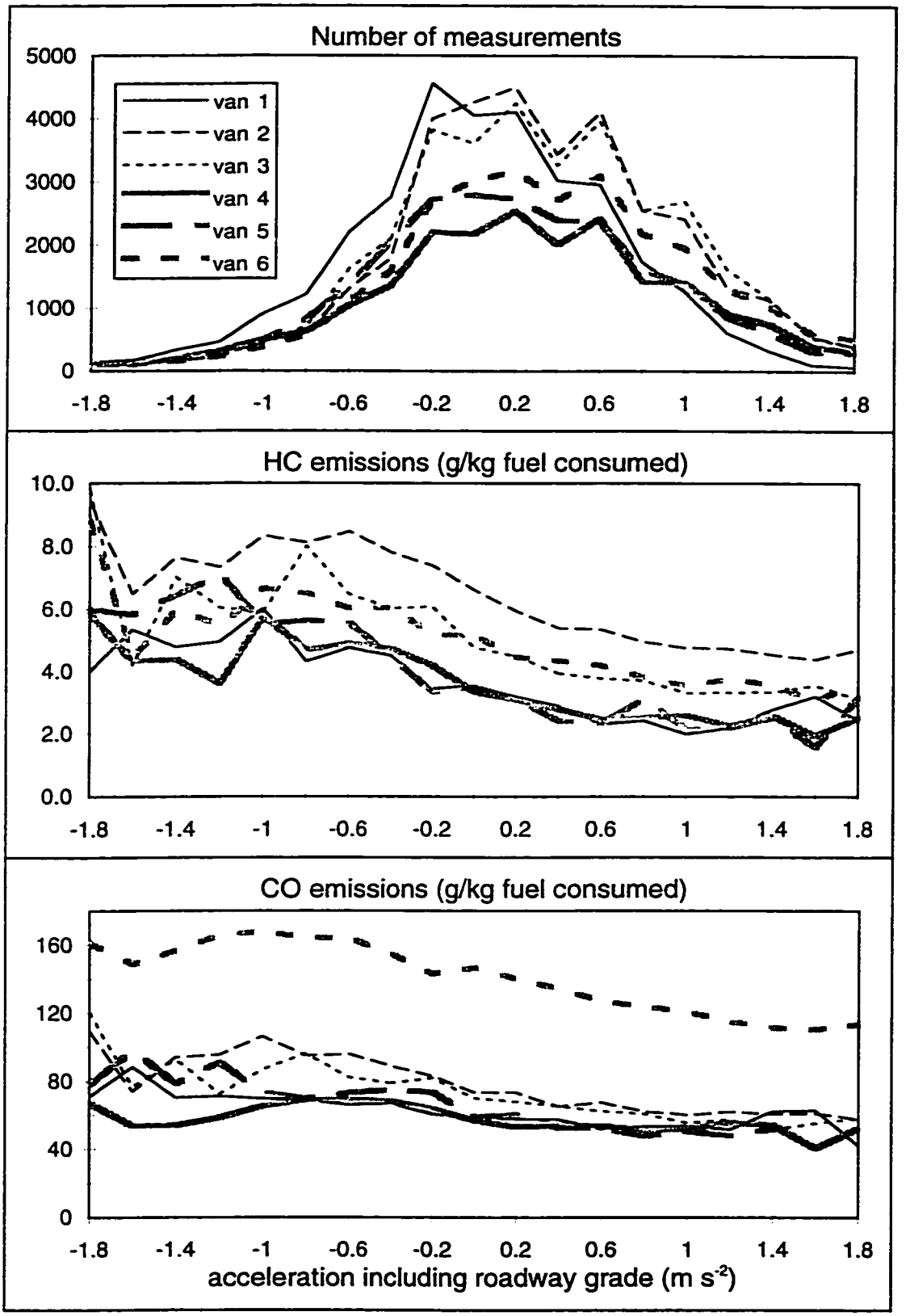

Figure 5.4. Dependence of fuel-normalized HC and CO emission factors on acceleration and roadway grade, as measured by remote sensing in Phoenix, AZ.

of negative accelerations. HC emissions during decelerations were about 50% higher and CO emissions about 20% higher than emissions during positive accelerations.

Figure 5.5 shows that CO emissions were stable when vehicles were measured at speeds of 60-100 km h^{-1} and decreased gradually at lower speeds. HC emissions peaked at moderate speeds, decreased sharply at lower speeds, and decreased gradually at higher speeds. The apparent dependence of emissions on vehicle speed results, in part, because the distribution of accelerations was not identical for all measured speeds. Figure 5.6 shows the mean acceleration for all measurements by each van in each speed bin. The lower accelerations observed in the speed range of ~35-65 km h^{-1} correlate to higher HC emissions at these speeds, whereas the higher accelerations associated with speeds below 35 km h^{-1} and above 65 km h^{-1} produce higher loads and as a result, lower HC emissions. The lower HC emissions observed at higher speeds may also result from higher loads caused by increased aerodynamic drag at higher speed.

Overall, Figures 5.2-5.6 indicate that fuel-normalized emission factors for HC and CO are most sensitive to whether vehicles are measured in a loaded or non-loaded mode, but less sensitive to the exact level of load. For the Arizona remote sensing data, acceleration and roadway grade were the most important determinants of driving mode. Vehicle speed is less useful here an indicator of load due to the relatively narrow distribution of speeds observed at the freeway on-ramps and off-ramps at which vehicles were sampled (see Figure 5.5).

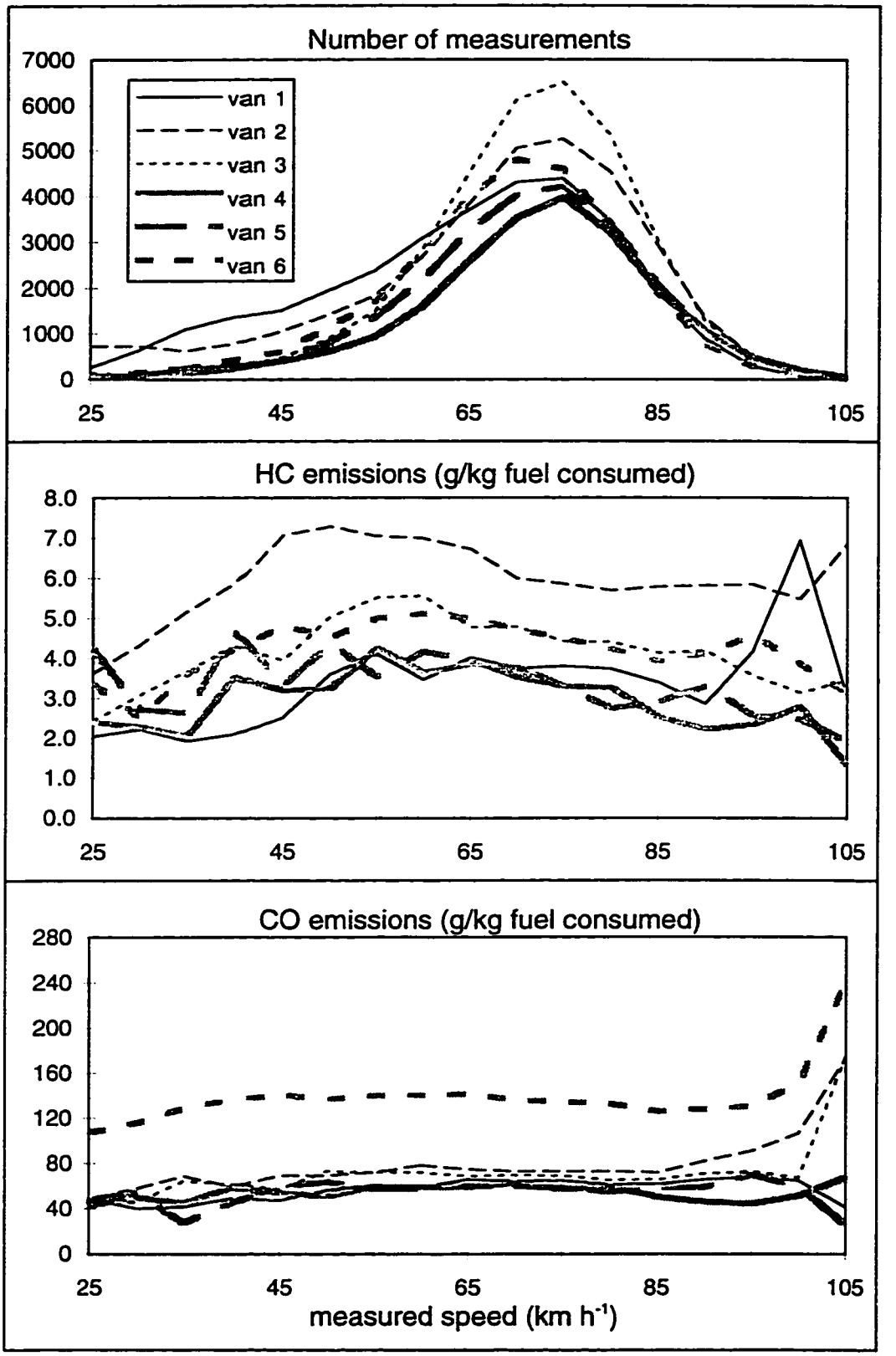

Figure 5.5. Dependence of fuel-normalized HC and CO emission factors on vehicle speed, as measured by remote sensing in Phoenix, AZ.

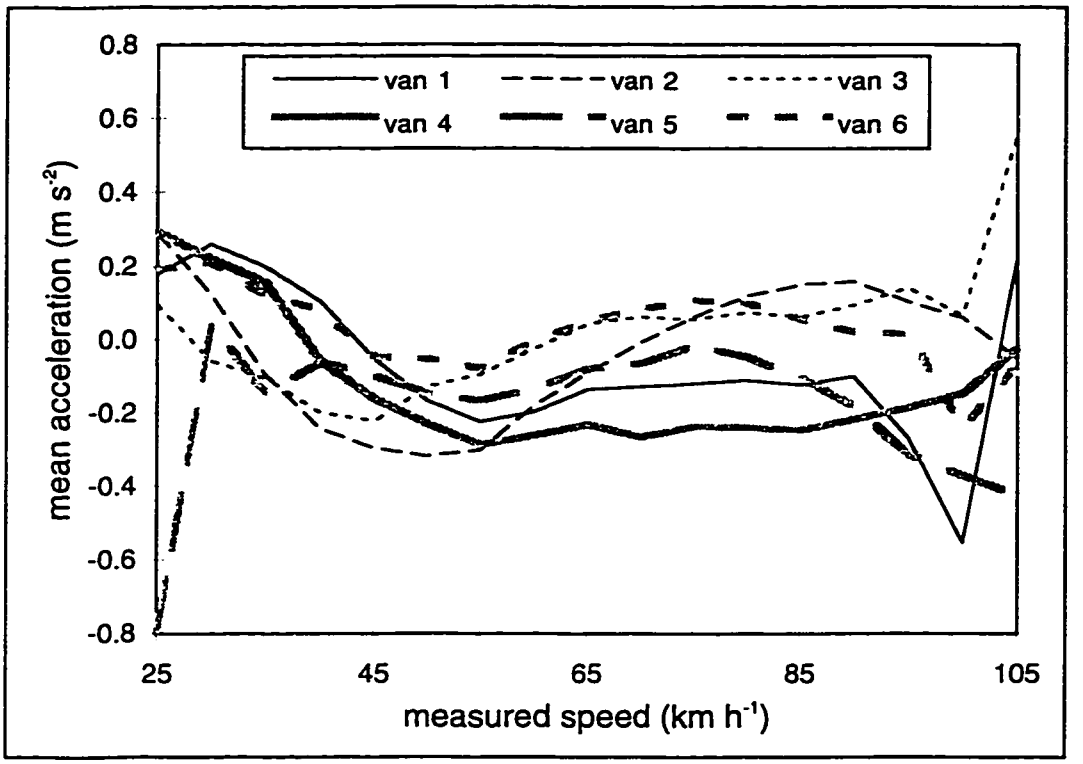

Figure 5.6. Mean acceleration of vehicles measured in each speed bin. Lower accelerations may explain the increase in HC emissions at moderate speeds.

Figure 5.7 shows the results of analyzing each van-day of data independently to quantify the relationship between emissions and load. For each van-day, mean emissions at each road load were divided by the emission levels at 10 kW of road load. The solid lines in Figure 5.7 trace the average of the emissions ratios measured from 64 days of remote sensing data. Figure 5.7 indicates that when normalized to fuel consumption, both HC and CO emissions were consistent over a range of positive loads, but increased during deceleration and braking events. HC emissions decreased by about 10% as load increased from 10 to 30 kW, while HC emissions at higher loads were slightly lower still. HC emissions during braking were about 50% higher than emissions at a moderate positive load. CO emissions during braking were about 20% higher than emissions at moderate road load and the difference between CO emissions at high and moderate loads was very small.

5.3.2 Idle Emissions

Mean ASM and idle emissions results from the California I/M Pilot Program vehicles are shown in Table 5.2. For this vehicle sample, idle emissions were lower than moderate loaded mode emissions by about 20% for CO and by 40-50% for HC. Figure 5.8, which shows the HC emissions distribution for the 618 vehicle sample, indicates that less than 10% of the vehicles contributed over half of the total emissions measured during each test. A similar degree of skewness is observed in on-road vehicle fleets (Zhang et al., 1994).

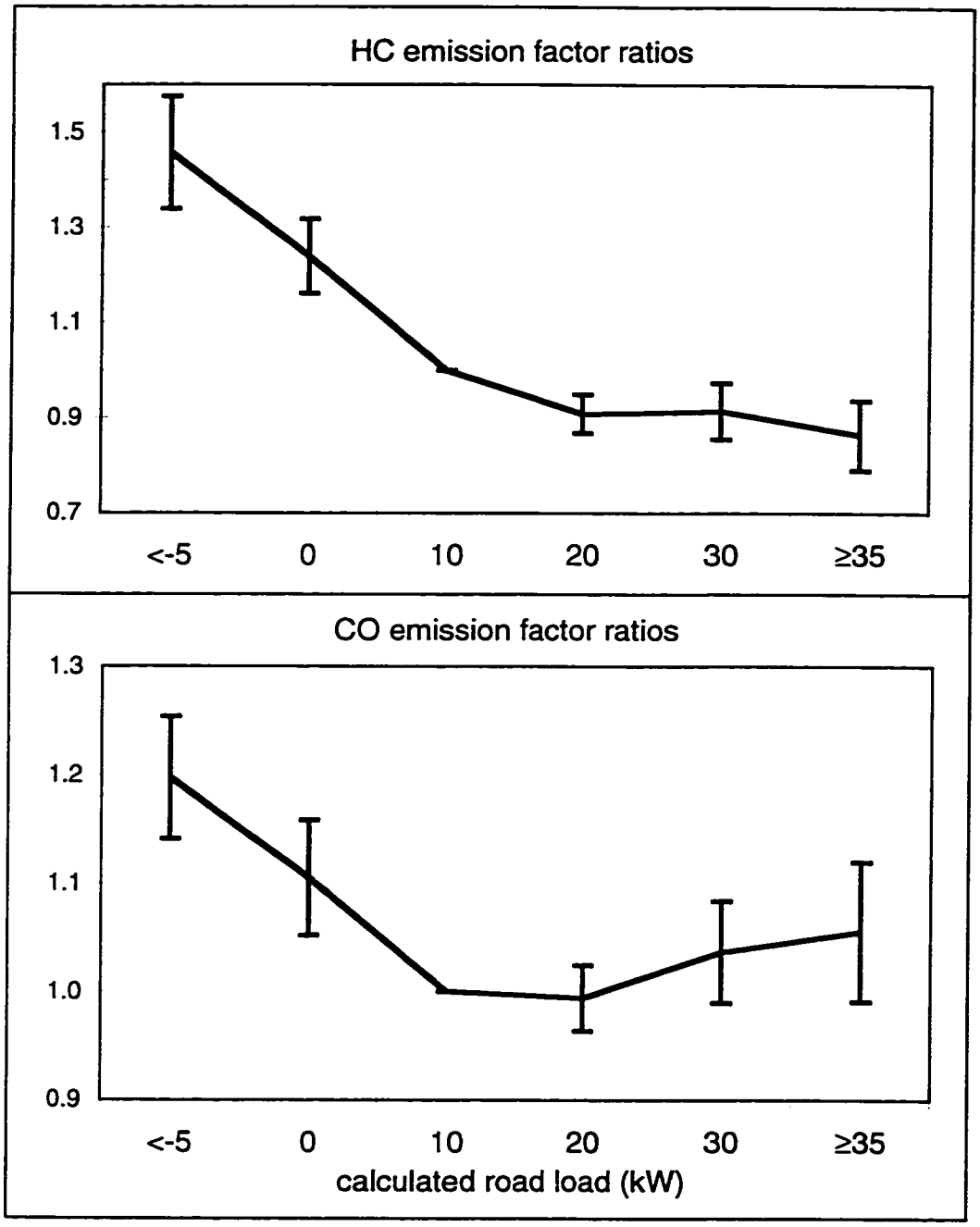

Figure 5.7. Ratios of fuel-normalized emissions measured at a range of road loads to emissions at 10 kW calculated road load. Mean ± 95% CI ratios calculated from 64 van-days of remote sensing measurements in Arizona.

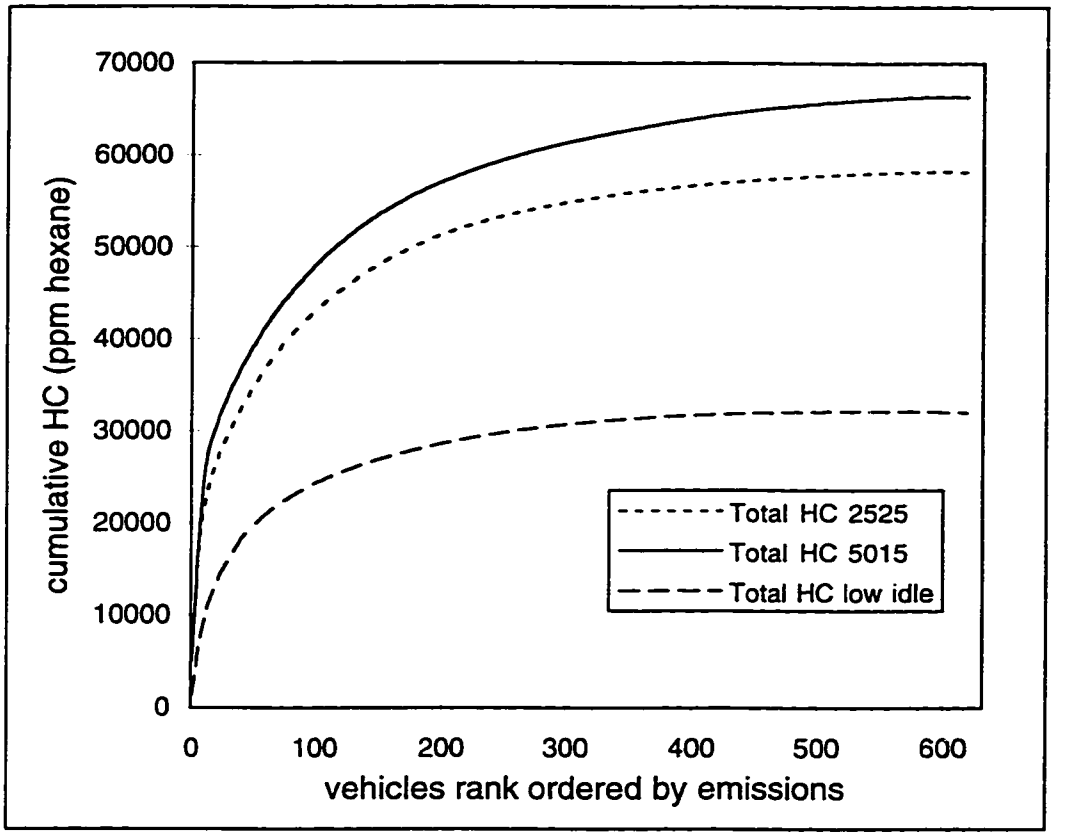

Figure 5.8. Distribution of HC emissions for ASM and idle emissions tests administered during CARB I/M Pilot program.

5.3.3 Modal Distribution of Fuel Use

The distributions of time spent and fuel used in various driving modes of the Unified cycle are shown in Table 5.3. Loaded modes occur during 63% of driving time but account for 87% of fuel energy use; of this total, approximately 10-15% of the fuel is used during loads which are greater than the maximum load of the FTP test. Idle and braking occupy 40% of the time, but only 12% of total fuel use occurs in these modes. Much less fuel is used during idle and braking events because the fuel use rate during each second of idle or braking is much lower than the fuel use rate during loaded mode driving.

Table 5.3. Apportionment of fuel use by driving mode[a] and comparison of emissions measured at 10 kW to emissions averaged over the full distribution of driving in California's Unified driving cycle.

Mode	Criteria[b]	Fraction driving time (%)	Fraction fuel used (%)	Fraction RSD msmts (%)	Ratio of emissions at stated mode to 10 kW emissions[c] HC	CO
Idle	Speed < 1mph	23	7	-	0.5-0.6	0.8
Braking	$P_b \leq -5$ kW	17	5	17	1.46±0.12	1.20±0.06
Loaded	$-5 \leq P_b < 5$ kW[d]	23	12	20	1.24±0.08	1.11±0.05
	$5 \leq P_b < 15$ kW	23	33	21	1	1
	$15 \leq P_b < 25$ kW	9	21	16	0.91±0.04	0.99±0.03
	$25 \leq P_b < 35$ kW	4	15	12	0.91±0.06	1.04±0.05
	$P_b \geq 35$ kW	1	5	14	0.86±0.07	1.06±0.06
Emissions during all driving vs. emissions at 10 kW					0.96±0.04	1.00±0.03

(a) Based on California's Unified driving cycle, which simulates the distribution of on-road driving conditions observed using chase cars in Los Angeles in 1992.

(b) P_b = road load calculated from measured speed and acceleration, and assuming typical 1993 vehicle characteristics. See text for details.

(c) For loaded modes and braking, values are mean ± 1 std dev of emissions ratios measured on 64 van-days of remote sensing in Phoenix, AZ in 1996-97. Figures 5.2-5.6 include data from 66 days; data from two remote sensors which were used for 1 day each are not included in this table.

(d) Positive loads result when engine friction of ~7 kW is added to the calculated road load. The fraction of time and fuel used during idle events was subtracted from this group.

For example, about 55 kJ of fuel energy is expended during each second that a vehicle encounters a road load of 20 kW, whereas only about 7 kJ are required for each second of idle operation. These results indicate that loaded modes should be emphasized when fuel-normalized emission factors are to be measured from the on-road fleet.

Table 5.3 also shows the ratio of HC and CO emissions in each mode to emissions at 10 kW of road load. These ratios are combined with the fraction of fuel used during each mode to estimate the relationship between fleet-average emission factors measured from vehicles at moderate road load and emission factors weighted by the distribution of on-road fuel use. For both HC and CO, the measurement of emissions at 10 kW provides a reasonable estimate of emissions averaged over almost the entire distibution of on-road driving (recall that the highest load driving may be underrepresented in the Unified cycle). Fleet-average emissions measured at 20 kW of road load would be similar for CO, and only about 10% lower for HC. This is true because both HC and CO emissions are consistent over the range of loaded modes during which most fuel use occurs. The slight changes in CO emissions during braking and idle are not very important since very little fuel is used during these modes. The higher CO emissions during braking are in any case offset by the lower emissions during idle. Likewise, the higher HC emission factors during braking and near-zero road loads are offset by the lower emission factors during idle and higher road loads.

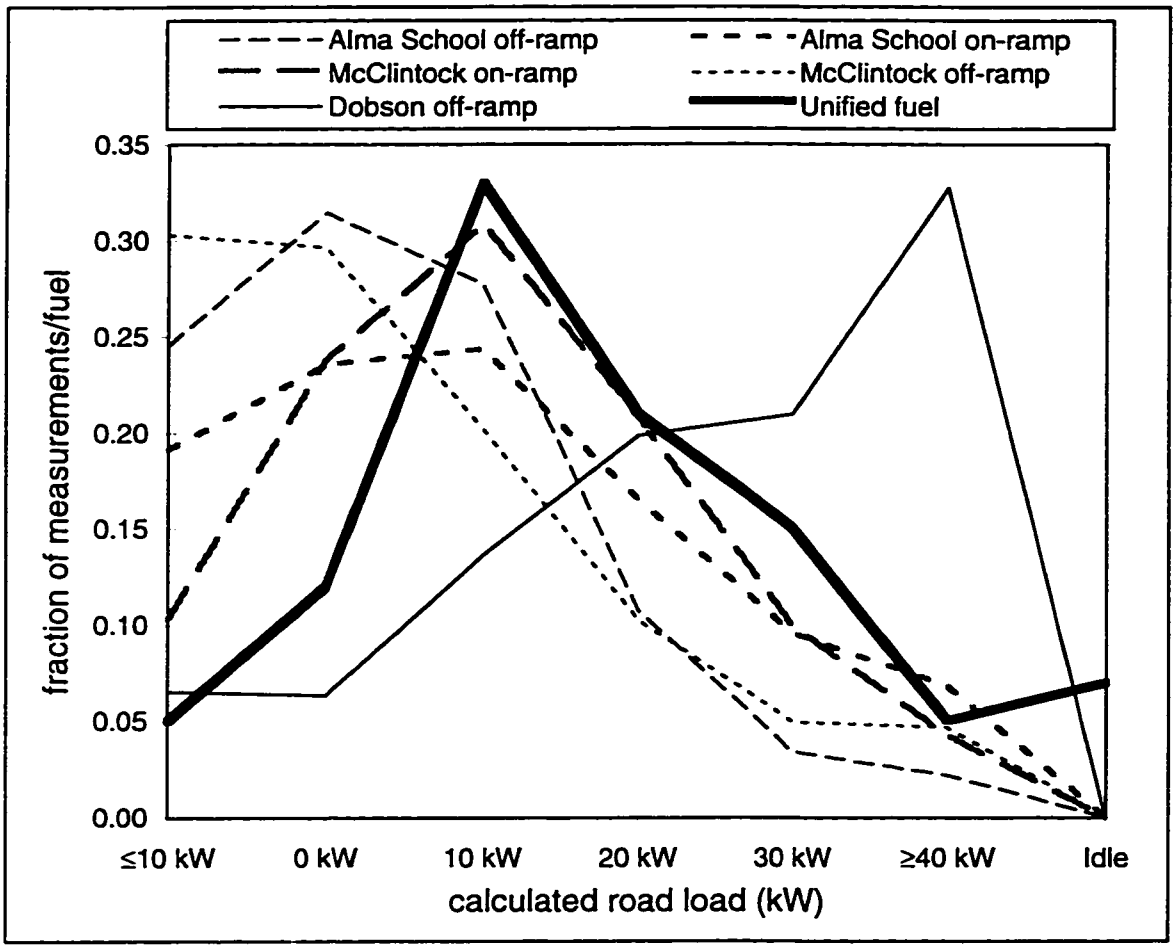

Figure 5.9. Distribution of activity by driving mode at several remote sensing sites in Arizona. The distribution of fuel use during CARB's Unified cycle is presented as a representation of how overall fuel use is distributed among on-road driving modes.

5.3.4 Distribution of Driving Modes Measured by On-Road Remote Sensors

Figure 5.9 compares the distribution of road loads observed at several of the remote sensing sites in Arizona to the distribution of fuel used in each driving mode during the Unified cycle. The distribution of road loads was roughly similar at all remote sensing sites except the Dobson off-ramp, at which much higher loads were caused by the 7% uphill grade. The distribution of driving modes at the McClintock on-ramp was most similar to the distribution of fuel use during on-road driving, as represented by the Unified cycle, even though no idle operation was observed at the remote sensing site. The modal distribution at the Dobson on-ramp was shifted to lower loads because of the downhill grade of the ramp. A higher percentage of driving at lower road loads was observed at the Alma School and McClintock off-ramps; average HC and CO emissions measured at these sites may therefore be higher than emissions during all Unified cycle driving. These results show that it is possible to select remote sensing sites at which the distribution of driving is *similar* to the distribution of fuel use during the Unified cycle.

5.3.5 Limitations of this Work

The data analyzed for this study included only HC and CO emissions measurements; no similarly representative NO_x emissions data were available. On an individual vehicle basis, NO_x formation is known to depend on load (Heywood, 1988). Fleet-average exhaust emission rates of NO_x may be influenced by many addtional factors, including the malfunction rate of fuel-delivery systems and in-use catalyst efficiencies (Wenzel and

Ross, 1998). The dependence on driving mode of fleet-average NO_x emissions should be determined from an analysis of a large, representative set of on-road emissions data.

This analysis may not have assessed completely the effects of very high road loads on fuel-normalized emission factors. The remote sensing sites in Arizona were selected to minimize the number of vehicles observed driving at very high loads, and as mentioned previously, some of the very high road loads shown in Figure 5.2 may result from imprecision in the acceleration measurements. Previous studies have indicated that very high load driving can cause otherwise low-emitting vehicles to run fuel-rich, which leads to much higher emissions of CO and HC (Kelly and Groblicki, 1993; St. Denis et al., 1994; Goodwin and Ross, 1996). The emissions measurements from Arizona suggest that fuel-normalized emissions of CO and HC do not increase substantially at very high loads. Additional measurements of on-road emissions from vehicles driving at very high loads may be needed to resolve this discrepancy. For the purpose of estimating fuel-normalized emissions for all on-road driving, better estimates of the frequency of the highest load driving are required.

Ideally, the relationship between emissions during idle and emissions during loaded modes would have been determined from a larger, on-road test fleet. This is not seen as a critical issue because the analysis of fuel use by driving mode demonstrated the relative unimportance of idle emissions in determining fleet-average emissions over the full range of in-use vehicle operation.

5.4 CONCLUSIONS

The analysis presented here demonstrates that fuel-normalized emissions of HC and CO are consistent over a wide range of positive vehicle loads, and that loaded-mode driving is most relevant when estimating on-road vehicle emissions. The bulk of this analysis was based on 175,000 combined emissions, speed, and acceleration measurements made at 6 on-road sites over a one year period in Phoenix, AZ. These results support the use of remote sensing measurements of vehicles under moderate load to calculate fuel-based motor vehicle exhaust emission inventories.

5.5 REFERENCES

An, F. and M. Ross (1993). A model of fuel economy and driving patterns. *SAE Tech. Pap. Ser.* **939328**.

Brown, H. J., C. Kirschenmann and D. Nelson (1996). Influence of real world vehicle operating modes on remote sensing measurements. *Sixth CRC On-Road Vehicle Emissions Workshop*, San Diego, CA, March 18-20, 1996. Coordinating Research Council, Atlanta, GA.

Brown, J. (1997). *Personal Communication.* Hughes Santa Barbara Research Center, Santa Barbara, CA.

CARB (1995). *Methodology for estimating emissions from on-road motor vehicles, MVEI 7G.* Mobile Source Emission Inventory Branch, California Air Resources Board, Sacramento, CA. Volumes I-V.

Cox, F., J. Walls and M. Carrel (1996). Assessment of remote sensing device (RSD) emissions measurement without vehicle pullover option. *Sixth CRC On-Road Vehicle Emissions Workshop*, San Diego, CA, March 18-20, 1996. Coordinating Reseach Council, Atlanta, GA.

Cullen, K. and T. Liberty (1996). Summer-time emissions from modern vehicles with A/C operating. *Sixth CRC On-Road Vehicle Emissions Workshop*, San Diego, CA, March 18-20, 1996. Coordinating Research Council, Atlanta, GA.

Gammariello, R. T. and J. Long (1993). An emissions comparison between the unified cycle and the federal test procedure. *The Emissions Inventory: Perception and Reality*, Pasadena, CA, October 18-20, 1993. Air & Waste Management Association, California Air Resources Board, and The South Coast Air Quality Management District.

Goodwin, R. W. and M. H. Ross (1996). Off-cycle exhaust emissions from modern passenger cars with properly-functioning emissions controls. *SAE Tech. Pap. Ser.* **960064**.

Grubbe, D. (1998). *Personal Communication.* Arizona Department of Environmental Quality, Phoenix, Arizona.

Heywood, J. B. (1988). *Internal Combustion Engine Fundamentals.* McGraw-Hill Publishing Company: New York, NY.

Hughes Environmental Systems (1994-5). *State of Arizona vehicle emission remote sensing program: Site selection plan.* Draft Report to the Arizona Department of Environmental Quality, Phoenix, Arizona, Volumes 1-3.

Jack, M. (1996). Remote sensing (RES) - an adjunct to I/M HEV identification and clean car pre-screening. *Sixth CRC On-Road Vehicle Emissions Workshop*, San Diego, CA, March 18-20, 1996. Coordinating Research Council, Atlanta, GA.

Kelly, N. A. and P. J. Groblicki (1993). Real-world emissions from a modern production vehicle driven in Los Angeles. *J. Air Waste Manage. Assoc.* **43**:1351-1357.

Kirchstetter, T. (1998). *Impact of reformulated fuels of motor vehicle emissions.* Ph.D. Dissertation, Department of Civil and Environmental Engineering, University of California, Berkeley, CA.

Kite, C., P. A. Walsh and M. O' Connor (1997). Overview of the Texas 1996 remote sensing feasibility study. *Seventh CRC On-Road Vehicle Emissions Workshop*, San Diego, CA, April 9-11, 1997. Coordinating Research Council, Atlanta, GA.

Klausmeier, R., S. Kishan, A. Burnette and J. McFarland (1995). *Evaluation of the California pilot inspection/maintenance (I/M) program.* Radian Corportation, Austin, TX. Draft Final Report to the California Bureau of Automotive Repair, Sacramento, CA.

Lawson, D. R., P. J. Groblicki, D. H. Stedman, G. A. Bishop and P. L. Guenther (1990). Emissions from in-use motor vehicles in Los Angeles: a pilot study of remote sensing and the inspection and maintenance program. *J. Air Waste Manage. Assoc.* **40**:1096-1105.

Lyons, C. E. and D. H. Stedman (1991). *Remote sensing enhanced motor vehicle emissions control for pollution reduction in the Chicago metropolitan area: siting*

and issue analysis. University of Denver, Atmospheric Science Center, Denver, CO. Report to the Illinois Department of Energy and Natural Resources, Office of Reseach and Planning, Springfield, IL. ILENR/RE-AQ-91/15.

O'Connor, M., P. A. Walsh and C. Kite (1997). 1996 Texas remote sensing feasibility study: data analyses and I/M implications. *Seventh CRC On-Road Vehicle Emissions Workshop*, San Diego, CA, April 9-11, 1997. Coordinating Research Council, Atlanta, GA.

Patel, D., S. Magbuhat, J. Long and M. Carlock (1996). *Comparison of the IM240 and ASM tests in CARB's I&M pilot program*. Mobile Source Division, California Air Resources Board.

Petherick, D. (1997). Ontario's vehicle emissions pilot project - a detailed look at the final results for "CleanScreen" and IM240. *Seventh CRC On-Road Vehicle Emissions Workshop*, San Diego, CA, April 9-11, 1997. Coordinating Research Council, Atlanta, GA.

Pierson, W. R., A. W. Gertler, N. F. Robinson, J. C. Sagebiel, B. Zielinska, G. A. Bishop, D. H. Stedman, et al. (1996). Real-world automotive emissions – summary of recent tunnel studies in the Fort McHenry and Tuscarora Mountain tunnels. *Atmos. Environ.* **30**:2233-2256.

Rendahl, C. S. (1998). *Personal Communication*. Remote Sensing Technologies, Inc.

Ross, M. (1994). Automobile fuel consumption and emissions: Effects of vehicle and driving conditions. *Annual Review Energy Environment* **19**:75-112.

Ross, M. and F. An (1993). The use of fuel by spark ignition engines. *SAE Tech. Pap. Ser.* **930329**.

St. Denis, M. J., P. Cicero-Fernandez, A. M. Winer, J. W. Butler and G. Jesion (1994). Effects of in-use driving conditions and vehicle/engine operating parameters on "off-cycle" events: comparison with federal test procedure conditions. *J. Air Waste Manage. Assoc.* **44**:31-38.

Stedman, D. H. and G. A. Bishop (1990). *An analysis of on-road remote sensing as a tool for automobile emissions control*. University of Denver, Chemistry Department, Denver, CO. Report to the Illinois Department of Energy and Natural Resources Office of Research and Planning, Springfield, IL. ILENR/RE-AQ-90-05.

Walsh, P. A. and A. W. Gertler (1997). *Texas 1996 remote sensing feasibility study*. Desert Research Institute, Energy and Environmental Engineering Center, Reno, NV. Final Report to the Texas Natural Resources Conservation Commission, Austin, Texas.

Wenzel, T. and M. Ross (1998). Characterization of recent-model high-emitting automobiles. *SAE Tech. Pap. Ser.* **981414.**

Zhang, Y., G. A. Bishop and D. H. Stedman (1994). Automobile emissions are statistically gamma-distributed. *Environ. Sci. Technol.* **28**:1370-1374.

CHAPTER SIX

Exhaust Emissions in the South Coast Air Basin

6.1 INTRODUCTION

Since 1991, new programs to reduce motor vehicle emissions have been implemented in California. New vehicle standards changed in 1994 to require improved control of reactive organic gases, nitrogen oxides, and exhaust particle emissions, and enhanced durability of emission controls for all pollutants (Calvert et al., 1993). California's reformulated gasoline program, which was implemented in two phases in 1992 and 1996, has led to significant changes in fuel formulation intended to reduce the mass, toxicity, and atmospheric reactivity of motor vehicle emissions (Kirchstetter, 1998). California's inspection and maintenance (smog check) program also has been enhanced with the goal of effectively identifying and repairing vehicles with malfunctioning emission control systems (Patel et al., 1996). Additional emissions reductions may have resulted from the retirement of older vehicles with less sophisticated and robust emissions control equipment. The emission control programs and fleet turnover are estimated by CARB (1996) to have reduced motor vehicle exhaust emissions significantly between 1991 and 1997.

The objective of this chapter is to use the fuel-based approach to estimate stabilized exhaust CO and VOC emissions for the Los Angeles area in summer 1997. Fuel-based inventory results for 1997 are compared to the 1991 fuel-based estimates calculated in Chapter 2 to assess CO emission reductions between 1991 and 1997. Emission factors measured on-road during 1991 and 1997 are compared as a function of vehicle age. The 1997 fuel-based inventory results also are compared to CO and VOC emissions estimates of California's MVEI 7G model. The relationship between emissions and the income level of vehicle owners is examined using census economic data resolved to the zip code level. Motor vehicle exhaust emissions are estimated for 1997 to coincide with the Southern California Ozone Study (SCOS97). SCOS97 was an intensive field study of ambient air pollutant concentrations, pollutant emission sources, and meteorological variables that was designed to update and improve understanding of air pollution problems in Southern California.

6.2 APPROACH

6.2.1 Overview

Fuel-based estimates of stabilized exhaust CO and VOC emissions from motor vehicles in California's South Coast Air Basin (SoCAB) were developed following the approach outlined in Chapter 2. Emission factors and activity for vehicles of each model year were calculated from over 60,000 on-road remote-sensor measurements made at 35 locations around the Los Angeles area. Total fuel use was estimated from fuel sales records and apportioned using average fuel economy for each vehicle model year.

6.2.2 Emission Factors

On-road vehicle emissions were measured by the Mobile Source Operations Division of the California Air Resources Board at 38 sites in the greater Los Angeles area between May and October of 1997 (CARB, 1998). Exhaust concentrations of CO_2, CO, and HC were measured using an infrared remote emissions sensor manufactured by Hughes Santa Barbara Research Center (Jack, 1996; CARB, 1998); a description of the predecessor to the Hughes sensor is available in the literature (Stephens and Cadle, 1991). The system used by CARB was equipped with dual independent sensors for duplicate emissions measurements and multiple video cameras to record the license number of each vehicle passing through the infrared beams (CARB, 1998). License numbers were identified with pattern recognition software and subsequently matched to Department of Motor Vehicles registration records to obtain the make, model year, and zip code where the vehicle was registered. About half of the automatically read license numbers were verified and corrected when necessary by CARB personnel (CARB, 1998). A sample of this data showed the license plate reader to be accurate for 95% of the plates read; of the 5% of license numbers which contained an error, only 1 in 4 resulted in the assignment of an incorrect model year (CARB, 1998).

Exhaust concentration and vehicle data for 36 sampling days (35 remote sensing sites) were provided by CARB (Long, 1997). The data included over 60,000 valid emissions measurements and vehicle registration data for all but 7,900 of the vehicles measured. Although vehicle classification data were not included in the dataset, it was assumed that most of the vehicles sampled were passenger cars, sport utility vehicles and

light-duty trucks. A small number of medium-duty trucks may also have been sampled. The location of the infrared beam limits sampling to vehicles with rear exhaust pipes which are about 30 cm from the ground. The sampling sites are listed in Table 6.1, along with the number of valid emissions measurements at each site. The sites were distributed geographically throughout the SoCAB, and as described below, the distribution of vehicles sampled by remote sensing was representative of overall vehicle and economic distributions in the SoCAB.

Mass emission factors were computed using eq 6.1:

$$E_P = \frac{Q_P}{1+\left(CO/CO_2\right)+3\cdot\left(HC/CO_2\right)} \cdot \frac{w_c \rho_f}{12} \cdot M_P \qquad (6.1)$$

where E_P is the HC or CO emission rate [g L^{-1}]; Q_P is the HC/CO_2 or CO/CO_2 molar exhaust ratio measured by the remote sensor; w_c = 0.85 is the carbon mass fraction and ρ_f = 750 g L^{-1} is the density of California reformulated gasoline (Kirchstetter, 1998); M_P is the molecular mass of the pollutant being considered (28 for CO, 44 for HC as propane); and 12 is the atomic mass of carbon. The first quotient of eq 6.1 reduces to the molar ratio of CO or HC to total carbon atoms in vehicle exhaust; the second set of terms defines the molar concentration of carbon atoms per liter of unburned gasoline. The remote sensor used by CARB was calibrated with propane and HC concentrations were reported as propane equivalents; eq 6.1 thus includes a factor of 3 in the denominator to convert from moles of propane to moles of carbon. The HC/CO2 ratio in the denominator could also be multiplied by a factor of 2 to account for the partial VOC

Table 6.1. Remote sensing sampling locations as described in CARB (1998).

Date	City	Road/Cross St.	N
5/6/97	South El Monte	Rosemead Blvd. near Rush St.	3407
5/7/97	El Monte	Santa Anita Ave. near Valley Blvd.	1156
5/8/97	Montebello	Potrero Grande	1367
5/9/97	Montebello	Montebello and Madison	1738
5/16/97	San Gabriel	San Gabriel Blvd.	2744
6/6/97	Long Beach	Studebaker Rd. near Sterns	1352
7/15/97	Irwindale	Arrow Highway near Irwindale	2441
7/16/97	El Monte	Peck Rd. near Mtn. View	1357
7/17/97	Montebello	Paramount Blvd.	2616
7/18/97	Montebello	Paramount Blvd.	2006
8/13/97	Westminster	Garden Grove Blvd.	1174
8/14/97	Lakewood	Harvey Way near Woodruff Ave.	669
8/15/97	Santa Ana	Flower St. near Santa Clara	700
8/18/97	La Mirada	Marquardt St. near Imperial Hwy.	606
8/19/97	Rolling Hills Estates	Palos Verdes Dr. near Roanwood	2095
8/20/97	Anaheim Hills	Fairmount Blvd. nr Santa Ana Canyon	589
8/21/97	Newport Beach	17th St. near Superior	2343
8/22/97	Garden Grove	Nelson St. near Lamosen	970
8/26/97	Southgate	Southern Ave.	1163
8/27/97	Signal Hill	Obispo Ave.	1220
9/2/97	Chatsworth	Topanga Blvd.	3170
9/3/97	Northridge	Reseda Blvd. near Devonshire	1660
9/4/97	Woodland Hills	Valley Circle	1472
9/5/97	Granada Hills	Sepulveda Blvd.	1717
9/19/97	Claremont	Baseline Rd. near Indian Hill Ave.	1164
9/23/97	Claremont	Arrow Hwy. near Geneva St.	2082
9/26/97	Riverside	Chicago Ave. near Linden	1650
9/30/97	North Hollywood	Riverside Dr.	1263
10/1/97	West Hills	Valley Circle Dr.	1483
10/2/97	Lawndale	Manhattan Beach Blvd. near Prairie	2248
10/3/97	Huntington Beach	Glodenwest Blvd. near Summit St.	2421
10/6/97	Lawndale	Prairie St. near 154th St.	2227
10/7/97	Long Beach	Paramount Blvd. near Artesia Blvd.	1721
10/8/97	El Segundo	Aviation near El Segundo	1872
10/9/97	Downey	Lakewood Blvd. near Bellflower Rd.	1792
10/10/97	Lynwood	Imperial Hwy.	2176

response of IR sensors; however, since less than 1% of the fuel carbon is emitted as organic carbon, this adjustment will have little effect on calculated emissions factors.

HC emission factors computed using eq 6.1 were scaled up to reflect the total mass of VOC in vehicle exhaust. Scaling was necessary because infrared analyzers do not respond equally to all individual VOC (Stephens et al., 1996). As discussed in Chapter 4, remote sensors calibrated with propane or hexane report most of the alkane mass, but only a fraction of the alkenes and aromatics that would be measured by a flame ionization detector. Since reformulated gasoline was in use at the time of this study, infrared HC measurements were multiplied by a factor of 2.0±0.1 to calculate fleet-average VOC emission factors.

6.2.3 Fuel Use and Vehicle Activity

When calculating a fuel-based inventory, vehicle activity is measured by fuel use. California gasoline sales totalled 2.7×10^{10} L during the period May 1 through October 31, 1997 (USDOT, 1998). The fraction of this total used in the SoCAB was estimated at 42%, based on the fraction of California population (44%) and vehicle registrations (40%) which are in the SoCAB. Gasoline use by construction and farm equipment, boats, and other off-road engines has been estimated at 3% of the statewide total on a yearly basis (Macias, 1994). Motorcycles and gasoline-powered heavy-duty trucks were estimated to account for 2% of SoCAB gasoline use during summer 1997 (CARB, 1996). Deducting these amounts, average summertime gasoline use by passenger cars, light-duty trucks, and medium-duty trucks in the SoCAB is estimated at 5.9×10^7 L day^{-1}.

The previous estimate of summer 1991 SoCAB gasoline use (see Chapter 2) has been revised to be consistent with a change in the definition of heavy-duty trucks between versions 7F and 7G of the MVEI model (CARB, 1993; CARB, 1995). Estimated gasoline use by heavy-duty trucks dropped from 11% to 2% of total gasoline sales corresponding to a rise in the minimum weight of heavy-duty trucks from 3864 kg (8500 lb) to 6400 kg (14,000 lb) gross vehicle weight. The revised estimate of gasoline use in the SoCAB in summer 1991 is 5.5×10^7 L day^{-1}, which indicates an increase of 8% in gasoline use by passenger cars and light/medium-duty trucks in the SoCAB between summer 1991 and summer 1997.

Remote sensors sample vehicles of various classes and model years according to the frequency with which they travel past the monitoring site. A simple average of vehicle emissions measured by remote sensing thus yields a travel-weighted average emission factor of the vehicles measured. To calculate a fuel-weighted fleet-average emission factor, the relative fuel economy of each vehicle class and model year must be considered. Consideration of vehicle age is most important for pre-1980 vehicles, which on average have higher emissions and lower fuel economy than newer vehicles. The distribution of travel by vehicle model year was calculated directly from the vehicle populations observed at 35 remote sensing sites. Relative fuel economies were estimated using measurements of new vehicle fuel economy weighted by nationwide sales of each vehicle model (Murrell et al., 1993; Davis, 1997). Table 6.2 shows the sales-weighted average fuel economy for new passenger cars and light trucks, along with the number of new cars

and trucks sold for each model year (Automotive News, 1996; Automotive News, 1998). These data were combined to calculate a sales-weighted average fuel efficiency of the light-duty vehicle fleet for each model year, which is also shown in Table 6.2. New vehicle fuel economy measurements have been shown to overstate in-use fuel economy, but the bias has been shown to be consistent from year to year (Mintz et al., 1993); the data presented in Table 6.2 can thus be used as a relative measure of fuel economy.

The fraction of total fuel f_i used by vehicles of each model year i was estimated as:

$$f_i = \frac{\left(v_i / FE_i\right)}{\sum_i \left(v_i / FE_i\right)} \tag{6.2}$$

where v_i is the fraction of travel by vehicles of each model year ($v_i = n_i/N$ where n_i is the count of model year i vehicles and N is the total number of remote sensor measurements) and FE_i is the average fuel economy of model year i vehicles.

6.2.4 Combining Activity and Emission Factors

Fleet-average emission factors $\overline{E_P}$ were calculated using the fuel fractions f_i and emission factors $E_{P,i}$ for each vehicle model year:

$$\overline{E_P} = \sum_i f_i E_{P,i} \tag{6.3}$$

Total stabilized exhaust emissions of CO and VOC were calculated as the product of the fleet-average emission factors $\overline{E_P}$ and total gasoline use by cars and trucks in the SoCAB. Mass emissions from vehicles of each model year were calculated as the product of fuel use and the emission factors for each model year.

Table 6.2. New vehicle sales and sales-weighted fuel economy of cars and light trucks.

Model Year	Fuel economy[a] (km L^{-1})		New vehicle sales[b] (1000s)		Light-duty vehicle fuel economy[c] (km L^{-1})
	Cars	Trucks	Cars	Trucks	
1974	6.0	5.8	8580	2399	6.0
1975	6.7	5.8	8500	2249	6.5
1976	7.4	6.1	9961	2915	7.1
1977	7.7	6.6	11012	3350	7.4
1978	8.4	6.4	11136	3771	7.8
1979	8.6	7.7	10538	3228	8.4
1980	10.3	7.8	8961	2227	9.7
1981	11.0	8.5	8519	2036	10.4
1982	11.3	8.7	7962	2392	10.6
1983	11.2	8.8	9153	2996	10.5
1984	11.4	8.7	10333	3878	10.5
1985	11.7	8.8	10983	4419	10.7
1986	11.9	9.1	11409	4618	10.9
1987	12.1	9.2	10186	4709	11.0
1988	12.2	9.0	10554	4878	11.0
1989	12.0	8.8	9770	4779	10.7
1990	11.9	8.8	9296	4591	10.7
1991	12.0	9.0	8170	4159	10.8
1992	11.8	8.8	8211	4675	10.5
1993	12.0	8.9	8520	5398	10.6
1994	12.0	8.8	8991	6098	10.5
1995	12.1	8.7	8636	6130	10.4
1996	12.1	8.8	8529	6611	10.4
1997	12.1	8.6	8289	6871	10.2

(a) Sales-weighted average fuel economy of new cars and trucks; calculated from combined city/highway fuel economy reported by the manufacturers to the EPA and yearly U.S. sales estimates. Data for model years 1979-1997 reported in Davis (1997); data for model years 1974-78 from Murrell et al. (1993).
(b) New vehicle sales for each vehicle class (Automotive News, 1996; Automotive News, 1998).
(c) Composite sales-weighted fuel economy of passenger cars and light-duty trucks.

6.2.5 Emissions and Activity vs. Income

Sorbo et al. (1996) reported a negative correlation between vehicle emissions and the income level of vehicle owners in the Los Angeles area. Emissions were measured by a remote sensor and income information was obtained by interviews with drivers who were pulled over after their vehicles passed through the sensor. This trend emphasizes the importance of measuring emissions from a sample of vehicles which represent the economic distribution of vehicle owners throughout the SoCAB.

For the current study, economic and vehicle use data were obtained for the zip code level from 1990 U.S. Census lookup tables available on the world wide web (Census Bureau, 1998). Data were obtained for most zip codes in Orange, Los Angeles, San Bernardino, and Riverside counties; data were unavailable for a small number of zip codes in these counties. The SoCAB boundaries encompass 100, 98, 81, and 72%, respectively, of the population living in these counties. The distribution of vehicle use by income was estimated as follows. The number of in-use vehicles in each zip code N_{zip} was calculated as follows:

$$N_{zip} = \sum_{i=1}^{7} \frac{N_i}{i} + \frac{N_{other}}{10} \tag{6.4}$$

where N_i is the number of persons commuting in a vehicle used by i persons. Income level was represented by the median household, which was found to correlate well with median family and per capita income by zip code. The number of vehicles used by Los Angeles, Orange, Riverside, and San Bernardino county residents with median household incomes within each $5,000 increment is shown in Figure 6.1.

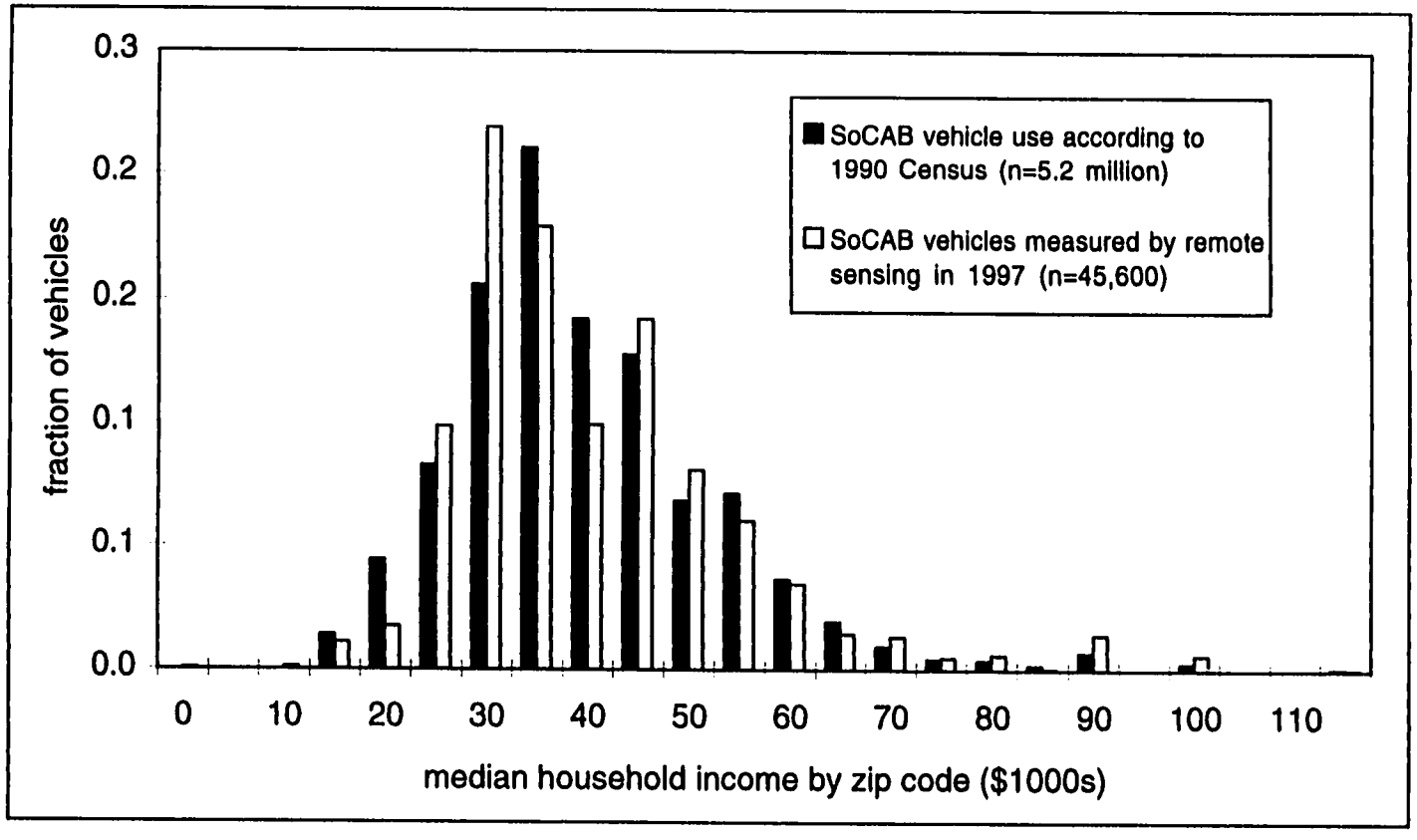

Figure 6.1. Distribution of 1997 remote sensor measurements by median household income in zip code where vehicle was registered. The distribution of SoCAB vehicle use by median household income, according to 1990 U.S. Census data, is also shown. See text for details.

To evaluate the economic distribution of the vehicle fleet sampled for this analysis, each vehicle measured by remote sensing and registered in the SoCAB was assigned to the income bin of the zip code where the vehicle was registered; this distribution is also shown in Figure 6.1. Figure 6.1 demonstrates that the population of SoCAB vehicles sampled by remote sensing is representative, vis-a-vis the median income where vehicles are registered, of the overall SoCAB vehicle fleet. The distribution shown in Figure 6.1 includes only 45,600 remote sensor measurements. An additional 3,750 of the vehicles measured by remote sensing were registered in SoCAB zip codes for which economic data were unavailable.

6.3 RESULTS

6.3.1 On-Road Emission Factors

Mean CO and VOC emission factors for each vehicle model year are shown in Figures 6.2-6.3. Consistent with past findings (Stephens and Cadle, 1991; Zhang et al., 1993; Stedman et al., 1994), emission factors for older vehicles are much higher on average than new vehicle emission factors. Emission factors were calculated for each model year at each site, and using data from all sites combined. Vehicles of model year 1974 and older were analyzed as a single group because very few measurements were available for individual older model years at each site; vehicles of model years 1975-1979 were likewise grouped together. Model year 1998 vehicles (n=107) and vehicles with dealer license plates (n=896) were included in the calculation of 1997 model year emission factors. The

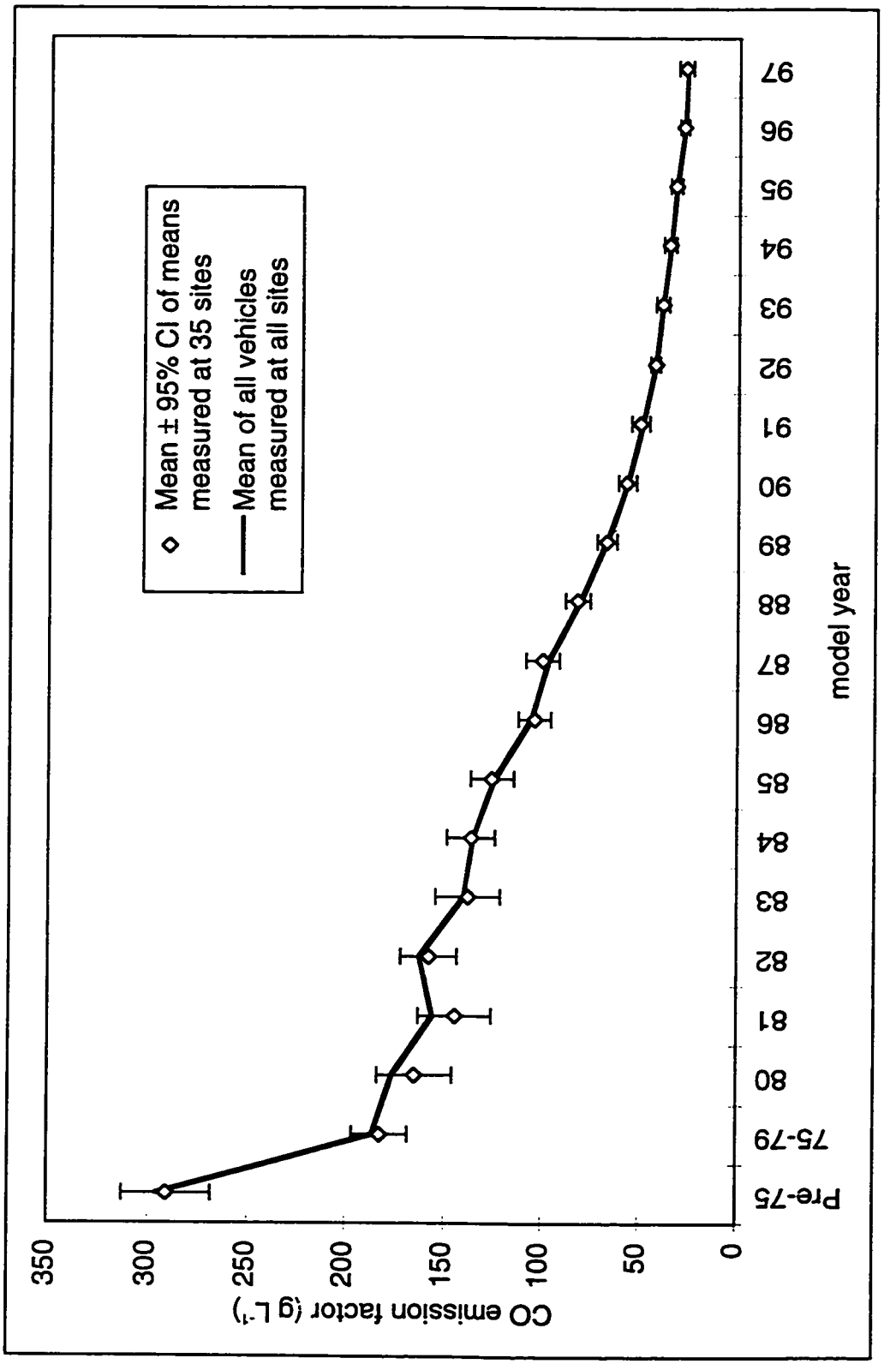

Figure 6.2. CO emission factors by model year measured on-road in the SoCAB during summer 1997.

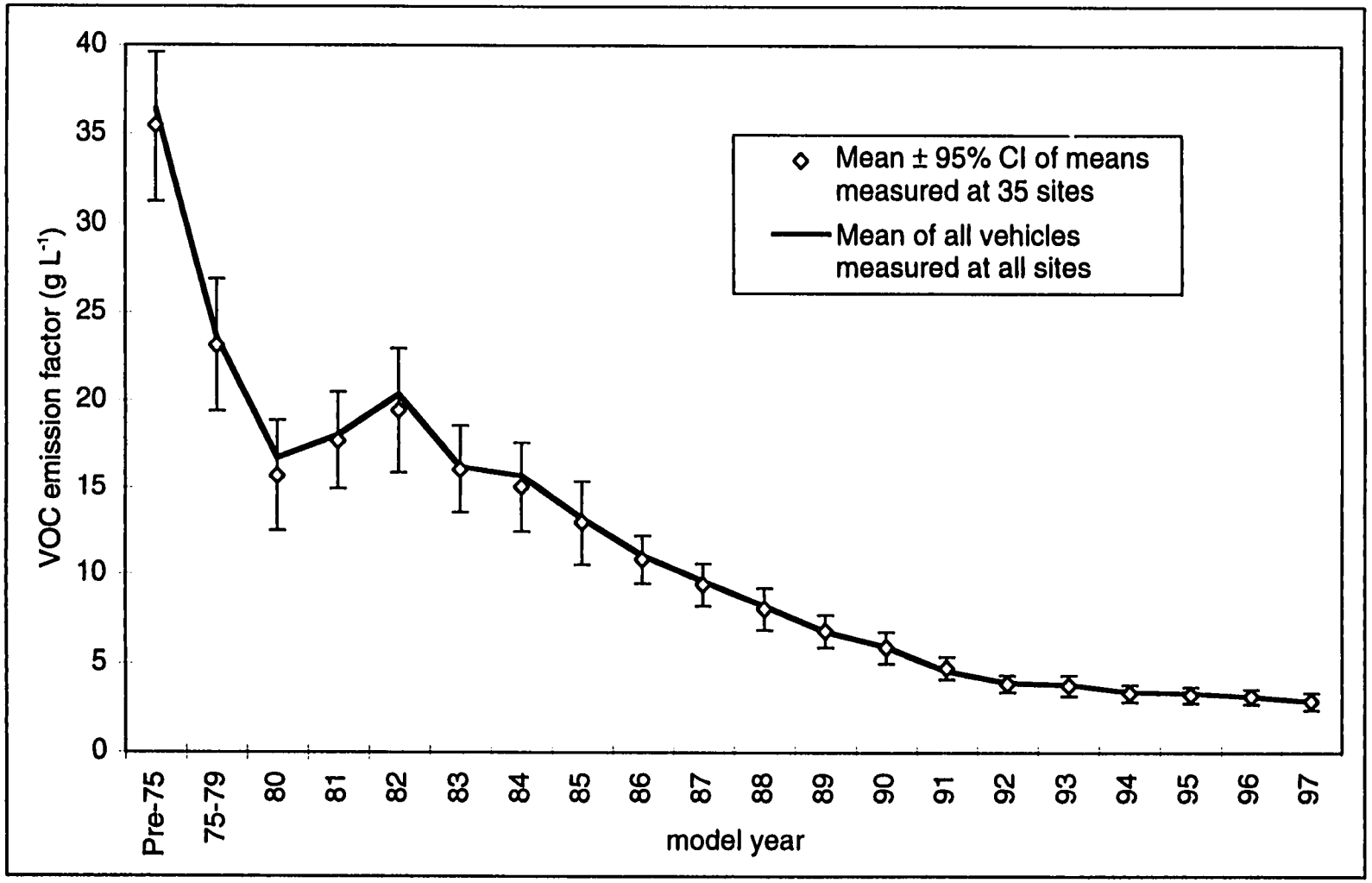

Figure 6.3. VOC emission factors by model year measured on-road in the SoCAB during summer 1997.

diamonds in Figures 6.2-6.3 represent the means over 35 sites of the emission factor for each vehicle model year; the uncertainty bounds represent the 95% CI about each mean. The confidence intervals are within ±10% and ±15%, respectively, of the calculated mean CO and VOC emission factors for most model years. The solid line traces the mean emission factors calculated from all measurements of each vehicle model year. The two approaches yield almost identical estimates of mean CO and VOC emisison factors for vehicles of each model year. For CO, the mean emission factors measured at 35 remote sensing sites are normally distributed for all but 5 model years/groups. For VOC, however, only about one third of the model year specific emission factors were normally distributed.

CO emission factors measured in 1991 (Stedman et al., 1994) and 1997 are shown in Figure 6.4 as a function of vehicle age. The emission factors shown in Figure 6.4 are for all vehicles measured during each sampling year; they include mostly passenger cars and light trucks, but a small number of medium duty trucks also may be included. These data show several interesting trends. First, on-road stabilized exhaust CO emissions of new vehicles in 1997 were the same as emissions from new vehicles in 1991. There is a large difference, however, in the emission factors for vehicles of other ages. Vehicles which were 5 years old in 1997 had emissions comparable to 3 year old vehicles in 1991, while vehicles which were 7 years old in 1997 had emissions comparable to 4 year old vehicles in 1991. In 1991, mean emissions increased roughly linearly with vehicle age starting with 3 year old vehicles; the rate of increase was about 12 g L^{-1} per model year. The inflection

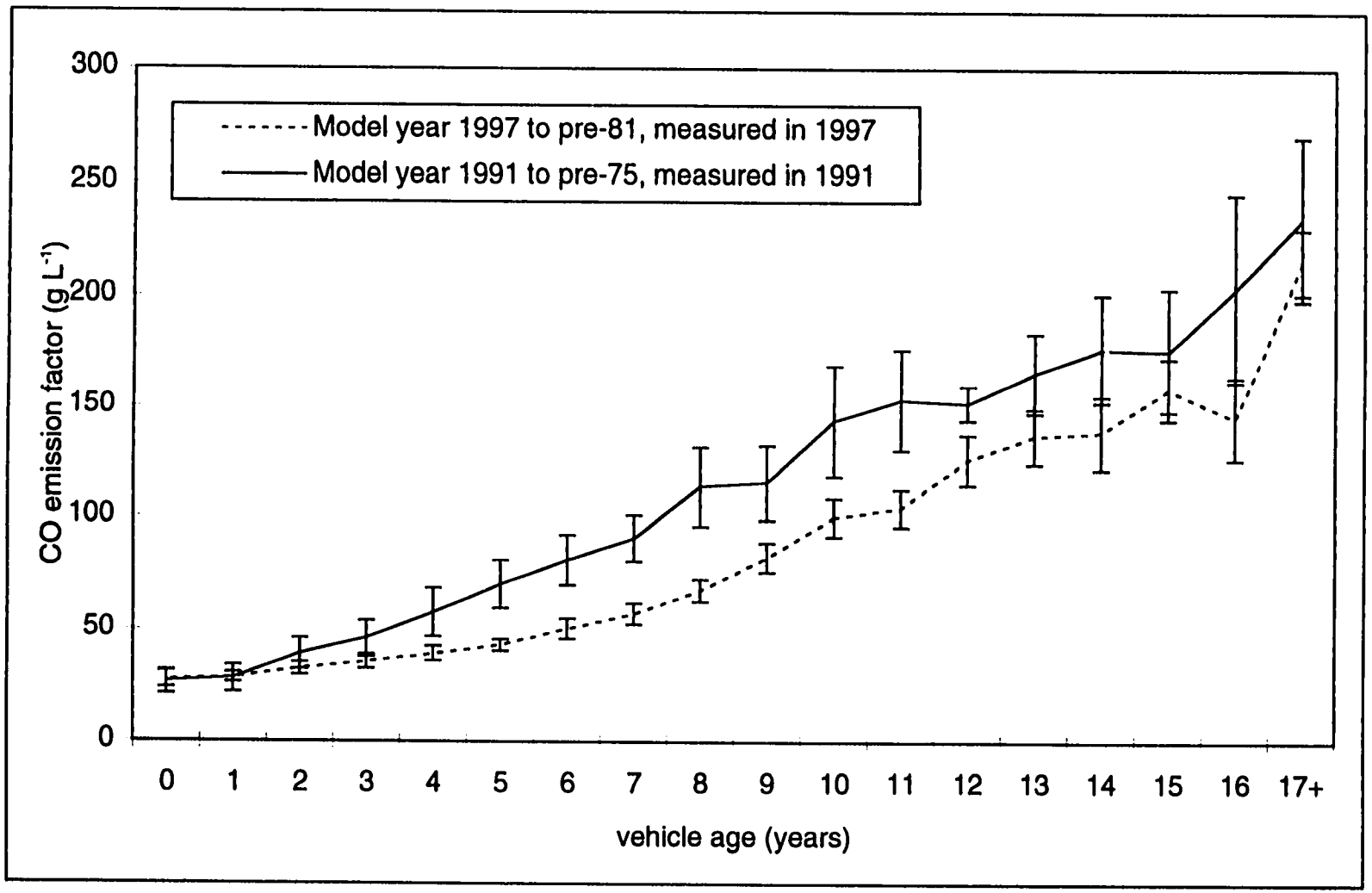

Figure 6.4. CO emission factors by vehicle model year measured by remote sensing in the SoCAB in 1991 and 1997.

point for the 1997 on-road fleet was at about 6 years of age; mean emissions increased at about 3 g L^{-1} per model year for vehicles aged 0-5 years and about 13 g L^{-1} per model year for vehicles aged 7 years or older.

6.3.2 On-Road Vehicle Activity

The distribution of travel by vehicle model year was calculated in an analogous fashion to the emission factors and the results are shown in Figure 6.5. The travel distribution calculated from 52,000 measurements for which vehicle model years were available is again almost identical to the mean distribution calculated from the 35 site-specific distributions. Confidence intervals were calculated independently for the mean travel fraction of each model year. It is important to note, however, that since the travel fractions must sum to unity, an underestimate of the travel fraction for one or more model years necessarily indicates an overestimate for other year(s).

The travel fractions shown in Figure 6.5 were combined with the light-duty fleet fuel economy estimates from Table 6.2 to calculate the fraction of fuel used by vehicles of each model year. Overall, the distribution of fuel use was similar to the distribution of travel across vehicle model years; this results because average fuel efficiency has remained relatively constant from the early 1980s through the present. Weighting of vehicle emissions by fuel use rather than distance traveled was most significant for pre-1980 vehicles, which contributed only 5.5% of total travel but accounted for 7.9% of gasoline use by SoCAB cars and trucks.

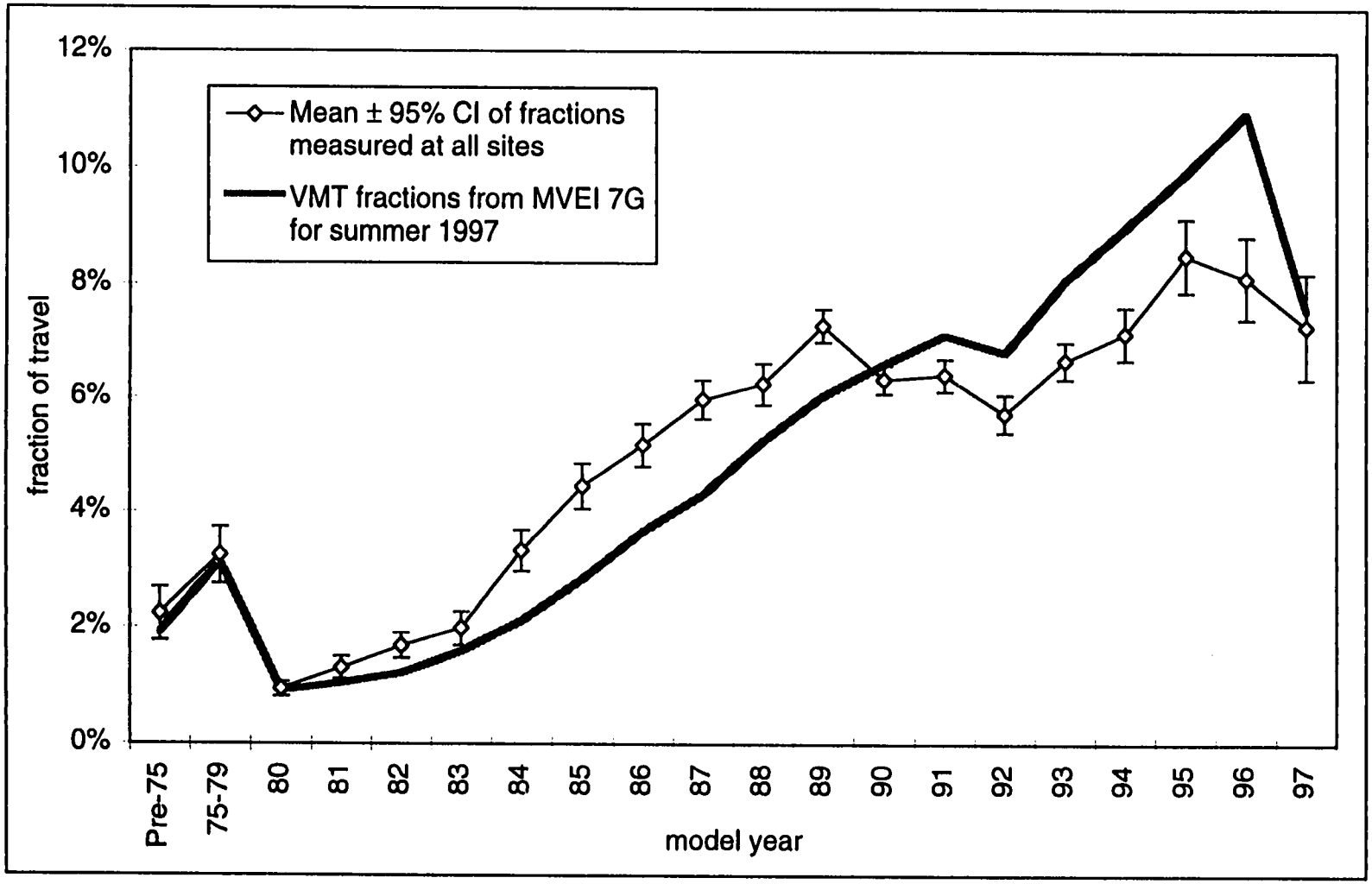

Figure 6.5. Distribution of travel by vehicle model year.

6.3.3 Exhaust Emission Inventory for 1997

Fuel-based inventory results are summarized in Table 6.3. Fleet-average emission factors were calculated using eq 6.3 and the emission factors measured from all vehicles of each model year. The emission factors shown in Table 6.3 include an upward adjustment of 2% for CO and 6% for VOC to account for the higher emissions from vehicles measured on-road for which no registration records were available. These adjustments were calculated by comparing the mean emission level of the entire 60,000 vehicle dataset to the mean emissions (unweighted by fuel economy) of the 52,000 vehicles for which model year was available.

Stabilized exhaust CO emissions for summer 1997 were lower than estimated emissions in summer 1991 by 20%, despite an 8% increase in fuel use. Overall CO mass emissions were reduced because the fleet-average CO emission factor in 1997 was lower by 26% than the fleet-average emission factor in 1991. The revised fuel-based inventory for 1991 reflects an updated fuel use estimate, as described in the Approach section.

Table 6.3. Comparison of motor vehicle exhaust emission inventories for the South Coast Air Basin, summer 1997[a].

Pollutant	Fleet-avg. emissions ($g\ L^{-1}$)	Fuel-based 1997 (metric tons per day)	MVEI 7G 1997	FB/MVEI 1997	Fuel-based 1991 (metric tons per day)	MVEI 7G 1991
CO	80±7	4700±400	1995	2.4±0.2	5900±1400	4074
VOC	9.3±1.5	550±90	159	3.5±0.6	N/A	275

(a) All values are for stabilized exhaust emissions from gasoline-powered passenger cars, light-duty trucks, and medium-duty trucks.

Stabilized exhaust CO emissions predicted by MVEI 7G for 1991 are lower than the fuel-based estimate by a factor of 1.4±0.3; this difference is much smaller than the factor of 2.3±0.5 which separated fuel-based and MVEI 7F estimates for 1991. For 1997, however, stabilized exhaust emissions estimates of 4700±400 metric tons day^{-1} CO and 550±90 metric tons day^{-1} VOC calculated using the fuel-based approach are greater than those predicted by MVEI 7G by factors of 2.4±0.2 and 3.5±0.6, respectively.

Uncertainty in fleet-average emission factors was quantified by propagating through eq 6.3 the uncertainty in emission factors for each pollutant and model year; the estimate does not account for uncertainty in fuel apportionment by model year. An upper-bound on the inventory uncertainty resulting from uncertainty in the distribution of fuel use by model year was estimated at 6% of the inventory value. This was calculated by assuming that the travel fractions of 1988 and older vehicles were understated, and the travel fractions of all newer vehicles overstated; the breakpoint was selected to maintain a sum of travel fractions equal to one. Such systematic bias would lead to an underestimate of fuel use by the highest-emitting vehicles, and as a result, understatement of the overall emissions inventory.

CO and VOC mass emissions from each vehicle model year are shown in Figure 6.6. The cumulative contribution to total mass emissions is also shown. Vehicles that were 7-13 years old in 1997 were responsible for the largest contributions and emitted about 40% of total exhaust CO and VOC. These "middle-aged" vehicles are an important source because their emission factors are 2-4 times those of new vehicles and they still see

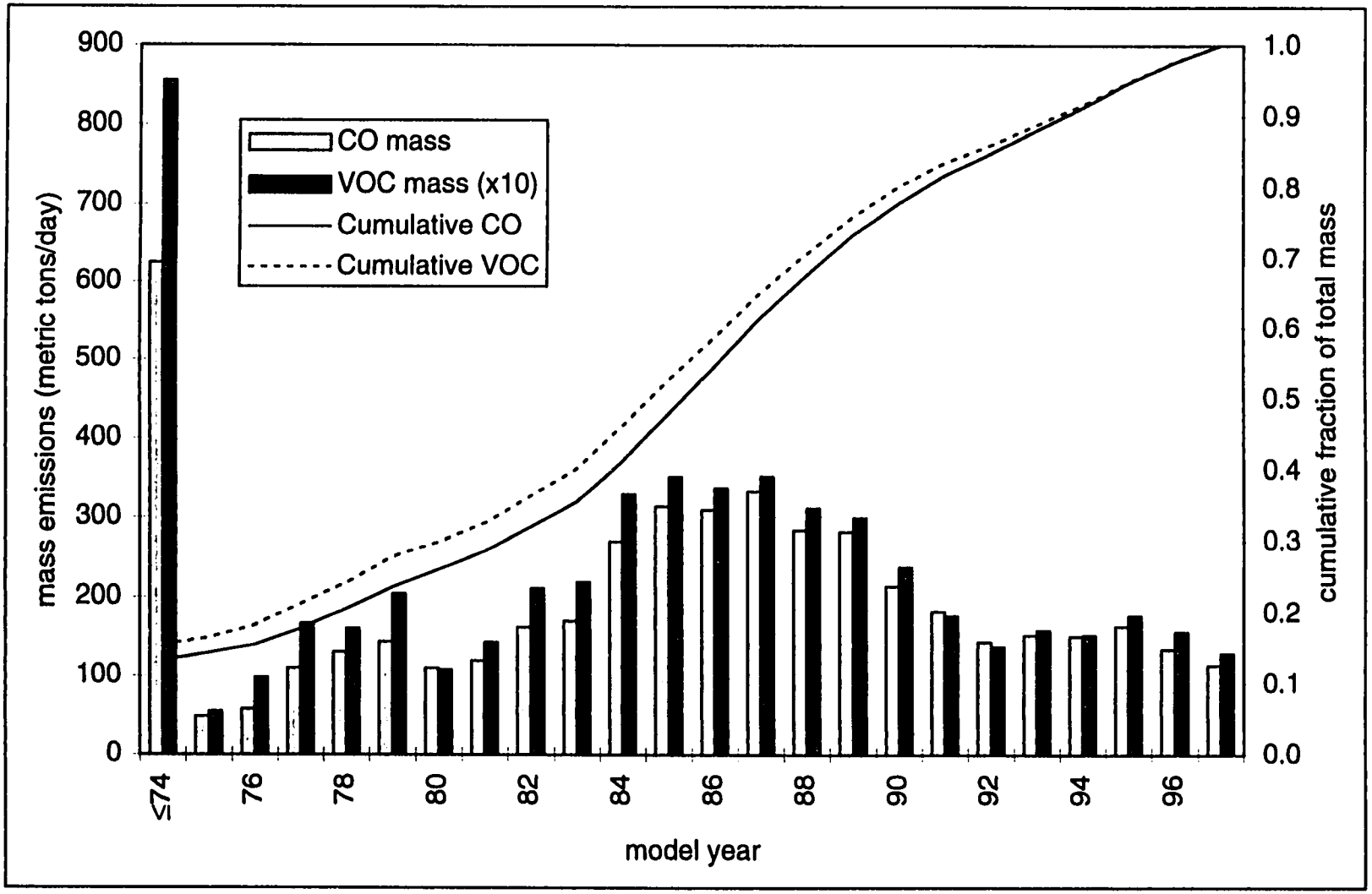

Figure 6.6. Contributions by model year to stabilized exhaust emissions from cars, light-duty, and medium-duty trucks in the South Coast Air Basin during summer 1997.

considerable use. Pre-catalyst vehicles also continue to be an important source of emissions: model year 1974 and older vehicles contributed about 15% of total exhaust CO and VOC emissions in 1997. Vehicles which were 10 or more years old in 1997 contributed 61% of total exhaust CO and 65% of total exhaust VOC in the SoCAB; in 1991, 58% of total exhaust CO was contributed by vehicles which were 10 or more years old.

6.3.4 Emissions vs. Economic Level

The relationship between emissions and the median household income in the zip code where a vehicle is registered is shown in Figure 6.7. This figure was produced by assigning to each vehicle the median household income in the zip code where the vehicle was registered. Mean emissions were then calculated for all SoCAB vehicles within each $5,000 income group. Less than 50 vehicles were registered in zip codes with median incomes ≤ $10,000 and >$100,000. Figure 6.7 shows that fuel-normalized CO and VOC emissions of vehicles registered in zip codes with the lowest median incomes were about twice those of vehicles registered in zip codes with the highest median incomes. The disparity results in part because the vehicle fleets in higher income areas are newer on average than those in lower income areas. Vehicles registered in zip codes with median household incomes of $60,000 are 4 years newer on average than vehicles registered in zip codes with median household incomes of $20,000 (model year of 1992 vs. 1988, with a linear change in average vehicle age between the two income levels). Vehicles in lower income areas also have higher emissions than vehicles of the *same age* which are registered

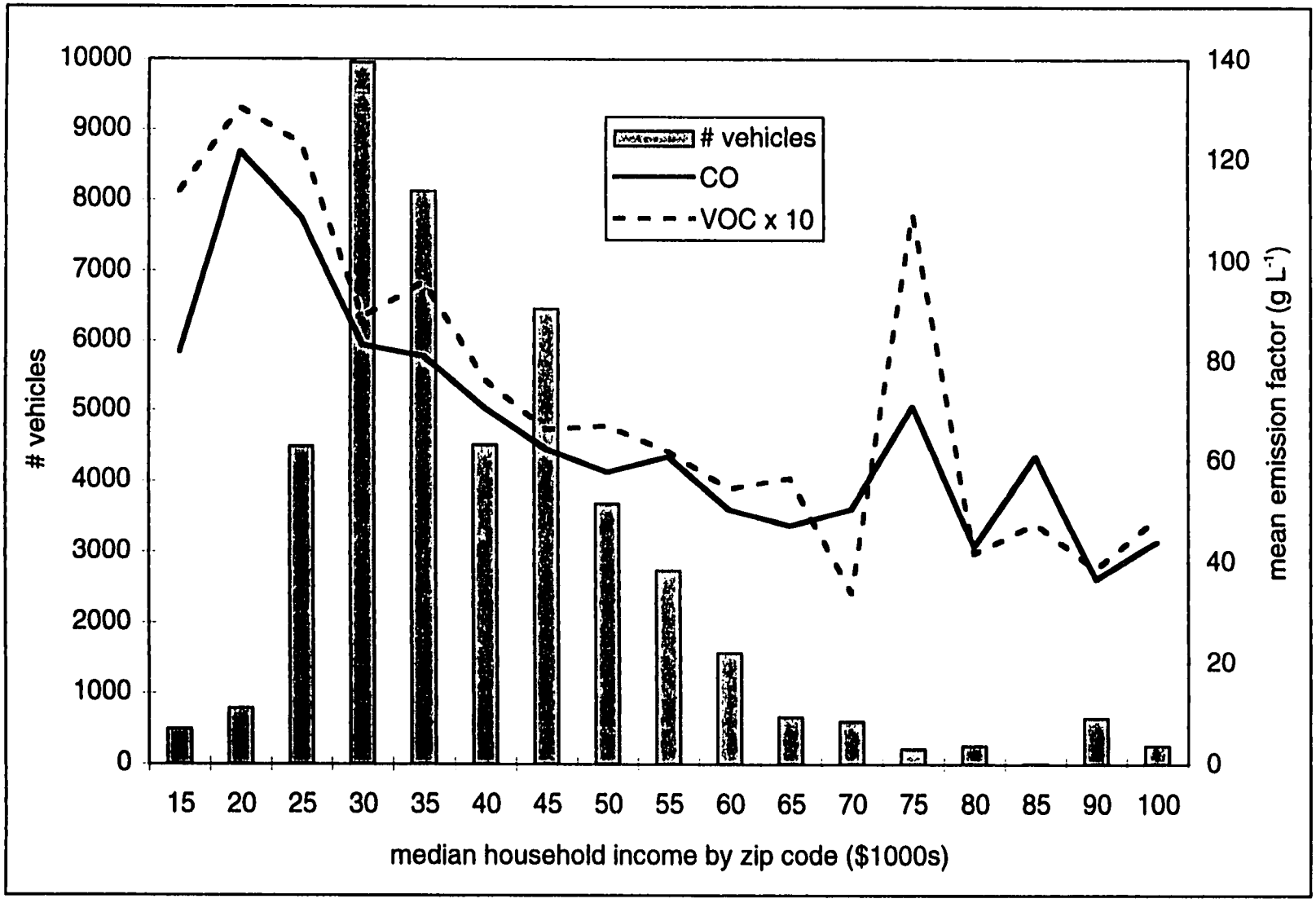

Figure 6.7. Correlation between on-road emissions and median income in the areas where vehicles are registered.

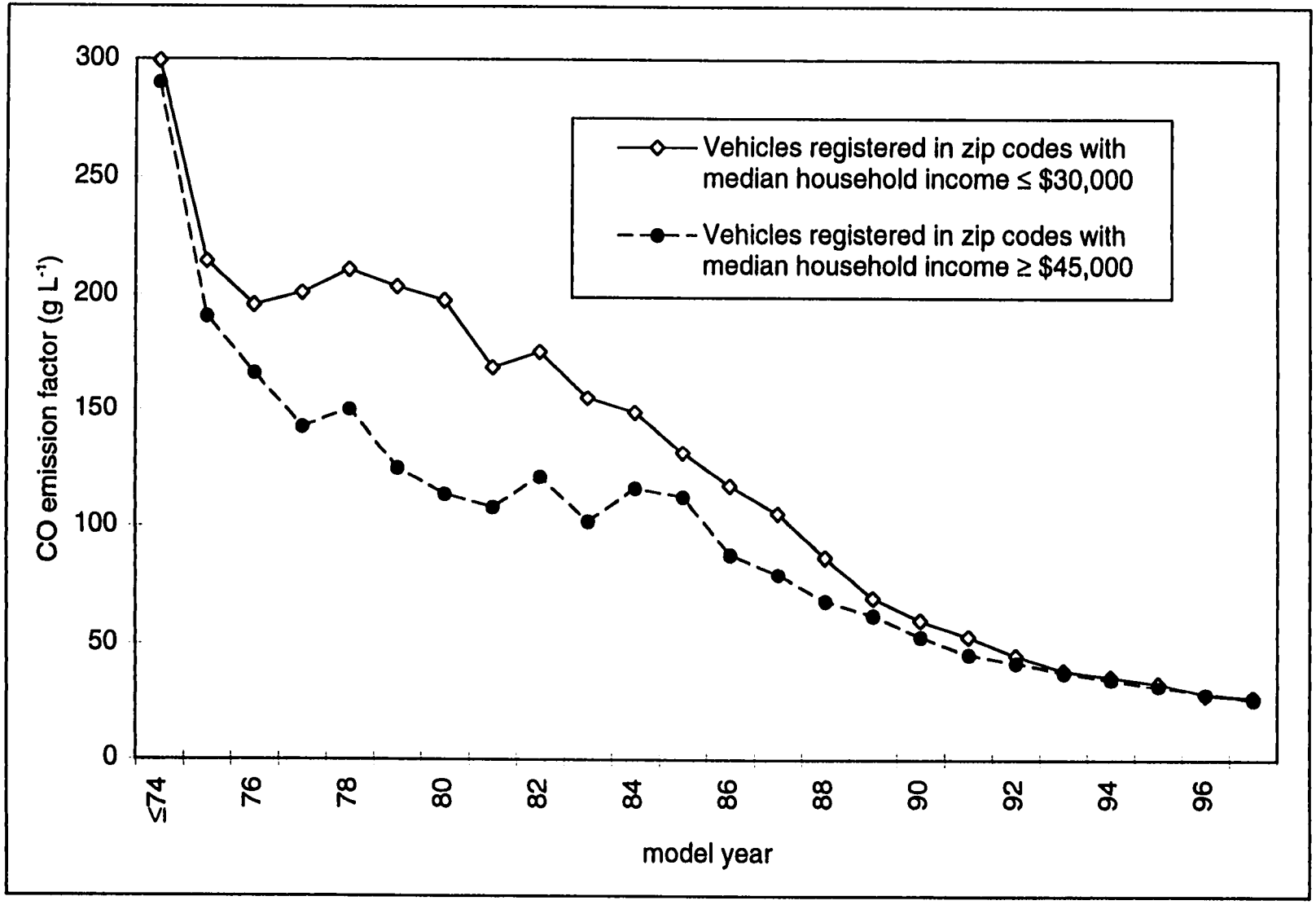

Figure 6.8. Emission factors by model year in lower-income and higher-income areas.

in higher income areas. Figure 6.8 shows model year specific CO emission factors for vehicles registered in zip codes with median household incomes ≤$30,000 and ≥$45,000. New vehicle emission factors are similar in the lower and higher income areas, but emissions increase more rapidly as vehicles age in the lower income areas.

6.4 DISCUSSION

The following discussion evaluates the data used to calculate the fuel-based inventory and attempts to identify causes for differences between MVEI and fuel-based estimates of stabilized CO and VOC emissions.

Fuel use estimates for this study are based on the actual amount of gasoline sold in California during the summer of 1997. The fraction of California gasoline used in the SoCAB was estimated at 42%, which is slightly higher than the value of 40% reported by MVEI 7G. For less than 40% of total California fuel use to be apportioned to the SoCAB, the distance driven per vehicle in the SoCAB would have to be lower than the statewide average (recall that 40% of California vehicles are registered in the SoCAB). In fact, studies of distance accrual rates reported in California's Smog Check program (Horie and Thiele, 1994; Heiken et al., 1996) have found that vehicles registered in Los Angeles and Orange counties travel slightly more (~2%) than the statewide average, while San Bernardino and Riverside county vehicles travel about 10% more than the state average. These estimates do not account for the presence of unregistered or out-of-state vehicles in the SoCAB relative to the presence of such vehicles in the remainder of the state.

SoCAB gasoline use reported by MVEI 7G for summer 1997 was 20% lower than the value estimated in this study for the same time period, and about equal to the gasoline use reported by MVEI 7G for summer 1991. The constant fuel use between 1991 and 1997 suggested by MVEI 7G conflicts with the 8% fuel use increase calculated in this study and the 10% increase in SoCAB travel between 1991 and 1997 reported by MVEI 7G.

Activity apportionment by vehicle model year differs between the fuel-based calculation and the MVEI 7G model, as shown in Figure 6.5. The distribution of vehicle activity observed on-road indicates more travel by 8-17 year-old vehicles (1981-1990 model years), and less travel by 1-6 year-old vehicles (1991-1996 model years) than does the age distribution used by MVEI 7G. The observed on-road data is consistent with the trend in new vehicle sales shown in Table 6.2. Fewer vehicles entered the fleet in the recession years of the early 1990s, while more new vehicles were sold in the mid- to late-1980s. If the MVEI 7G travel apportionment by model year is used in place of the travel apportionment derived from on-road observations, the calculated fuel-based CO and VOC inventories are about 10% lower than the values presented in Table 6.3.

Total vehicle activity estimates and activity apportionment by model year can together account for only ~20% of the difference between fuel-based and MVEI 7G inventory estimates; fleet-average emission factors used by MVEI 7G must therefore be lower than those measured on-road by factors of ~2 for CO and ~3 for VOC. Fleet-average emission factors used to calculate the fuel-based inventory were derived from over 60,000 on-road remote emissions measurements collected at 35 sites located throughout

the greater Los Angeles area. A disproportionate share (~80%) of the SoCAB vehicles measured by remote sensing were registered in Los Angeles county, as compared to the share of SoCAB vehicle registrations and population which are in Los Angeles (~60%). However, as shown in Figure 6.1, the economic distribution of SoCAB vehicle owners sampled is similar to the overall economic distribution of vehicle users in the SoCAB.

The use of remote sensors allowed for the measurement of all light-duty vehicles passing by the 35 sites during sampling, including vehicles registered outside of the SoCAB and vehicles which were not registered. By comparison, MVEI 7G emission factors are derived primarily from testing of registered vehicles which are submitted voluntarily by vehicle owners. The recruitment program targets an unbiased sample of California vehicles, but the unwillingness of some vehicle owners to participate introduces a possible source of bias. If owners of high-emitting vehicles are less likely to participate than owners of low-emitting vehicles, the fleet tested by CARB will have lower emissions on average than the overall fleet of registered vehicles. Such bias was observed in two Los Angeles area studies where vehicles were pulled over and drivers were asked to participate in the studies after their vehicles had been measured by remote sensing (Stedman et al., 1994; Hughes Environmental Systems, 1995).

It also may be significant that remote sensing occured exlusively on surface streets. The estimated distribution of travel by vehicle model year could potentially be biased because the age distribution of vehicles on Los Angeles freeways may not be identical to the distribution measured at the 35 surface street locations where remote sensing was used to measure emissions. Potentially, even the average emission factors by model year

could differ between vehicle populations on highways and on surface streets, e.g. if owners of poorly maintained vehicles are less likely to use their vehicles for highway driving. The extent to which these potential biases actually affect the fuel-based emission inventory cannot be determined. It is worthwile to note, however, that the distribution of vehicle activity by age measured from 35 surface streets in 1997 is similar to the distribution measured from 5 freeway on/off-ramps and 2 surface streets during 1991 (compare Figures 2.5 and 6.5).

In Chapter 5 it was shown that emission factors measured during moderate load provide a good estimate of fuel-normalized emissions averaged over the full distribution of driving in the Unified cycle; the Unified cycle provides a rough estimate of the distribution of on-road driving but probably underrepresents the highest load driving modes. Emission factors measured during deceleration and braking events were shown to be higher by 20% for CO and 50% for VOC. No measurements of speed and acceleration were available for the locations where emissions were measured by CARB in 1997, but the sites were selected to measure vehicles during moderate loads. Since vehicle emissions were not measured under very high load driving conditions (e.g. high speed, high acceleration events), the emission inventory estimates of Table 6.3 do not include the effects of such driving.

One possible source of bias in the fleet-average emission factors measured by remote sensing is that emissions sampling occurred mostly between the hours of 9:00 and 14:00, and thus missed the morning and afternoon commute periods. Remote sensing measurements collected at Rosemead Boulevard in El Monte, CA during the summer of

1991 (Stedman and Bishop, 1994; Stedman et al., 1994) indicate that fleet-average CO emission levels were constant between the hours of 8:00 and 16:00 at this site. The extent to which emission levels throughout the entire day may differ from those measured for this study could not be determined.

While it is also possible that some fraction of the vehicles measured by remote sensing were not fully warmed up, it is unlikely that cold start effects can account for the difference between MVEI 7G and measured on-road emission factors. Cold start emissions measured in an Oakland, CA parking garage in summer 1997 were about a factor of 3 higher than stabilized exhaust emissions of CO and VOC (Chapter 3). In the 1991 study by Stedman et al. (1994), 3% of vehicles identified by remote sensing as high-emitters and pulled over for inspection were found to be in cold start mode. Even if 3% of all vehicles measured by remote sensing in 1997 were in cold start mode, the fleet-average emission factors reported in this study would be higher by only 6% than actual on-road stabilized emission levels.

Emission factors measured by remote sensing can be compared to those measured in Los Angeles area roadway tunnels. In 1995, Gertler et al. (1997) measured emission factors of 93±14 g L^{-1} CO and 6.6±1.3 g L^{-1} NMHC from vehicles passing through the Van Nuys tunnel, and emission factors of 56±3 g L^{-1} CO and 5.3±0.7 g L^{-1} NMHC at the Sepulveda tunnel. Emission factors of 47±4 g L^{-1} CO and 5.0±0.7 g L^{-1} NMHC were measured at Sepulveda in 1996, after SoCAB counties switched from federal reformulated gasoline to California phase 2 reformulated gasoline (Gertler et al., 1998). The average model year of vehicles sampled at the Van Nuys tunnel was about two years older than

the average model year used by MVEI 7F to characterize the SoCAB vehicle fleet; the average model year observed at the Sepulveda tunnel was comparable to the MVEI 7F default value. It is therefore expected that emission factors measured at the Van Nuys tunnel may be higher than the Los Angeles area average. The tunnel results corroborate the CO emission factors measured by remote sensing. Fleet-average exhaust VOC emission factors derived from remote sensing were higher by 40% than NMHC emission factors (including evaporative running losses) measured at the Van Nuys tunnel and higher by about 90% than running NMHC emission factors measured in the Sepulveda tunnel.

6.5 CONCLUSIONS

Robust fuel use estimates and fleet-average emission factors measured from over 60,000 on-road vehicles were used to calculate a stabilized exhaust inventory of 4700±400 metric tons day^{-1} CO and 550±90 metric tons day^{-1} VOC for the SoCAB during summer 1997. These values are higher than official inventory estimates for the same period by factors of 2.4±0.2 for CO and 3.5±0.6 for VOC. The primary cause for these differences appears to be in the fleet-average emission factors used to calculate each inventory. Fuel-based estimates indicate CO emissions reductions of 20% between 1991 and 1997. Fuel use increased by 8%, and the fleet-average CO emission factor decreased by 26% during this period. The MVEI 7G model predicts a 50% reduction in stabilized CO emissions, despite a 10% increase in estimated travel between 1991 and 1997.

The association between median income in an area and average vehicle emissions has been examined. Vehicles registered in high income areas have average CO and VOC

emission factors which are about one-half of the emission factors observed from vehicles registered in low income areas. This difference results in part because vehicle fleets in higher income areas are newer on average than vehicle fleets in lower income areas. New vehicle emissions are similar in high- and low-income areas, but emissions increase more rapidly with vehicle age in low-income areas.

6.6 REFERENCES

Automotive News (1996). *The 100 Year Almanac and 1996 Market Data Book.* Automotive News: Detroit, MI.

Automotive News (1998). *1998 Market Data Book.* Automotive News: Detroit, MI.

Calvert, J. G., J. B. Heywood, R. F. Sawyer and J. H. Seinfeld (1993). Achieving acceptable air quality: some reflections on controlling vehicle emissions. *Science.* **261**:37-45.

CARB (1993). *Methodology for estimating emissions from on-road motor vehicles. Volume III: BURDEN7F.*Technical Support Division, California Air Resources Board, Sacramento, CA.

CARB (1995). *Methodology for estimating emissions from on-road motor vehicles, MVEI 7G.* Mobile Source Emission Inventory Branch, California Air Resources Board, Sacramento, CA. Volumes I-V.

CARB (1996). *MVEI 7G, Version 1.0.* Mobile Source Emission Inventory Branch, Technical Support Division, California Air Resources Board, Sacramento, CA.

CARB (1998). *Summary report for 1997 ozone season remote sensing of motor vehicle on-road emissions.* Mobile Source Operations Division, California Air Resources Board, El Monte, CA. MSO 98-06.

Census Bureau (1998). *1990 Census lookup tables.* Bureau of the Census, United States Department of Commerce, Washington, DC. Data accessed via the internet at www.venus.census.gov in July, 1998.

Davis, S. C. (1997). *Transportation Energy Data Book: Edition 17.* Center for Transportation Analysis, Oak Ridge National Laboratory, U.S. Department of Energy, Oak Ridge, TN. ORNL-6919.

Heiken, J., B. Austin, A. Pollack, D. Coe, L. Chinkin and D. Eisinger (1996). Estimation of local fleet characteristics and activity data for improved emission inventory development. *Sixth CRC On-Road Vehicle Emissions Workshop*, San Diego, CA, March 18-20, 1996. Coordinating Research Council, Atlanta, GA.

Horie, Y. and M. Thiele (1994). *On-road motor vehicle activity data. Volume II - vehicle age distribution and mileage accumulation rate by county.* Valley Research Corporation, Northridge, CA. Prepared for California Air Resources Board Research Division, Sacramento, CA. Final Report, Contract No. A132-182.

Hughes Environmental Systems (1995). *City of Los Angeles remote sensing pilot project.* Prepared for the Mobile Sources Air Pollution Reduction Committee under the AB2766 Program and the City of Los Angeles Environmental Affairs Department. City Contract #C87060-1.

Jack, M. (1996). Remote sensing (RES) - an adjunct to I/M HEV identification and clean car pre-screening. *Sixth CRC On-Road Vehicle Emissions Workshop*, San Diego, CA, March 18-20, 1996. Coordinating Research Council, Atlanta, GA.

Kirchstetter, T. (1998). *Impact of reformulated fuels on motor vehicle emissions.* Ph.D. Dissertation, Department of Civil and Environmental Engineering, University of California, Berkeley, CA.

Long, J. (1997). *Personal Communication.* Mobile Source Control Division, California Air Resources Board, El Monte, CA.

Macias, K. (1994). *Personal Communication.* Stationary Source Division, California Air Resources Board, Sacramento, CA.

Mintz, M., A. D. Vyas and L. A. Conley (1993). Differences between EPA-test and in-use fuel economy: are the correction factors correct? *Transportation Research Record* **1416**:124-130.

Murrell, J. D., K. H. Hellman and R. M. Heavenrich (1993). *Light-duty automobile technology and fuel economy trends through 1993.* U.S. Environmental Protection Agency. EPA/AA/TDG/93-01.

Patel, D., S. Magbuhat, J. Long and M. Carlock (1996). *Comparison of the IM240 and ASM tests in CARB's I&M Pilot Program.* Mobile Source Division, California Air Resources Board, El Monte, CA.

Sorbo, N. W., D. Allen, L. Kawasaki and T. Beecham (1996). City of Los Angeles remote sensing pilot project: summary of key results. *Sixth CRC On-Road Vehicle Emissions Workshop*, San Diego, CA, March 18-20, 1996. Coordinating Research Council, Atlanta, GA.

Stedman, D. H. and G. Bishop (1994). *Personal Communication.* University of Denver, Denver, CO.

Stedman, D. H., G. A. Bishop, S. P. Beaton, J. E. Peterson, P. L. Guenther, I. F. McVey and Y. Zhang (1994). *On-road remote sensing of CO and HC emissions in California.* University of Denver, Denver, CO. Final Report to the California Air Resources Board, Contract No. A032-093.

Stephens, R. D. and S. H. Cadle (1991). Remote sensing measurements of carbon monoxide emissions from on-road vehicles. *J. Air Waste Manage. Assoc.* **41**:39-46.

Stephens, R. D., P. A. Mulawa, M. T. Giles, K. G. Kennedy, P. J. Groblicki, S. H. Cadle and K. T. Knapp (1996). An experimental evaluation of remote sensing-based hydrocarbon measurements: a comparison to FID measurements. *J. Air Waste Manage. Assoc.* **46**:148-158.

USDOT (1998). *Monthly fuel sales reported by states*. Federal Highway Administration, U. S. Department of Transportation, Washington, DC. Data accessed via the internet at www.fhwa.dot.gov.

Zhang, Y., D. H. Stedman, G. A. Bishop, P. L. Guenther, S. P. Beaton and J. E. Peterson (1993). On-road hydrocarbon remote sensing in the Denver area. *Environ. Sci. Technol.* **27**:1885-1891.

CHAPTER SEVEN

Conclusions

7.1 SUMMARY OF RESULTS

A fuel-based methodology for estimating motor vehicle exhaust emissions has been presented. The fuel-based approach uses fuel-normalized emission factors measured directly from large numbers of on-road vehicles; emissions are measured using roadside remote sensors and/or by sampling the exhaust air in roadway tunnels and parking garages. Vehicle activity is estimated from fuel sales records which can be resolved to the air basin or regional level.

The fuel-based approach was applied in Chapter 2 to calculate an inventory of motor vehicle carbon monoxide (CO) emissions in California's South Coast Air Basin (SoCAB) in summer 1991. Fleet-average emission factors of 105±21 g L^{-1} CO for cars and 120±35 g L^{-1} CO for light/medium trucks were calculated from over 70,000 infrared remote sensing measurements at 7 sites in the Los Angeles area. Gasoline use by passenger cars and trucks weighing less than 3860 kg (8500 lbs) was estimated to be 4.9×10^7 L day^{-1}. Total stabilized CO emissions from cars and trucks in the SoCAB were estimated to be 5400±1200 metric tons per day. Vehicles which were ten or more

years old in 1991 accounted for almost 60% of this total. Fuel-based inventory estimates were 2.3±0.5 times higher than the official stabilized exhaust CO inventory predicted by California's MVEI 7F model.

A fuel-based evaluation of real-world cold start emission factors was presented in Chapter 3. Hot stabilized exhaust emission factors were measured as vehicles arrived in the morning, and cold start emissions were measured as vehicles started and exited in the afternoon from an underground parking garage in Oakland, CA during March, 1997. The incremental, or excess emissions associated with vehicle starting were calculated by difference. Composite emissions from ~135 vehicles were sampled during each of 6 morning and 6 afternoon periods. Measured stabilized exhaust emissions were 5.0±0.6 g L^{-1} non-methane hydrocarbons (NMHC), 59±6 g L^{-1} CO, and 2.3±0.5 g L^{-1} nitrogen oxides (NO_x). Cold start emission factors of 18.3±1.0 g L^{-1} NMHC, 175±12 g L^{-1} CO, and 7.4±0.9 g L^{-1} NO_x were measured for vehicles spending an average of ~60 s in the garage after starting in the afternoon. Average fuel use during cold start was estimated to be ~0.26 L, and the cold start period was estimated to last for ~200 s. When cold start emission factors measured in the garage were scaled to represent the full 200 s cold start period, incremental start emission factors of 2.1±0.3 g NMHC, 16±3 g CO, and 2.1±0.4 g NO_x per vehicle start were calculated. The cold start emission factors derived from parking garage measurements were lower than predictions of California's MVEI 7G model by 45% for NMHC, 65% for CO and 12% for NO_x; these results suggest that current inventories overstate the excess emissions associated with vehicle starting.

Chapter 4 focused on the use of infrared remote sensor HC measurements for emission inventory calculations. Remote sensor HC measurements should not be used directly for emission inventory purposes because infrared (IR) analyzers calibrated with propane understate volatile organic compound (VOC) concentrations in vehicle exhaust by 30-70% when compared to flame ionization detectors (FID). The difference depends on VOC composition, and arises because many organic compounds in vehicle exhaust absorb less IR radiation than propane on a per-carbon basis. This study demonstrated an approach for scaling infrared measurements to reflect more accurately total exhaust VOC emissions from on-road motor vehicle fleets. Infrared versus flame ionization detector response to individual VOC was measured in the laboratory for MTBE and a range of alkanes, alkenes, and aromatics that are prominent in vehicle exhaust. Overall IR/FID response to real exhaust mixtures was calculated by summing the response contributions of all individual VOC constituents. Average IR/FID response factors were calculated for typical on-road vehicle fleets based on VOC speciation profiles measured in several U.S. roadway tunnels. Results indicate that HC concentrations measured by remote sensors with 3.4 μm filters should be multiplied by a factor of 2.0±0.1 for light-duty vehicles using either California or Federal reformulated gasoline blends and by 2.2±0.1 when conventional gasoline is used.

Chapter 5 addressed the importance of driving mode when measuring emission factors and developing fuel-based estimates of on-road motor vehicle emissions. The effect of load on fuel-normalized emission factors was analyzed using on-road remote

emissions measurements paired to individual vehicle speed and acceleration measurements from a Phoenix, AZ test program. Measured speed, acceleration, and roadway grade were combined with characteristic values of vehicle mass, frontal area, aerodynamic drag coefficient, and rolling resistance coefficient to estimate the load on each vehicle; average emissions were then calculated for all vehicles measured at each load level. Both CO and HC emission factors varied by less than 10% over a wide range of positive vehicle loads, but emissions under the highest load driving conditions could not be conclusively assessed. Emission factors measured during hard deceleration or braking events were higher than emissions measured during moderate positive loads by about 50% for HC and 20% for CO. The amount of fuel used during each driving mode was estimated using the Unified cycle, which is based on the distribution of driving observed on-road in Los Angeles in 1992. Results indicate that almost 90% of fuel use occurs during loaded mode driving, and that emissions measured during 10-20 kW of road load provide a good estimate of emissions averaged over the distribution of driving modes observed on-road.

In Chapter 6, the fuel-based approach was used to estimate stabilized exhaust CO and VOC emissions in the SoCAB during summer 1997. Fleet-average emission factors of 80±7 g L^{-1} CO and 9.3±1.5 g L^{-1} VOC were calculated from more than 60,000 infrared remote sensor measurements collected at 35 sites throughout the greater Los Angeles area. Gasoline use by SoCAB passenger cars and trucks weighing less than 6360 kg (14,000 lbs) was estimated at 5.9×10^7 L day^{-1} based on actual fuel sales during summer 1997. Stabilized exhaust emissions of 4700±400 metric tons per day CO and 530±90 metric

tons per day VOC calculated with the fuel-based approach were higher than estimates of California's MVEI 7G model by factors of 2.4±0.2 for CO and 3.5±0.6 for VOC. According to the fuel-based inventory estimates, stabilized CO emissions in 1997 were lower by 20% than emissions during summer 1991. Fuel use increased by 8% during this period while the fleet-average CO emission factor decreased by 26%. The relationship between income and vehicle emissions was examined using census data resolved to the zip code level. On average, vehicles registered in the lowest income areas had CO and VOC emission factors which were double those of vehicles registered in higher income areas. The difference results (1) because the vehicle population in lower income areas is older on average than the fleet in higher income areas, and (2) because average emissions increase with vehicle age more sharply in lower income areas.

7.2 CONCLUSIONS

The fuel-based approach can be used to estimate stabilized exhaust emissions from the in-use motor vehicle fleet. The accuracy of fuel-based inventory estimates depends upon the measurement of fleet-average emission factors which represent the entire in-use vehicle fleet in an area. The age distribution of the on-road fleet and the rate at which emissions increase with vehicle age both appear to depend strongly on the median household income in the area where emissions are measured. On-road emission factors should be measured at sampling sites which reflect the economic distribution of the larger air basin or region of interest. Emission factors measured from vehicles under moderate loads provide a good estimate of emissions averaged over most on-road driving because

fuel-normalized CO and HC emission factors are consistent over a wide range of positive loads and because most fuel is used during such driving modes; however, the effect of very high load driving events of fleet-average emissions is still uncertain. The fuel-based approach can be used to estimate stabilized exhaust emissions of CO, VOC, NO_x, and any other pollutants for which emission factors can be measured on-road. Real-world cold start emission factors can be measured in parking garages.

Fuel-based inventories are useful for validating and/or improving upon predictions of current motor vehicle emission inventory models. Application of the fuel-based inventory approach indicates that Calfornia's official motor vehicle emission inventory model, currently at version 7G, continues to underpredict stabilzed exhaust emissions of CO and VOC. In contrast, MVEI 7G overstates incremental cold start emission factors and therefore may overstate total incremental start emissions. The importance of cold starts relative to total CO and VOC exhaust emissions is overstated.

Prediction of future year emission inventories requires accurate estimates of current emissions. California's MVEI 7G model understates current stabilized exhaust emission levels, and overstates emissions reductions between 1991 and 1997; official inventory predictions for future years are therefore likely to be overly optimistic. As a result of this uncertainty, management plans which count on large reductions in vehicle emissions to achieve ambient air quality standards may fall short of their objectives.

7.3 RECOMMENDATIONS

This research has demonstrated the value of the fuel-based approach for estimating motor vehicle emissions. Many important issues – such as the dependence of fuel-normalized emissions on driving mode and the appropriate scaling factor for infrared HC measurements – were examined in this volume. Following are the areas which I believe should be the foci of future research related to on-road vehicle emission inventories.

7.3.1 On-Road NO_x Emissions

Motor vehicle emissions of nitrogen oxides are an important precursor to ozone, fine particles, peroxy acetyl nitrate (PAN), and nitric acid (HNO_3). The fuel-based approach can be applied to estimate NO_x emissions in a manner analogous to the CO and HC emission inventories presented in this thesis. Exhaust NO_x concentrations have been measured from individual vehicles using roadside remote sensors and on a fleet-average basis in roadway tunnels. The dependence of NO_x emission factors on driving mode should be determined by an analysis similar to that presented for CO and HC emissions. If fleet-average NO_x emissions are shown to depend significantly on load, then calculation of a NO_x emission inventory will require that emission factors be measured for an array of driving modes; mode-specific emission factors can then be weighted by the distribution of on-road driving among to calculate a fleet-average emision factor representative of all on-road driving. Calculation of on-road vehicle NO_x emission inventories should also include an assessment of emissions from heavy-duty deisel trucks.

7.3.2 Evaporative VOC Emissions

Evaporative VOC emissions from in-use motor vehicles are currently thought to be similar in magnitude to exhaust emissions. Studies involving small numbers of vehicles indicate that the distribution of evaporative emissions among the in-use fleet may be highly skewed. If this is the case, then current inventory models may significantly understate evaporative emissions for the same reasons that they understate exhaust emissions: i.e. the highest-emitting vehicles are not adequately represented in the test fleet from which emissions are measured. The development of methods to measure evaporative emissions from large, unbiased samples of in-use vehicles should be a high research priority. For example, hot soak emissions may be measured in parking structures. Meteorological flux techniques may be useful in measuring diurnal evaporation from cars in large open-air parking lots, such as those at airports (especially long-term parking).

7.3.3 VOC Speciation

Individual VOC can be directly toxic, highly reactive in the atmosphere (and thus contribute to ozone formation), or relatively inert and harmless. It is therefore essential that total VOC emission estimates be accurately speciated to estimate mass emissions of each important individual organic compound or compound group. Total VOC emissions estimates calculated with the fuel-basd approach may be combined with speciation profiles measured in roadway tunnels to calculate speciated VOC emission inventories. However, VOC speciation measured in a roadway tunnel may depend on the prevalent

driving mode(s) in the tunnel. If average VOC speciation differs substantially under driving modes not encountered in tunnels where speciation has been measured, then the overall mass emission estimates for individual VOC may be less accurate. The dependence of driving mode on fleet-average VOC speciation is also important in determining infrared HC scaling factors appropriate to various driving modes. Based on the results of Chapter 5, the accurate determination of VOC speciation under loaded driving modes appears to be most important, but VOC speciation should nevertheless be determined over a range of driving conditions.

7.3.4 Importance of High-Speed, High-Load Driving

The importance of the highest load driving events to the overall emission inventory remains uncertain. Emissions should be measured under very high load driving conditions and, if possible, from the same stream of vehicles under moderate load driving conditions to determine how emissions under the highest load driving conditions compare to fleet-average emissions under moderate load conditions. The amount of fuel used during the highest load driving conditions should be assessed using accurate estimates of the distribution of on-road driving (preferably data which has been collected since freeway speed limits were raised in the mid-1990s). These data could then be combined using the methodology described in Chapter 5 to estimate the contribution of very high load driving events to the overall emission inventory.

7.3.5 Analysis of Variables Which May Affect On-Road Vehicle Emissions

The present analysis did not examine all factors which may influence average emissions of the on-road vehicle fleet. Long-term remote sensing and tunnel-based monitoring programs should be established to determine which factors most affect fleet-average emissions at a given sampling site. Specifically, fleet composition and average emission levels should be analyzed as a function of time of day (commute vs. non-commute hours), day of the week (weekday vs. weekend), season of the year, and ambient temperature.

7.3.6 Spatial and Temporal Distribution of Emissions

The photochemical models which are used to understand ozone formation in urban air basins require that emission inventories be resolved temporally and spatially. At present total stabilized exhaust emissions are resolved according to the travel distribution predicted by travel demand models. From the analysis in Chapter 6, it is clear that average emission factors are not uniform across all neighborhoods throughout the Los Angeles area; older vehicle fleets and higher average emissions were observed in lower income areas. Any spatial distribution of emissions should account for the dependence of vehicle emissions on the median household income in each neighborhood of an urban area.

7.37 Vehicle Emissions and Socioeconomics

Median household income appears to be a useful predictor of average vehicle emissions in an area (see Chapter 6). One reason for this trend is that vehicle fleets in lower income areas are older on average than vehicle fleets in higher income areas. Another factor is that emission levels appear to increase more rapidly with vehicle age in lower income areas

than in higher income areas. By contrast, emission factors for the most recent model year vehicles are similar in higher and lower income areas. The difference in deterioration rates between lower income and higher income areas could result from differences in vehicle durability, differences in mileage accumulation rates, and/or differences in vehicle maintenance between higher and lower income areas. The causes for these trends should be examined.

7.3.8 Verification of Motor Vehicle Emission Inventories

The primary motivation for this reseach was the need for accurate inventories of motor vehicle emissions in polluted air basins. The fuel-based approach should be used to verify or adjust current year inventories of motor vehicle exhaust emissions in each of the most polluted urban areas of the U.S. Fuel-based inventories can be used to guage uncertainty in current official emission inventories and to identify areas requiring further study in motor vehicle emission inventory models. On-road emission factors should be measured and fuel-based inventories periodically recalculated in areas with persistent air pollution problems.

IMAGE EVALUATION
TEST TARGET (QA-3)

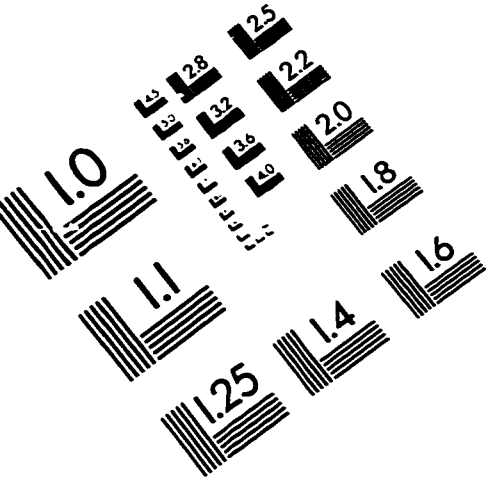

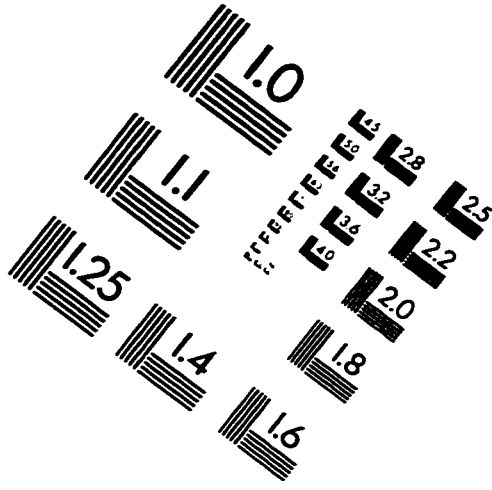

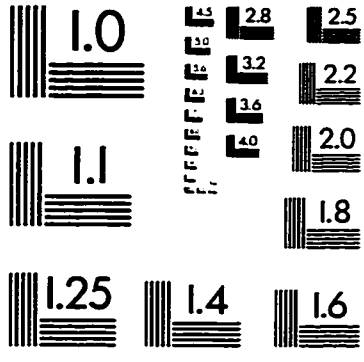

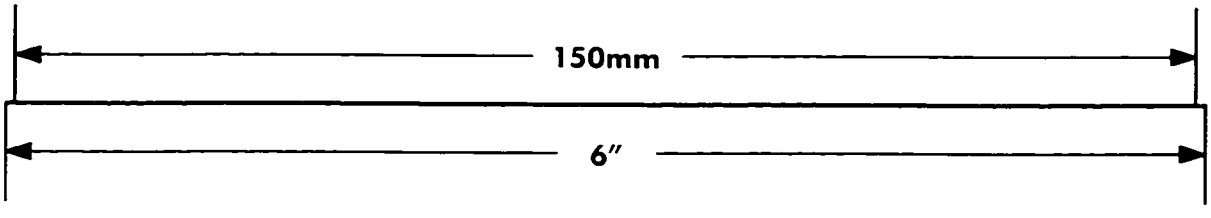

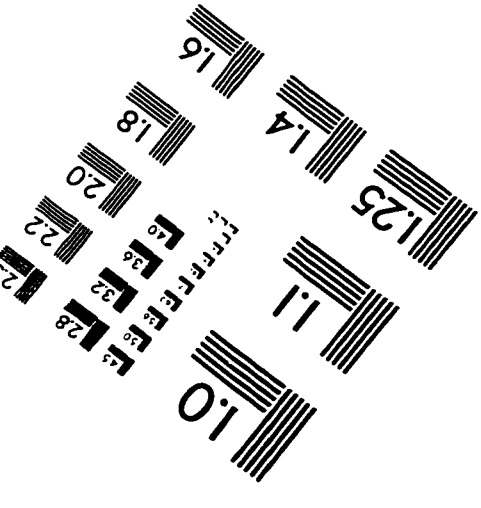

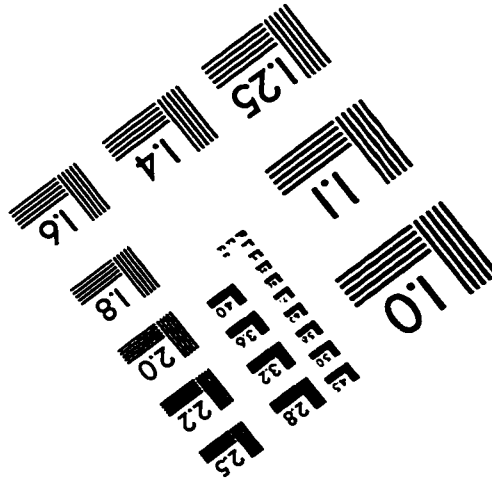

APPLIED IMAGE, Inc
1653 East Main Street
Rochester, NY 14609 USA
Phone: 716/482-0300
Fax: 716/288-5989